MARTIN MARIETTA ENERGY SYSTEMS LIBRARIES

3 4456 0374402 7

ORNL/NPR-92/64

ornl

OAK RIDGE NATIONAL LABORATORY

MARTIN MARIETTA

FINAL REPORT

PIPE BREAK TESTING OF PRIMARY LOOP PIPING SIMILAR TO DEPARTMENT OF ENERGY'S NEW PRODUCTION REACTOR-HEAVY WATER REACTOR

Materials/System Integrity Task of the HWR-NPR Program

Oak Ridge National Laboratory

OAK RIDGE NATIONAL LABORATORY
CENTRAL RESEARCH LIBRARY
CIRCULATION SECTION
4500N ROOM 175
LIBRARY LOAN COPY
DO NOT TRANSFER TO ANOTHER PERSON
If you wish someone else to see this report, send in name with report and the library will arrange a loan.
MCN-TRR (10-77)

MANAGED BY
MARTIN MARIETTA ENERGY SYSTEMS, INC.
FOR THE UNITED STATES
DEPARTMENT OF ENERGY

This report has been reproduced directly from the best available copy.

Available to DOE and DOE contractors from the Office of Scientific and Technical Information, P.O. Box 62, Oak Ridge, TN 37831; prices available from (615) 576-8401, FTS 626-8401.

Available to the public from the National Technical Information Service, U.S. Department of Commerce, 5285 Port Royal Rd., Springfield, VA 22161.

This report was prepared as an account of work sponsored by an agency of the United States Government. Neither the United States Government nor any agency thereof, nor any of their employees, makes any warranty, express or implied, or assumes any legal liability or responsibility for the accuracy, completeness, or usefulness of any information, apparatus, product, or process disclosed, or represents that its use would not infringe privately owned rights. Reference herein to any specific commercial product, process, or service by trade name, trademark, manufacturer, or otherwise, does not necessarily constitute or imply its endorsement, recommendation, or favoring by the United States Government or any agency thereof. The views and opinions of authors expressed herein do not necessarily state or reflect those of the United States Government or any agency thereof.

OE F 1332.15
3-93)
ombines previous
ersion of DOE
1332.15 and .16.
l other editions are
bsolete.

U. S. DEPARTMENT OF ENERGY
RECOMMENDATIONS FOR THE ANNOUNCEMENT AND DISTRIBUTION OF DEPARTMENT OF ENERGY (DOE) SCIENTIFIC AND TECHNICAL INFORMATION (STI)

(See instructions on reverse side. Use plain bond paper if additional space is needed for explanations.)

OMB Control No.
1910-1400
OMB Burden Disclosure Statement on reverse side

PART I *(DOE, DOE Contractors, Grantees, and Awardees complete)*

A. Product/Report Data

1. (Award) Contract No. DE-AC05-84OR21400

2. Title Pipe Break Testing of Primary Loop Piping Similar to Department of Energy's New Production Reactor-Heavy Water Reactor - Final Report

3. Product/Report Description

☒ a. Report *(Complete all that apply)*
(1) ☒ Print ☐ Nonprint *(specify)*
(2) ☐ Quarterly ☐ Semiannual ☐ Annual ☐ Final
☒ Topical ☐ Phase I ☐ Phase II
☐ Other *(specify)*

Dates covered ____ thru ____

☐ b. Conference/Meeting/Presentation *(Complete all that apply)*
(1) ☐ Print ☐ Nonprint *(specify)*
☐ Published proceedings
☐ Other *(specify)*

(2) Conference Title *(no abbreviations)*

Location *(city/state/country)*

Date(s) *(m/d/y)* / / thru *(m/d/y)* / /
Sponsor

☐ c. Software—Additional forms are required. Follow instructions on the back of this form.
☐ d. Other *(Provide complete description)*

B. Patent Information

Yes No
☐ ☒ Is any new equipment, process, or material disclosed? If yes, identify page numbers

☐ ☒ Has an invention disclosure been submitted? If yes, identify the disclosure number and to whom it was submitted. Disclosure number
Submitted to

☐ ☒ Are there patent-related objections to the release of this STI product? If so, state the objections.

C. Contact *(Person knowledgeable of content)*

Name
Phone
Position
Organization

PART II *(DOE/DOE Contractors complete/or as instructed by DOE contracting officer)*

A. DOE Identifiers

1. Product/Report Nos. ORNL/NPR-92/64

2. Funding Office(s) *(NOTE: Essential data)* 39 NP 01 00 0

B. Copies for Transmittal to AD-21 (OSTI)

(STI must be of sufficient quality for microfilming/copying.)

☐ 1. One for classified processing
☐ 2. *(number)* for standard classified distribution
☒ 3. Two unclassified for processing
☐ 4. *(number)* for program unclassified distribution
☒ 5. UC/C Category 940

☐ 6. Additional instructions/explanations

(Do not identify Sigma categories for Nuclear Weapons Data reports, and do not provide additional instructions that are inconsistent with C below.)

C. Recommendation *("X" at least one)*

☒ 1. Program/Standard Announcement/Distribution *(Available to U.S. and foreign public)*
☐ 2. Classified *(Standard Announcement only)*
☐ 3. Special Handling *(Legal basis must be noted below.)*
☐ a. Unclassified Controlled Nuclear Information (UCNI)
☐ b. Export Control/ITAR/EAR
☐ c. Temporary hold pending patent review
☐ d. Translations of copyrighted material
☐ e. Small Business Innovation Research (SBIR)
☐ f. Commercializable information
☐ (1) Proprietary
☐ (2) Protected CRADA information
Release date / /
☐ (3) Other *(explain)*

☐ 4. Program Directed Special Handling *(copy attached)*

D. Releasing Official

A. Patent Clearance *("X" one)*
☐ Has been submitted for DOE patent clearance
☒ DOE patent clearance has been granted

B. Released by
(Name) D.R. Hamrin
(Signature) D. R. Hamrin (RB)
(Phone) (615) 574-6752
(Date) May 17, 1993

ORNL/NPR-92/64

New Production Reactor

FINAL REPORT
PIPE BREAK TESTING OF PRIMARY LOOP PIPING SIMILAR TO DEPARTMENT OF ENERGY'S NEW PRODUCTION REACTOR-HEAVY WATER REACTOR

A. B. Poole
R. L. Battiste
J. A. Clinard

Materials/System Integrity Task of the NPR-HWR Program

Oak Ridge National Laboratory

January 1993

Prepared by the
OAK RIDGE NATIONAL LABORATORY
Oak Ridge, Tennessee 37831
managed by
MARTIN MARIETTA ENERGY SYSTEMS, INC.
for the U.S. Department of Energy
under Contract No. DE-AC05-84OR21400

MARTIN MARIETTA ENERGY SYSTEMS LIBRARIES

3 4456 0374402 7

TABLE OF CONTENTS

Page

Foreward iv

List of Figures ..... v, vi

List of Tables vii

1. Executive Summary 1

2. Introduction 1

3. Background 2

4. Degraded Piping Material Tests 2

5. Test Results 8

6. Discussion 12

7. Post-Test Examination 27

8. Piping Integrity Review Group (PIRG) Comments 31

9. PIRG Conclusions/Recommendations 36

10. Acknowledgements 37

11. References 37

Appendix A. First Report of the Piping Integrity Review Group (PIRG) 38

Appendix B. Final Report of the Piping Integrity Review Group (PIRG) 65

Appendix C. Final Report on Battelle NP-HWR Analytical Assistance Program 77

Appendix D. Parametric Study of the Probability of Leaks in the NPR-HWR Pressurizer surgeline. (by Argonne National Laboratory) 133

FOREWARD

This report provides information about and results from specific tests completed at Oak Ridge National Laboratory (ORNL). The subject of the program was failure testing of a Savannah River C-reactor piping weldment, which will be referred to as the C-pipe in the remainder of the report.

Prior to completion of the ORNL high load cycling of the C-pipe, Battelle Columbus Laboratory completed analytic studies simulating both a modeling of crack growth and realistic dynamic fracture assessment of a typical New Production Reactor (Heavy Water) primary pipe system. Provided in this report are specific comparisons between the Battelle analysis results and ORNL C-pipe test data which confirm the analytic techniques. These studies have confirmed that the analytic techniques used can predict observed experimental behavior with an acceptable degree of accuracy. The analytic results are discussed in the report and specific sections of the Battelle report are provided in Appendix C.

LIST OF FIGURES

Figure — Page

1. Life prediction analysis for NPR-HWR plant piping and test design for confirmatory impact testing 11

2. Leakage rate versus pipe load for small cracks 13

3. Sketches of the opening crack were made at zero load at completion of various cycles 14

4. Pipe load versus pipe centerline displacement for "C"-Pipe 100 kip loadings 15

5. Pipe load versus crack opening displacement for "C"-Pipe 100 kip loadings 15

6. Battelle calculated load-displacement curve for cracked pipes loaded under four-point bending. The initial crack lengths assumed are indicated 16

7. Battelle calculated load-displacement curve for cracked pipes loaded under four-point bending. The initial crack lengths assumed are indicated. The ORNL "C"-Pipe data are shown for various load cycles 17

8. Battelle calculated power-law fit for crack growth resistance for the base metal, heat affected zone, and weld metal. The data points shown on the graph are estimated J values developed by ORNL using "C"-Pipe test data 19

9. The ORNL test fixture is shown here with the hydraulic ram in position to load the pipe in four-point bending 20

10. The "C"-Pipe is shown here after 40 cycles of bending at +/- 400 ft-kips moment. The original 2-in. crack has grown to 16.5-in. in length 21

11. The top portion of the 16.5-in. crack is shown in this picture. The crack has twisted to the west (left side) and is tearing along the weld fusion-line 22

12. The bottom portion of the 16.5-in. crack is shown in this picture. The crack has twisted to the east (right side) and is tearing along the weld fusion-line 23

13. Preliminary NPR-HWR Coolant Piping 24

14. Design and Analysis Spectra used in the piping analysis 25

15. SSE Spectrum Compatible Time History used in the Piping Analysis 26

16. Fracture surface on East Side of C-Pipe 29

LIST OF FIGURES (cont'd)

Figure Page

17. Fatigue crack growth through the SS304 pipe wall during fully reversed bending cycles at a bending moment of +/- 110 ft-kips 32

18. Fatigue crack growth data for 304 stainless steel in PWR water at 25°C, f = 1 Hz 33

LIST OF TABLES

Table Page

1. Test Histogram for C-Pipe 9-11
2. P-scan indication locations in weld 3C-PW15-16"W15 31
3. C-Pipe Fatigue Crack Data 31

1. EXECUTIVE SUMMARY

This report provides information about and results from specific tests completed at Oak Ridge National Laboratory (ORNL) in support of the Department of Energy's (DOE's) New Production Reactor-Heavy Water Reactor (NPR-HWR) program. The report also provides detailed analytical studies completed by Battelle Columbus Laboratory and Argonne National Laboratory. All of this information is presented in a demonstration that the primary piping of the NPR-HWR, with its relatively moderate temperature and pressure should not suffer an instantaneous double-ended-guillotine-break (DEGB) under design basis loadings and conditions.

The first ORNL test series obtained pipe crack extension data representative of large dynamic loads applied to a flawed stainless steel 316L pipe weldment. The results of that testing was reviewed by a special Piping Integrity Review Group (PIRG) established by DOE. Members of this group are identified in Appendix A.

The PIRG review comments were such as to necessitate a second series of tests. This report provides results of that second series of pipe tests. An aged section of 304 stainless steel pipe was obtained from the C-reactor at Savannah River and it was subjected to large fully reversed cyclic bending loads. An initial flaw size was based on leakage flow testing at prototypic NPR-HWR pressure and temperature. The detectable leakage flaw was cycled in bending at large loads for 40 cycles.

The members of PIRG assessed these results together with analytic work by Battelle and stated that provided the caveats cited in the Applicability of Results section of Appendix B are in force, then the following conclusion is applicable:

- For DOE low pressure, ($\leq$ 1.72 MPa) low temperature (100° C) reactors with austenitic stainless steel piping, the DEGB should not be a design basis condition.

2. INTRODUCTION

The United States Department of Energy (DOE) initiated the design of a new generation of production reactors to replace the aging production reactors at the Savannah River Site (SRS) in Aiken, South Carolina. A heavy water reactor was one of the options considered during the Title I design phase. This program was continued through the design phase; however, a decision was made not to construct a new production reactor.

The increase in understanding and the vast experience gained from existing production reactors and commercial nuclear power plants led to proposed improvements in several areas of the proposed NPR-HWR design. One such area of improvement was to confirm that for the tough austenitic piping of the NPR-HWR at the moderate temperatures and pressures expected, an instantaneous DEGB was highly improbable.

The Pipe Impact Test Facility (PITF) at ORNL was designed to load pipes in four-point

bending. The maximum bending stress is located at the center of the pipe. This loading condition provides a uniform constant bending stress across the three foot (914.4 mm) long center section of the pipe. The flaw being studied is located in a weld in the exact center of the constant bending section of the pipe. Static slow oscillatory cyclic (SOC) and dynamic loadings have been used to produce bending in the pipe. These bending loads tend to open the flaw in the pipe. Therefore, the PITF can be used to show crack stability in tough austenitic piping when being loaded at safe-shutdown earthquake (SSE) load levels and above.

3. BACKGROUND

The PITF at ORNL was designed to test a 16 in. (406 mm) diameter schedule 40 stainless steel pipe. The pipe is approximately 20 ft (6.1 m) long and has a circumferential weld at the center. For the first test series, the center weld was completed using a tungsten inert gas (TIG) weld joint design that provided a lack of penetration 360 degrees around the pipe and 0.17 in. (4.45 mm) deep at the inside surface. This represented a worst case 60-year flaw at the pipe inside diameter. At the center of the pipe weld, a 0.03 in. (0.76 mm) wide by 1 in. (25.4 mm) long slot was machined by metal disintegration from the outside pipe surface totally through the 0.5 in. (12.7 mm) thick pipe wall. This design represented the estimated worst case complex crack that could exist after 60 years of service.

The test facility design is such that the pipe can be loaded in bending using a hydraulic ram and/or a 3,100 lb (13.79 KN) swing weight. Figure 1 provides the life prediction analysis for NPR-HWR plant piping and test design for confirmatory impact testing. The worst case 60 year flaw was impact tested and shown to be stable at SSE loads. This crack was then extended along the circumferential weld by fatigue using the hydraulic ram. At various crack lengths the flaw was tested by dynamic impact loading using the swing weight. The first test article was subjected to considerable overloadings. The pipe was impacted 104 times at levels equal to and well beyond the one SSE load level. In addition, 569,751 fatigue cycles and 20 purposeful static overloads were applied to extend the flaw completely around the pipe. At no time during the first test series did the crack grow in an unstable manner.

The testing concept and results of the initial first test series on the 316LN stainless steel pipe were discussed in a previous ORNL report [1], and at the American Society of Mechanical Engineers (ASME) 1992 Pressure Vessels and Piping Conference [2]. The results were reviewed by a special Piping Integrity Review Group (PIRG) established by DOE. Members of this review group are identified in Appendix A. The initial meeting of this group was held in August 1992 and the last meeting in December 1992. Based on their review of the first test series, the PIRG was impressed by the pipe flaw stability. However, in order to ensure very low probabilities of failure during an SSE, the PIRG stated that a second test be completed at high load levels. Also, the high load levels should be applied in a slow oscillatory cyclic manner until at least 40 cycles of bending had been obtained. Successful completion of this test (e.g. no unstable crack growth) would provide for a very low probability of pipe failure during an SSE.

In order to bound age effects relative to the pipe material, the second pipe test series was scheduled so that a degraded pipe weldment from the Savannah River C-reactor could be used as the test piece. This testing is discussed in the following sections of this report.

4. DEGRADED PIPING MATERIAL TESTS

This report addresses the recent failure testing of the Savannah River C-reactor piping weldment, referred to as the C-pipe in the remainder of the report. The intent is to further familiarize the technical community with Oak Ridge National Laboratory's (ORNL) pipe test program and activities associated with the C-pipe test (as conducted on behalf of the DOE-NPR Program).

The C-pipe is a 16 in. (406 mm) diameter schedule-40 [0.5 in (13 mm) wall pipe of type-304 stainless steel (SS304) which saw service in the Savannah River Plant (SRP) C-reactor for 27 years (1957-1984). The two foot (610 mm) pipe piece containing the subject butt weld was selected because of its availability, because it could be decontaminated to levels that allow its handling under DOE regulations, and because it appeared from outside-surface in-service inspection (ISI) by ultrasonic methods (UT) to suffer from inside-surface stress corrosion cracking (SCC) in sensitized material near the weld.

The C-pipe weld was taken from the reactor hot leg near the entrance to the loop heat exchanger. This weld was completed in approximately 1957 using a gas metal-arc welding process. After completion of the weld, grinding was performed on the pipe inside surface. This grinding was probably completed in an effort to remove areas with a lack of penetration at the weld root. The final inspection at that time accepted the pipe weld for reactor operation. During later inservice inspection this weld (3C-PW15-16, Weld 15) was identified as having two indications of intergranular stress corrosion cracking (IGSCC).

After decontamination, additional detailed inspections were performed in July 1992. These inspections included dye penetrant examination of the pipe weld inside surface and a full volumetric ultrasonic (UT) examination of the weld. These inspections were completed by Westinghouse Savannah River Company (WSRC) K-reactor ISI team members. The dye penetrant examination showed that a lack-of-penetration (LOP) ran circumferentially in a dashed/broken pattern at the inside center of the weld for much of the pipe's circumference. This LOP was estimated to be approximately 0.030 in. (0.76 mm) deep. The UT examination revealed that one of the IGSCC crack indications was most likely due to the UT equipment sensing grinding marks on the inside surface of the pipe.

The two foot (610 mm) C-pipe piece was selected for testing, because it had seen considerable service in the various production campaigns of the SRP C-reactor, because it was degraded in a natural manner, and because it was judged to provide a weld condition that would represent a very worst case, degradation beyond current acceptable nuclear plant weld practice and acceptance standards. The two foot (610 mm) piece was welded to spool pieces of SS304 at both ends with the original butt weld centered in the test section of the 20-ft (6.1 m) article. The largest LOP signal location was positioned for maximum stress.

The testing of the C-pipe commenced on August 18, 1992, and was completed on November 20, 1992. A large number of individual tests was performed using the C-pipe in order to drive the initial weld flaw through the 0.5 in. (13 mm) pipe wall and around the pipe's circumference to produce separation. The more important tests (listed in chronological order) are the following:

1. Ten original hammer drops (8/18/92),
2. 118,000 cycles of fatigue to break through-wall and create a leak before break (LBB) crack (ending 10/13/92),
3. Reverse loadings to establish the 2*Sy loading for C-pipe (ending 10/13/92),
4. Flow tests of the pipe's LBB crack (ending 10/15/92),
5. 40-cycle failure test of the LBB crack (ending 10/21/92),
6. 188 cycles of fatigue to grow 25 in. crack (11/09/92),
7. 12-cycle failure test of the 25 in. crack (11/09/92),
8. 9 hammer drops to the 30-35 in. crack (11/18/92),
9. 305 fatigue cycles to grow 45 in. crack (11/19/92),
10. 8 hammer drops with the 45 in. crack (11/20/92),
11. Fatigue separation of the remaining 5 in. ligament (11/20/92).

Of the above 11 test items, by far, the most important is the fifth item, a test intended to address most of the important questions raised by reviews, particularly the first PIRG review.

Relationship of C-Pipe Test to the First ORNL Pipe Test. The original SS316L pipe [1] was tested to supply failure-related data for the case of a representative bounding initial flaw in a representative weld under representative loadings anticipated for the New Production Reactor's (NPR's) SSE. For various through-wall crack lengths from 1 to 47 in. (25 to 1,194 mm), dynamic impacts (104 hammer drops representing earthquake cycles) were interspersed with fatigue sequences (16 sequences totaling 561,000 cycles) to extend the one inch (2.5 mm) initiating crack to pipe separation (50 in. or 1,270 mm). Loads were cyclicly applied, with dynamic loadings being statically reversed, normally at the level estimated to be the SSE level in terms of peak opening moment applied to the circumferential crack. (Discussion of load level will be elaborated on in the following paragraphs.) The applied load level was below the crack tearing-instability level for all cases of SS316L pipe testing. For short cracks (< 1/2 the circumference), the duration of loading and the system stored energy were not sufficient to sustain crack growth and the SSE moment produced only small amounts of stable crack extension per cycle of load. In an actual piping system subject to realistic seismic input, crack growth might have occurred. For crack lengths in excess of 25 in. (635 mm), the test loads were limited in magnitude to levels below the estimated SSE peak moment because of inherent limitations in the static loading system composed of the hydraulic ram (because of limitations on stroke capacity) and limitations in the dynamic loading system based on hammer drops from various heights (because impact loads transmitted through the load cell were purposely kept below levels that would destroy the load cell).

As identified by the reactor system designer (EBASCO), the central important purpose of the original SS316L failure test was to determine the minimum time-to-failure of the cracked pipe as such failure would be assumed to occur during the actual SSE event. EBASCO imagined that a small departure from the 10CFR50 Appendix K's instantaneous double-ended guillotine break (DEGB) would be acceptable in NPR-HWR "regulatory space" as the design basis of the HWR ECCS. The small departure would be to define the minimum timing surrounding the design-basis loss-of-coolant accident (DBLOCA) where the LOCA size would be assumed to remain that of double-ended pipe separation of the primary piping [(or a flow area of 400 in.^{2} (0.26 m^2)]. Pipe-test-supplied specific information concerning timing of the break development (in terms of flow area versus time during the SSE) would then be fed into the designer's thermal/hydraulic models to analytically demonstrate that significant voiding in the HWR core would be avoided as the cooling/protection systems would have sufficient time for

activation and successful core cooling. Therefore, the worst case DBLOCA of the primary piping would be mitigated without core damage.

The purpose of the C-pipe test. Simply stated, the purpose of this test was to perform an overwhelmingly convincing test that would demonstrate that a leak-before-break (LBB) crack in the NPR-HWR large primary piping could not lead to tearing instability under seismic loads. Analytical work completed by Battelle (see Appendix C) provided confirmation of the test data and showed large margins to failure. This analytical work as supported by the C-pipe testing was the basis for LBB and for eliminating a DEGB/LBLOCA as the design basis for the NPR emergency core cooling system (ECCS). The phrases "overwhelmingly convincing" and "could not" simply equate to the statement that the test was intended to demonstrate with high confidence that the HWR large primary pipe break is a very low probability event. Additional probability work has been completed by Argonne National Laboratory using the Praise Code. These Praise Code evaluations (see Appendix D) also confirm very low probabilities of failure. Confidence and probability levels would need further quantification that would presumably be determined during the NPR-HWR seismic margin assessment (for example, as per NRC generic letter 88-20) required to be conducted to support the final design.

For the SS316L pipe the center load for the pipe test configuration in the Pipe Impact Test Facility (PITF) used to represent the estimated SSE level was the following:

1XSSE = 27.5 kips(load) [122 kN] or 110 ft-kips(moment) [149 kN·m]
or 14.5 ksi(stress) [100 MPa]

The 1XSSE level was estimated in an attempted-conservative fashion by ORNL. Since the PIRG commented in great depth concerning appropriate load level and appropriate designation of load level, we, in this document, will be less specific concerning the relationship of test load to the actual SSE load. Certainly the subject is one of high importance being reviewed and reconsidered at many levels of the current reactor design and regulatory process and merits additional discussion and associated analysis. For the remainder of the report we will refer to the normal load level of the first test simply as L1.

Simple specimen tests show the 0.2 percent-offset yield for the SS316L base material to be between 36 and 39 ksi (248 and 269 MPa) at room temperature. This is lower than the preliminary value reported earlier which was based on the ball-indentation method. Since the SS316L pipe testing was performed at a maximum temperature of only about 135°F (57°C), it is expected that the actual yield of the pipe material for the SS316L test condition was only slightly below the 36-39 ksi (248 - 269 MPa) range. This means that the applied stress of 14.5 ksi (100 MPa) was about 38-40 percent of the yield stress of the test article base metal.

The SS316L pipe impact load level applied to open the crack was controlled through adjustment of the drop height and calculated from measurements of elastic strain in the pipe. The control and measurement methods were quite reliable for through-wall cracks to about 1/2 the pipe's circumference. For essentially all hammer drops, the stress levels were controlled to be the same as the normal static stress level, or L1.

Here it should be noted that the minimum American Society of Mechanical Engineers (ASME) yield strength of the subject material is of the order of 30-35 ksi (207 - 241 MPa) depending on temperature assumptions. For the remainder of this discussion, however, we will

not refer to the ASME yield stress values, but rather reference the test stress levels to the yield stress of the base metal of the specific test article. Recall that the ASME yield (Sy) is a minimum value provided for conservative design and is used in acceptance criteria when stresses are being calculated using linear-elastic stress analysis assumptions. Also, recall that the allowable level of calculated stress for the SSE evaluation is, for the primary piping, the Level D value of twice the yield strength (2Sy). As pointed out by several of the PIRG members, these statements mean that the L1 load level would be of the order of 20-25 percent of the ASME allowed value (from elastic calculations) for the case of the SS316L test. Further, the L1 level would likewise be only about 20 percent of the ASME allowed value for the SS304 (C-pipe) test.

Confusion over appliled load level versus estimated seismic loads potentially arise when the plastic straining in the test is significant or when other nonlinearities such as crack opening occur. This is the case for the C-pipe test. Here, a few statements, perhaps oversimplifying statements, will be interjected to keep notation and definition straight. High load level earthquakes are expected to yield reactor primary pipes at certain localized regions. The C-pipe was tested at high load levels to address pipe response to loads corresponding to an SSE that has a very low probability of occurence. The only quantities relating to stresses that can be measured during testing of the pipes are the applied loads and the response deflections and certain specimen response strains. At points where strain gages are located, stresses cannot be directly measured for plastic loading levels.

In the case of the C-pipe, the PIRG recommended testing at levels which represent loads required to produce the "real" elastic-plus-plastic strains associated with the 2Sy ASME Level-D. In an attempt to determine a Level D load as per PIRG recommendation, we employed strain measurements from the reference base-metal strain gage on the C-pipe (on the side of the pipe opposite the cracked region). These measurements represent the maximum strain obtained during the crack-closing half of the load cycle. We attempted to find a load level that would produce 0.4 percent plastic-offset strain. At the maximum load that the system could provide and control we were unable to place the C-pipe at such high strain levels because of the rather high apparent yield stress of the C-pipe SS304 material, likely somewhere around 40-45 ksi (276 - 310 MPa).

It should be noted that stress and plastic strain are not uniquely related for a strain-hardening material such as stainless steel due to the nonlinear path-dependent behavior of the material. This explains why there is uncertainty regarding (and sometimes confusion) when defining the Level D stress and/or load since that stress is not uniquely defined by the 0.4 percent "value" of plastic strain. Also, the pipe is a structure that everywhere obeys the material response behavior and structural equilibrium and compatibility requirements; indeed, once yielding occurs stress redistribution in the pipe results and the relationships of applied load to resulting stress and strain are difficult to state in terms such as the elastic simplifications of M/z for bending stress and stress/E for strain.

Larger and more difficult questions arise in relating load used in the test to the load level that might be experienced by the HWR primary piping system for SSE earthquakes of various g-level ground motions. Additional details of analyses conducted at ORNL and Battelle to complement the C-pipe test are discussed later.

To characterize the C-pipe test loads in simple terms, certain values of stress and strain will be given without complete explanation. As with the first pipe, test loads could be increased

only to maximum levels permitted within the limitations of the PITF static hydraulic-ram load and control systems. As it turns out, this maximum level of load was +/- 100 kips (445 kN), and it will be referred to below as L2. The SS304 base material of the C-pipe has a room temperature average yield value quoted by WSRC of 38 ksi (262 MPa) and an average yield at 257°F (125°C) of 29 ksi (200 MPa). As observed during testing, the SS304 base material exhibited a yield stress more like 40-45 ksi (276 - 310 MPa). For the C-pipe test load of 100 kips (445 kN) the following is approximately correct, with strains quoted for the base metal away from the crack and for a test temperature maintained at 135-140°F (57 - 60°C):

L2 = 3.6 X L1 = 100 kips (load) [445 kN] or 400 ft-kips (moment) [542 kN·m]
or 0.3% (peak measured strain),
or about 0.16% (peak measured offset plastic strain),
or about 48 ksi (331 MPa)(estimated peak stress of uncracked pipe),
or a peak stress of 52.5 ksi (362 MPa) if no yielding had occurred.

It is not clear from this test observation exactly what load would have caused 0.4 percent plastic strains for the C-pipe uncracked base metal. Our guess would be a load of about 120-130 kips (534 - 579 kN) which would be somewhere between 4.4 - 4.7 L1.

Testing of the pipe specimen. This second PITF series of tests on the C-pipe was conducted in four major sequences. Table 1, Test Histogram for C-pipe, shows all tests in sequence and major test parameters. The nominal load range (LOAD) in kips, the periodicity (PRD.) in seconds, and the number of test cycles (CYC.) executed are listed when the test was under servo-hydraulic actuator control. When a test was a dynamic test, "HIT" is listed in the LOAD column, and the load reversal (LD.RV.) value in kips, the pre-load (PR.LD.) value in kips, and the drop height (DR.HT.) in inches are given. The C-pipe temperature (TEMP.) in degrees Fahrenheit, the internal pipe pressure (PRES.) in psi, and the full/empty (WET/DRY respectively) status for every test are also listed.

The first test sequence was conducted on August 18, 1992. A compliance test (hwp2t1c1) of four cycles to ±L1 load with a four second periodicity was performed to verify proper operation of the data-acquisition system, the servo-hydraulic control system, and the instrumentation installed on the pipe. Then, a series of 10 hits (hwp2t1h1 through hwp2t1h10) was conducted on the as-received C-pipe. The pre-load was five kips (22.3 kN applied in conjunction with the dynamic load), the drop height was 5.5 in. (139.7 mm), and the load reversal value was L1 (performed after each hit).

The second test sequence started with a set of fatigue cycles (Tests hwp2t2f1, hwp2t2f2, hwp2Tt2f3, and hwp2t2f4) in an attempt to drive the existing fusion line inside crack through-wall. A total of 104,134 fatigue cycles was conducted, but a through-wall, 14 in. (356 mm) long crack in one of the C-pipe spool piece welds [the connection of one end of the 28 in. (.71 m) long spool C-pipe to a nine ft. (2.74 m) long pipe end piece] developed. The weld was repaired, and the pipe was re-instrumented with strain gages. These gages had been removed during ultrasonic crack inspection. Tests hwp2t2f5, hwp2t2c3, and hwp2t2c4 were executed to assess the effects of a facility weld repair and the pipe weld repair. After assuring these modifications did not affect overall structural behavior and localized near-crack behavior, a series of tests (hwp2t2c5 through hwp2tc13) was conducted. This series loaded the pipe in the crack closing direction only. Low-cycle fatigue test hwp2t2f7 drove the inside crack through-wall with only an additional 14,076 cycles for a total of 118,210 cycles.

The third test sequence started with a set of tests (hwp2t3c1 through hwp2t3c18). These tests were an attempt to obtain crack opening, load, and flow data for many conditions. New strain gages at different locations and a crack-opening displacement gage (COD gage) were installed. Tests hwp2t3c19 and hwp2t3c20 were executed to validate the performance of this new instrumentation. The main test sequence of 40 cycles under hydraulic actuator load control to ±L2 (test hwp2t3c21 through hwp2t3c62) was conducted. The periodicity was increased from 16-sec. on cycle one, to 32-sec. on cycle two, to 64-sec. on cycle three. A .5-sec. hold period at the load peaks was added for cycle four (hwp2t3c24). This hold period was increased to one-sec. on cycle five (hwp2t3c25). All modifications to the test parameters were to allow the servo-hydraulic control system to attain the ±L2 load range. The test parameters were constant from cycle 5 to cycle 39 (hwp2t3c60). On cycle 39, a maximum actuator stroke limit in the crack opening direction was exceeded and the nominal -L2 load was not achieved. The first half (hwp2t3c61) of cycle 40 (crack closing) was conducted as in all the previous cycles. Then the actuator was shimmed to attain 1.5 more inches stroke in the crack opening direction, and the last half (hwp2t3c62) of cycle 40 was conducted. The cycle halves were combined post-test and stored as hwp2t3c63. Post-test analysis showed unstable crack growth below the L2 load level during the last half of cycle 40, thus, ending this test sequence.

The purpose of the fourth and final testing sequence was two fold; investigate the behavior of the pipe with a large crack [approximately 25 in. (635 mm) long] during a dynamic event, and to grow the through-wall crack completely around the circumference so fractography of the crack surfaces could be easily performed. A series of load controlled fatigue cycles (hwp2t4f1, hwp2t4f2, and hwp2t4f3) was executed to lengthen and sharpen the crack. Then, a series of dynamic hits was conducted on November 18, 1992. The drop height was increased from 6 in. (152 mm) to 60 in. (1.52 m) as shown in Table 1 for tests hwp2t4h1 through hwp2t4h9. Also, due to actuator stroke limitations, the pre-load of -2 kip (-8.9 kN) was not imposed after Hit five (hwp2t4h5), but lowered to -1.5 kip -(6.7 kN) on Hit six and then to zero thereafter. To hasten crack growth, a series of stroke control fatigue cycles (hwp2t4f4 through hwp2t4f9) of ±3 in. (±76.2 mm) was performed. Next, another series of hits (hwp2t4h10 through hwp2t4h16) was conducted with two more stroke control fatigue sequences interspersed. The last fatigue test drove the crack around the circumference, thus, ending the test.

5. TEST RESULTS

This section provides results from the C-pipe tests to determine the LBB crack sizing and results from the 40-cycle PIRG test.

Crack Sizing Wet Tests. The initial through-wall fatigue crack in the C-pipe was 1.7 in. (43 mm) long. This initial fatigue crack was very tight allowing measurements of near minimum anticipated leakage flows for the NPR-HWR reactor large primary piping conditions. The leakage flow rate as a function of pipe stress is provided on plot a of Fig. 2. Data taken during these tests represent a condition of 200 psig (1.4 MPa) pressure and 138°F (59°C) temperature. The nominal NPR-HWR plant primary pipe cold-leg operating stress condition ($\sigma_m + \sigma_b$) is estimated to be approximately 6.8 ksi (47 MPa). The leakage rate measured at this condition was 0.15 gpm (9.5 ml/s). In order to develop larger leak rates at normal operating conditions, the pipe was slowly cycled at higher loads. This slow cycling enlarged the crack length and caused the crack to open wider at the centerline. This higher load

Table-1 , Test Histogram for C-pipe

DATA SET or TEST	DATE mo/dy/yr	LOAD kip.	PRD. sec.	CYC.	WET/ /DRY	TEMP. deg. F	PRES. psi.	LD.RV. kip	PR.LD. KIP	DP.HT. inches
hwp2t1c1	8/18/92	"-/+ 27.5"	4	4	DRY	75	0	N/A	N/A	N/A
hwp2t1h1	8/18/92	HIT	N/A	N/A	WET	135	125	27.5	-5	5.5
hwp2t1h2	8/18/92	HIT	N/A	N/A	WET	135	125	27.5	-5	5.5
hwp2t1h3	8/18/92	HIT	N/A	N/A	WET	135	125	27.5	-5	5.5
hwp2t1h4	8/18/92	HIT	N/A	N/A	WET	135	125	27.5	-5	5.5
hwp2t1h5	8/18/92	HIT	N/A	N/A	WET	135	125	27.5	-5	5.5
hwp2t1h6	8/18/92	HIT	N/A	N/A	WET	135	125	27.5	-5	5.5
hwp2t1h7	8/18/92	HIT	N/A	N/A	WET	135	125	27.5	-5	5.5
hwp2t1h8	8/18/92	HIT	N/A	N/A	WET	135	125	27.5	-5	5.5
hwp2t1h9	8/18/92	HIT	N/A	N/A	WET	135	125	27.5	-5	5.5
hwp2t1h10	8/18/92	HIT	N/A	N/A	WET	135	125	27.5	-5	5.5
hwp2t2f1	8/18/92	"-/+ 27.5"	4	20,000	DRY	75	0	N/A	N/A	N/A
hwp2t2c1	8/19/92	"-/+ 27.5"	4	4	DRY	76	0	N/A	N/A	N/A
hwp2t2c2	8/19/92	"-/+ 27.5"	4	4	DRY	77	0	N/A	N/A	N/A
hwp2t2f2	8/20/92	"-/+ 27.5"	4	20,000	DRY	75	0	N/A	N/A	N/A
hwp2t2f3	8/21/92	"-/+ 27.5"	4	64,134	DRY	66	0	N/A	N/A	N/A
hwp2t2f4	8/24/92	"-/+ 27.5"	4	4	WET	73	0	N/A	N/A	N/A
hwp2t2f5	9/4/92	"-/+ 27.5"	4	4	WET	76	0	N/A	N/A	N/A
hwp2t2c3	10/12/92	"-10/10"	4	4	DRY	75	0	N/A	N/A	N/A
hwp2t2c4	10/12/92	"-/+ 27.5"	4	4	DRY	75	0	N/A	N/A	N/A
hwp2t2c5	10/12/92	"0/-55"	8	2	DRY	75	0	N/A	N/A	N/A
hwp2t2c6	10/12/92	"0/-75"	8	1	DRY	75	0	N/A	N/A	N/A
hwp2t2c7	10/12/92	"0/-85"	8	1	DRY	75	0	N/A	N/A	N/A
hwp2t2c8	10/13/92	"0/-90"	8	1	DRY	72	0	N/A	N/A	N/A
hwp2t2c9	10/13/92	"0/-95"	8	1	DRY	72	0	N/A	N/A	N/A
hwp2t2c10	10/13/92	"0/-96"	8	1	DRY	72	0	N/A	N/A	N/A
hwp2t2c11	10/13/92	"0/-97"	8	1	DRY	73	0	N/A	N/A	N/A
hwp2t2c12	10/13/92	"0/-100"	8	1	DRY	73	0	N/A	N/A	N/A
hwp2t2c13	10/13/92	"-/+ 27.5"	8	4	DRY	75	0	N/A	N/A	N/A
hwp2t2f6	10/13/92	"-/+ 27.5"	4	6	DRY	75	0	N/A	N/A	N/A
hwp2t2f7	10/13/92	"-/+ 27.5"	4	14,076	DRY	75	0	N/A	N/A	N/A
hwp2t3c1	10/14/92	0	N/A	N/A	WET	75	241	N/A	N/A	N/A
hwp2t3c2	10/14/92	"-5/5"	6	4	WET	75	221	N/A	N/A	N/A
hwp2t3c3	10/14/92	"-10/10"	N/A	N/A	WET	75	192	N/A	N/A	N/A
hwp2t3c4	10/14/92	"-/+ 27.5"	N/A	N/A	WET	75	206	N/A	N/A	N/A
hwp2t3c5	10/14/92	"-15/15"	6	4	WET	75	212	N/A	N/A	N/A
hwp2t3c6	10/14/92	"-/+ 27.5"	6	4	WET	75	206	N/A	N/A	N/A
hwp2t3c7	10/15/92	"-55/55"	6	4	WET	75	200	N/A	N/A	N/A
hwp2t3c8	10/15/92	"-55/55"	8	4	WET	75	200	N/A	N/A	N/A
hwp2t3c9	10/15/92	"-70/70"	8	4	WET	75	200	N/A	N/A	N/A
hwp2t3c10	10/15/92	"-70/70"	8	4	WET	75	200	N/A	N/A	N/A
hwp2t3c11	10/15/92	"-10/10"	8	4	WET	75	204	N/A	N/A	N/A
hwp2t3c12	10/15/92	"-70/70"	8	4	WET	75	180	N/A	N/A	N/A
hwp2t3c13	10/15/92	"-70/70"	8	4	WET	75	180	N/A	N/A	N/A
hwp2t3c14	10/15/92	"-10/10"	8	4	WET	75	205	N/A	N/A	N/A
hwp2t3c15	10/15/92	"-10/10"	8	4	WET	75	26	N/A	N/A	N/A
hwp2t3c16	10/15/92	"-15/15"	8	4	WET	75	24	N/A	N/A	N/A
hwp2t3c17	10/15/92	"-10/10"	8	4	WET	75	104	N/A	N/A	N/A
hwp2t3c18	10/15/92	"-15/15"	8	4	WET	75	106	N/A	N/A	N/A
hwp2t3c19	10/19/92	"-/+ 27.5"	8	4	DRY	75	8	N/A	N/A	N/A
hwp2t3c20	10/19/92	"-/+ 27.5"	8	4	DRY	75	8	N/A	N/A	N/A
hwp2t3c21	10/19/92	"100/-100"	16	1	WET	136	0	N/A	N/A	N/A
hwp2t3c22	10/19/92	"100/-100"	32	1	WET	136	0	N/A	N/A	N/A

Table-1 , Test Histogram for C-pipe

DATA SET or TEST	DATE mo/dy/yr	LOAD klp.	PRD. sec.	CYC.	WET/ /DRY	TEMP. deg. F	PRES. psi.	LD.RV. klp	PR.LD. KIP	DP.HT. inches
hwp2t3c23	10/19/92	"100/-100"	64	1	WET	136	0	N/A	N/A	N/A
hwp2t3c24	10/19/92	"100/-100"	66	1	WET	136	0	N/A	N/A	N/A
hwp2t3c25	10/19/92	"100/-100"	66	1	WET	136	0	N/A	N/A	N/A
hwp2t3c26	10/19/92	"100/-100"	66	1	WET	134	0	N/A	N/A	N/A
hwp2t3c27	10/19/92	"100/-100"	66	1	WET	133	0	N/A	N/A	N/A
hwp2t3c28	10/19/92	"100/-100"	66	1	WET	133	0	N/A	N/A	N/A
hwp2t3c29	10/19/92	"100/-100"	66	1	WET	132	0	N/A	N/A	N/A
hwp2t3c30	10/19/92	"100/-100"	66	1	WET	131	0	N/A	N/A	N/A
hwp2t3c31	10/19/92	"100/-100"	66	1	WET	131	0	N/A	N/A	N/A
hwp2t3c32	10/20/92	"100/-100"	66	1	WET	137	0	N/A	N/A	N/A
hwp2t3c33	10/20/92	"100/-100"	66	1	WET	136	0	N/A	N/A	N/A
hwp2t3c34	10/20/92	"100/-100"	66	1	WET	136	0	N/A	N/A	N/A
hwp2t3c35	10/20/92	"100/-100"	66	1	WET	136	0	N/A	N/A	N/A
hwp2t3c36	10/20/92	"100/-100"	66	1	WET	136	0	N/A	N/A	N/A
hwp2t3c37	10/20/92	"100/-100"	66	1	WET	135	0	N/A	N/A	N/A
hwp2t3c38	10/20/92	"100/-100"	66	1	WET	135	0	N/A	N/A	N/A
hwp2t3c39	10/20/92	"100/-100"	66	1	WET	134	0	N/A	N/A	N/A
hwp2t3c40	10/20/92	"100/-100"	66	1	WET	134	0	N/A	N/A	N/A
hwp2t3c41	10/20/92	"100/-100"	66	1	WET	133	0	N/A	N/A	N/A
hwp2t3c42	10/20/92	"100/-100"	66	1	WET	140	0	N/A	N/A	N/A
hwp2t3c43	10/20/92	"100/-100"	66	1	WET	142	0	N/A	N/A	N/A
hwp2t3c44	10/20/92	"100/-100"	66	1	WET	142	0	N/A	N/A	N/A
hwp2t3c45	10/20/92	"100/-100"	66	1	WET	142	0	N/A	N/A	N/A
hwp2t3c46	10/20/92	"100/-100"	66	1	WET	142	0	N/A	N/A	N/A
hwp2t3c47	10/20/92	"100/-100"	66	1	WET	141	0	N/A	N/A	N/A
hwp2t3c48	10/20/92	"100/-100"	66	1	WET	140	0	N/A	N/A	N/A
hwp2t3c49	10/20/92	"100/-100"	66	1	WET	140	0	N/A	N/A	N/A
hwp2t3c50	10/20/92	"100/-100"	66	1	WET	139	0	N/A	N/A	N/A
hwp2t3c51	10/20/92	"100/-100"	66	1	WET	139	0	N/A	N/A	N/A
hwp2t3c52	10/21/92	"100/-100"	66	1	WET	140	0	N/A	N/A	N/A
hwp2t3c53	10/21/92	"100/-100"	66	1	WET	138	0	N/A	N/A	N/A
hwp2t3c54	10/21/92	"100/-100"	66	1	WET	137	0	N/A	N/A	N/A
hwp2t3c55	10/21/92	"100/-100"	66	1	WET	137	0	N/A	N/A	N/A
hwp2t3c56	10/21/92	"100/-100"	66	1	WET	133	0	N/A	N/A	N/A
hwp2t3c57	10/21/92	"100/-100"	66	1	WET	132	0	N/A	N/A	N/A
hwp2t3c58	10/21/92	"100/-100"	66	1	WET	131	0	N/A	N/A	N/A
hwp2t3c59	10/21/92	"100/-100"	66	1	WET	129	0	N/A	N/A	N/A
hwp2t3c60	10/21/92	"100/-100"	66	1	WET	128	0	N/A	N/A	N/A
hwp2t3c61	10/21/92	"0/100"	33	0.5	WET	120	0	N/A	N/A	N/A
hwp2t3c62	10/21/92	0/-100"	33	0.5	WET	120	0	N/A	N/A	N/A
hwp2t3c63	10/28/92		66	1	WET	120	0	N/A	N/A	N/A
hwp2t4f1	11/9/92	"30/-30"	8	172	DRY	72	0	N/A	N/A	N/A
hwp2t4f2	11/9/92	"31/-31"	8	16	DRY	72	0	N/A	N/A	N/A
hwp2t4f3	11/9/92	"31/-31"	8	12	DRY	72	0	N/A	N/A	N/A
hwp2t4h1	11/18/92	HIT	N/A	N/A	WET	72	0	0	-2	6
hwp2t4h2	11/18/92	HIT	N/A	N/A	WET	72	0	0	-2	12
hwp2t4h3	11/18/92	HIT	N/A	N/A	WET	72	0	0	-2	24
hwp2t4h4	11/18/92	HIT	N/A	N/A	WET	72	0	0	-2	30
hwp2t4h5	11/18/92	HIT	N/A	N/A	WET	72	0	0	-2	36
hwp2t4h6	11/18/92	HIT	N/A	N/A	WET	72	0	0	-1.5	42
hwp2t4h7	11/18/92	HIT	N/A	N/A	WET	72	0	0	0	48
hwp2t4h8	11/18/92	HIT	N/A	N/A	WET	72	0	0	0	54
hwp2t4h9	11/18/92	HIT	N/A	N/A	WET	72	0	0	0	60

Table-1 , Test Histogram for C-pipe

DATA SET or TEST	DATE mo/dy/yr	LOAD kip.	PRD. sec.	CYC.	WET/ /DRY	TEMP. deg. F	PRES. psi.	LD.RV. kip	PR.LD. KIP	DP.HT. inches
hwp2t4f4	11/19/92	STROKE	24	40	DRY	72	0	N/A	N/A	N/A
hwp2t4f5	11/19/92	STROKE	24	29	DRY	72	0	N/A	N/A	N/A
hwp2t4f6	11/19/92	STROKE	24	96	DRY	72	0	N/A	N/A	N/A
hwp2t4f7	11/19/92	STROKE	24	4	DRY	72	0	N/A	N/A	N/A
hwp2t4f8	11/19/92	STROKE	24	36	DRY	72	0	N/A	N/A	N/A
hwp2t4f9	11/19/92	STROKE	24	100	DRY	72	0	N/A	N/A	N/A
NO NAME	11/20/92	HIT	N/A	N/A	WET	72	0	NONE	NONE	12
hwp2t4h10	11/20/92	HIT	N/A	N/A	WET	72	0	NONE	NONE	16
hwp2t4h11	11/20/92	HIT	N/A	N/A	WET	72	0	NONE	NONE	20
hwp2t4h12	11/20/92	HIT	N/A	N/A	WET	72	0	NONE	NONE	24
hwp2t4h13	11/20/92	HIT	N/A	N/A	WET	72	0	NONE	NONE	36
hwp2t4h14	11/20/92	HIT	N/A	N/A	WET	72	0	NONE	NONE	36
hwp2t4f10	11/20/92	STROKE	24	20	WET	72	0	N/A	N/A	N/A
hwp2t4h15	11/20/92	HIT	N/A	N/A	WET	72	0	NONE	NONE	36
hwp2t4h16	11/20/92	HIT	N/A	N/A	WET	72	0	NONE	NONE	48
hwp2t4f11	11/20/92	STROKE	12	163	WET	72	0	N/A	N/A	N/A

Results of Life Prediction Analysis Provide Basis for ornl Test Plan

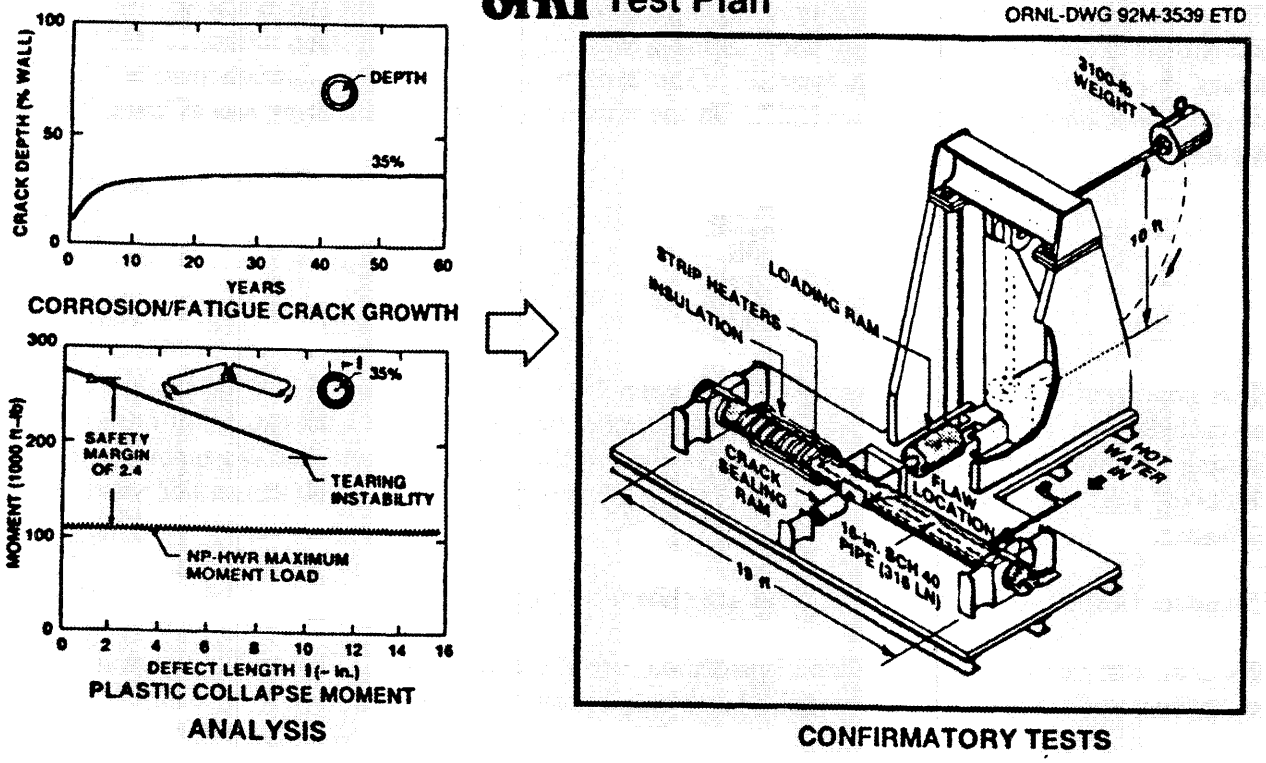

Fig. 1. - Life prediction analysis for NPR-HWR plant piping and test design for confirmatory impact testing.

cycling was completed for six cycles. These higher load cycles would represent plant heat-up and cool-down conditions on a small flaw.

The normal operating load condition was then applied to the pipe, and a leakage rate of approximately two gpm (0.126 l/s) was measured. The crack length was measured to be two-in. (50.8 mm), and this was defined to be the detectable leakage flaw size, or LBB crack.

With the crack length at two inches (50.8 mm) a series of tests was completed to define leakage flow as a function of pipe stress and pressure. These data are provided on plot b of Fig. 2.

Large Load Cycling Test. The referenced two-in. (50.8 mm) crack was then loaded in fully reversed bending cycles at the ram maximum load of 100 kips (445 kN) as previously discussed. This loading provided a bending moment in the pipe center section of 400 ft-kips (542 kN·m) which is a factor of 3.6 times larger than the previous testing completed on the SS316L piping. For this load, three strain gages located 180° away from the crack developed on the average over 0.2 percent strain (with peak strains approaching 0.3%).

After ten cycles of loading, the surface crack length was measured at 3.0 in. (76 mm). The crack length at the end of 20 cycles was established at 3.7 in. (94 mm); and at 30 cycles was 4.8 in. (122 mm). At the end of 30 cycles the top of the crack had twisted over to the west weld fusion line, while the bottom of the crack tip had twisted over to the east weld fusion line (see Fig. 3). From this position, the remaining 10 cycles caused the crack to tear essentially along the weld fusion line. Tearing was essentially evenly incremental at 0.3 in./cycle (7.6 mm/cycle) through cycle 33. The incremental tearing then increased to 0.7 in./cycle (18 mm/cycle) through cycle 37. On the remaining load cycles, tearing was as listed below:

Cycle	Crack Growth
38	1.2 in. (30.5 mm)
39	1.5 in. (38.1 mm)
40	5.0 in. (127.0 mm)

It is important to note that the crack was between 10 and 11 inches (254 - 279 mm) when, in cycle 39, the 100 kip (445 kN) load could no longer be supported. Crack extension rates during the tearing instability were of modest value on the order of two-in./sec (51 mm/sec). Further, it is noted that the frequency of loading programmed into the controller was 1/60 Hz.

Sketches of the crack length dimensions are shown on Fig. 3.

Plots of load versus pipe centerline displacement are shown on Fig. 4. The cyclic variation of load versus crack mouth opening displacement is provided on Fig. 5.

6. DISCUSSION

Prior to completion of the ORNL high load cycling of the C-pipe, Battelle completed sensitivity studies of the effect of crack length on the pipe loading [3]. This was done for the ORNL configuration (circumferentially through-wall cracked pipes under four-point bending)

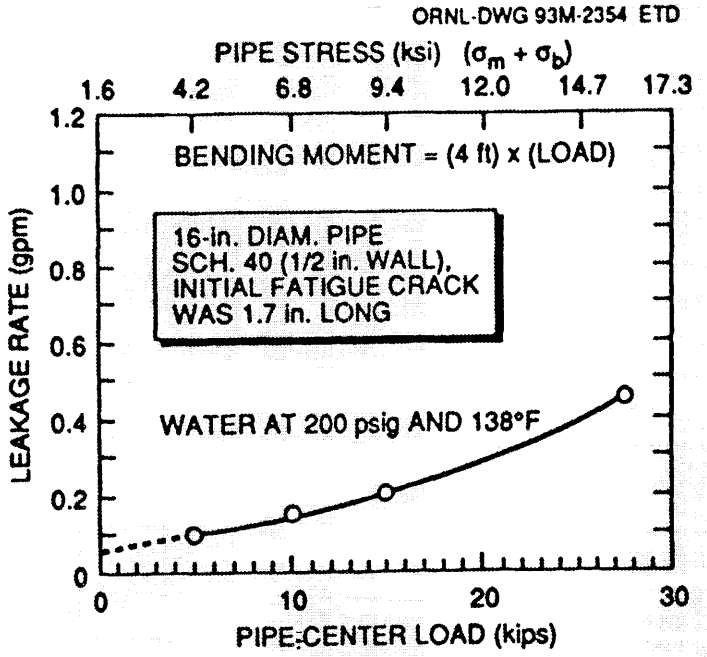

Plot a - Leakage rate for small tight fatigue cracks.

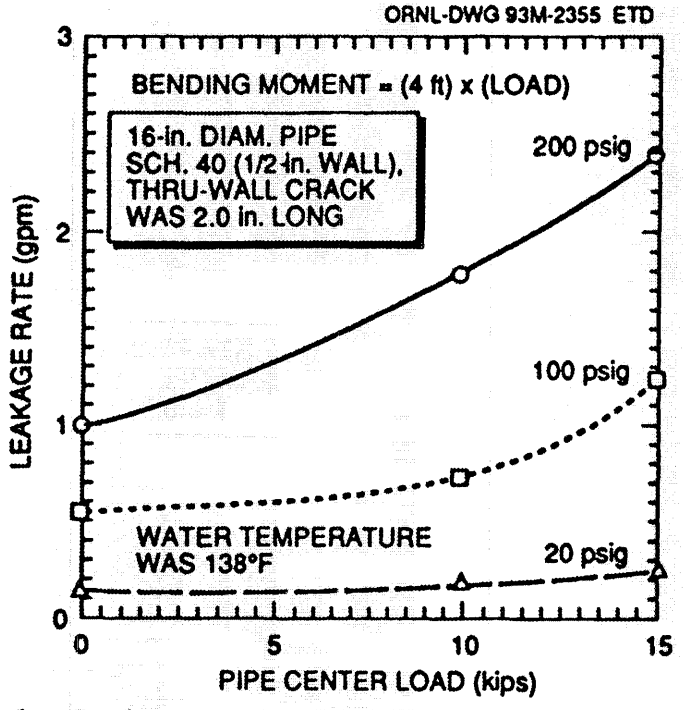

Plot b - Leakage rate for small cracks that have been cycled with a small number of large bending loads to open the crack.

Fig. 2. - Leakage rate versus pipe load for small cracks.

ORNL-DWG 93M-2356 ETD

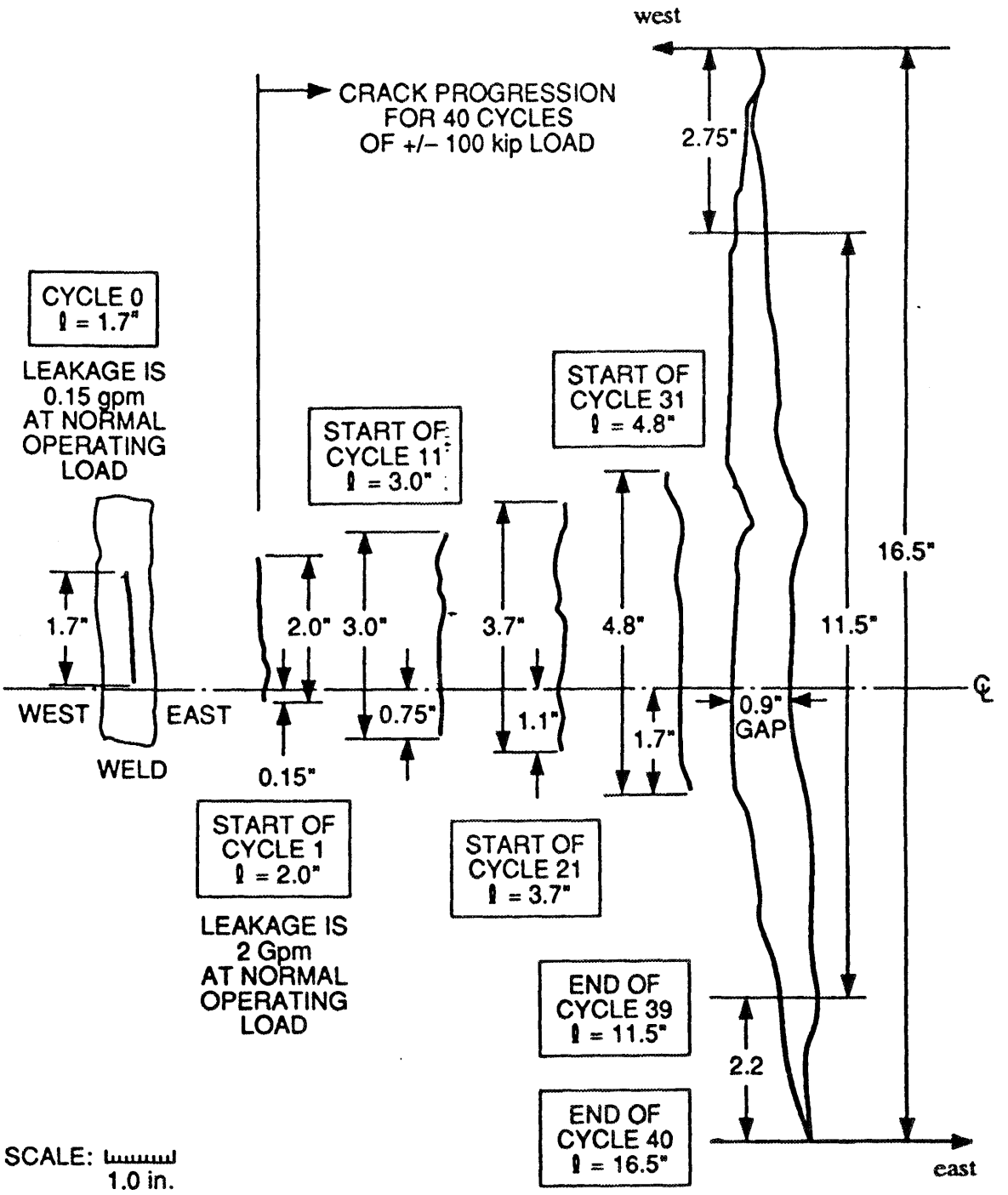

Fig. 3. - Sketches of the opening crack were made at zero load at completion of various cycles.

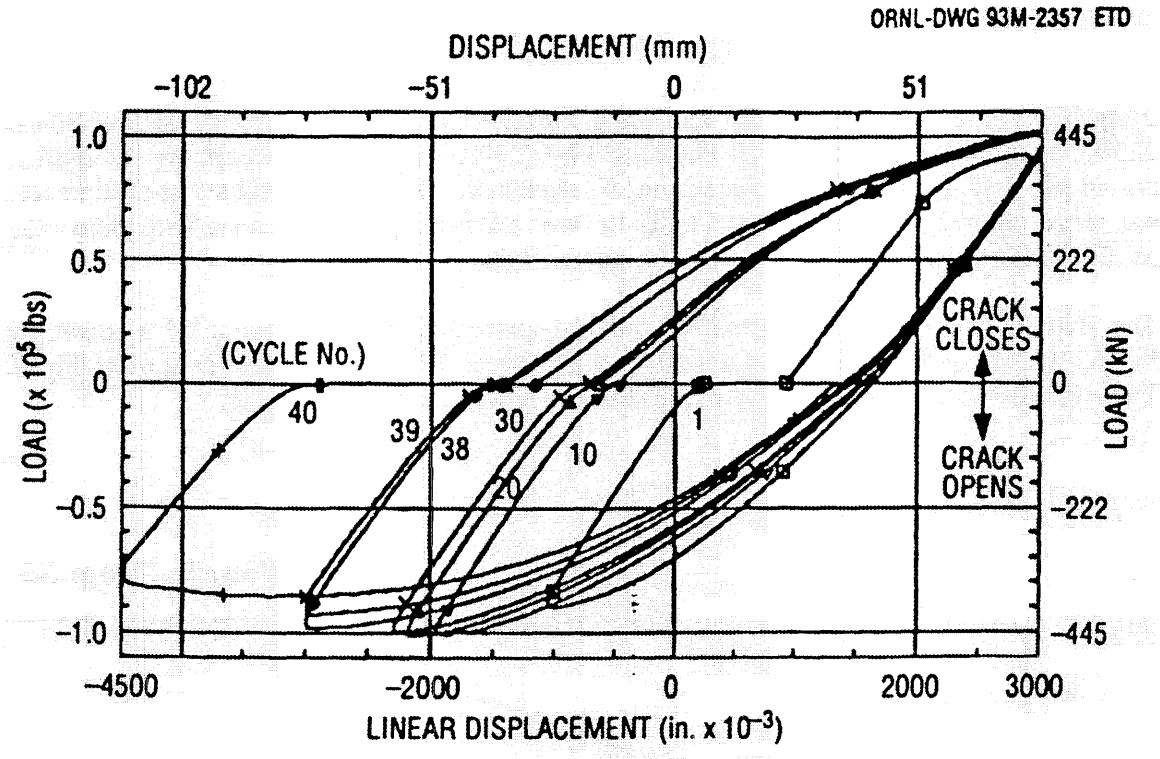

Fig. 4. - Pipe load versus pipe centerline displacement for "C" pipe 100 kip loadings.

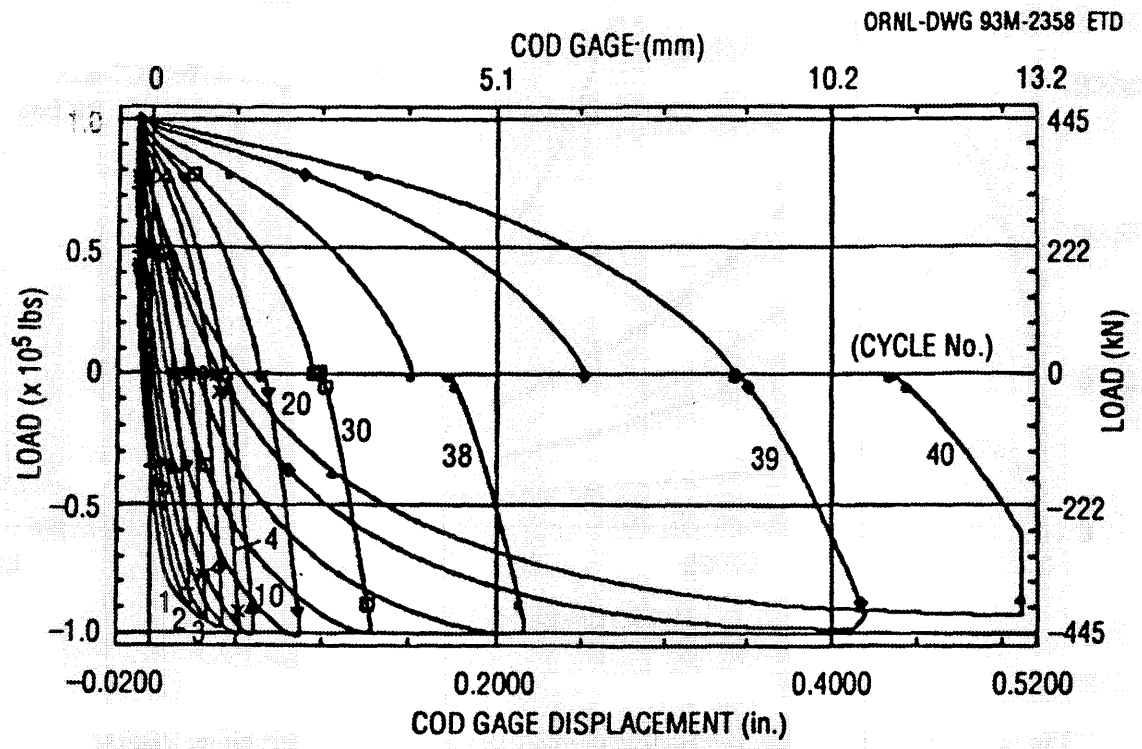

Fig. 5. - Pipe load versus crack opening displacement for "C" pipe 100 kip loadings.

using NRC-Pipe Code version 1.4 and using average material properties of SRP SS304 at 125°C, as provided by WSRC [4]. The LBB.ENG2 J-estimation scheme option was used to obtain predictions of load versus load-line displacement. The base metal stress-strain curve was represented by WSRC and used by Battelle as a Ramberg-Osgood curve with yield = 29 ksi (200 MPa), epsilon-0 = 0.001, N = 5, and α = 2.

The Battelle estimate of load versus load-line displacement for weld metal [3] is shown on Fig. 6. This Battelle estimate is compared to measured ORNL C-pipe test data using Fig. 7. The estimate correlates surprisingly well with the ORNL measured values.

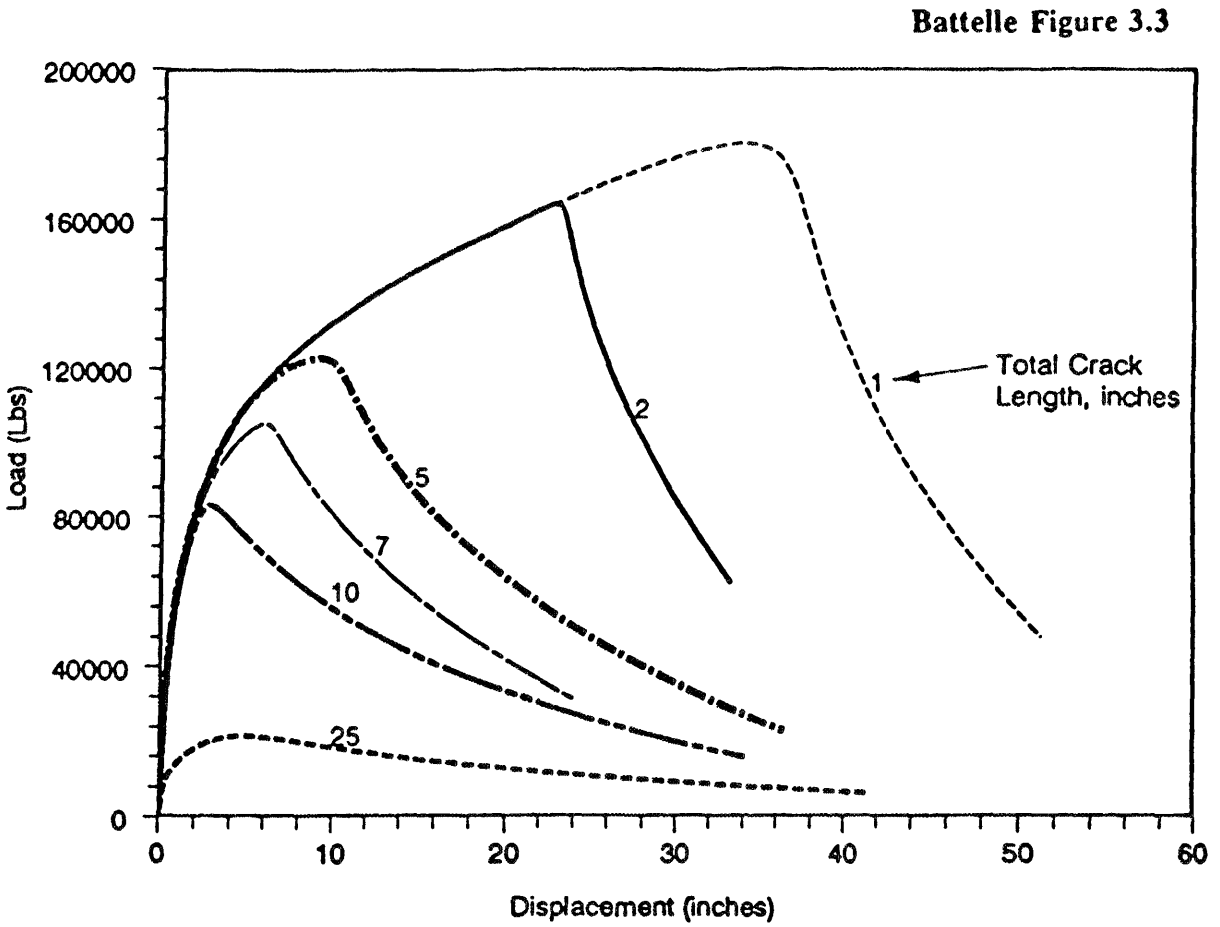

Fig. 6. - Battelle calculated load-displacement curve for cracked pipes loaded under four-point bending. The initial crack lengths assumed are indicated. This load versus load-line displacement prediction was completed using the LBB.ENG2 J-estimation scheme for the ORNL C-pipe experiment assuming the crack is in the TIG weld metal.

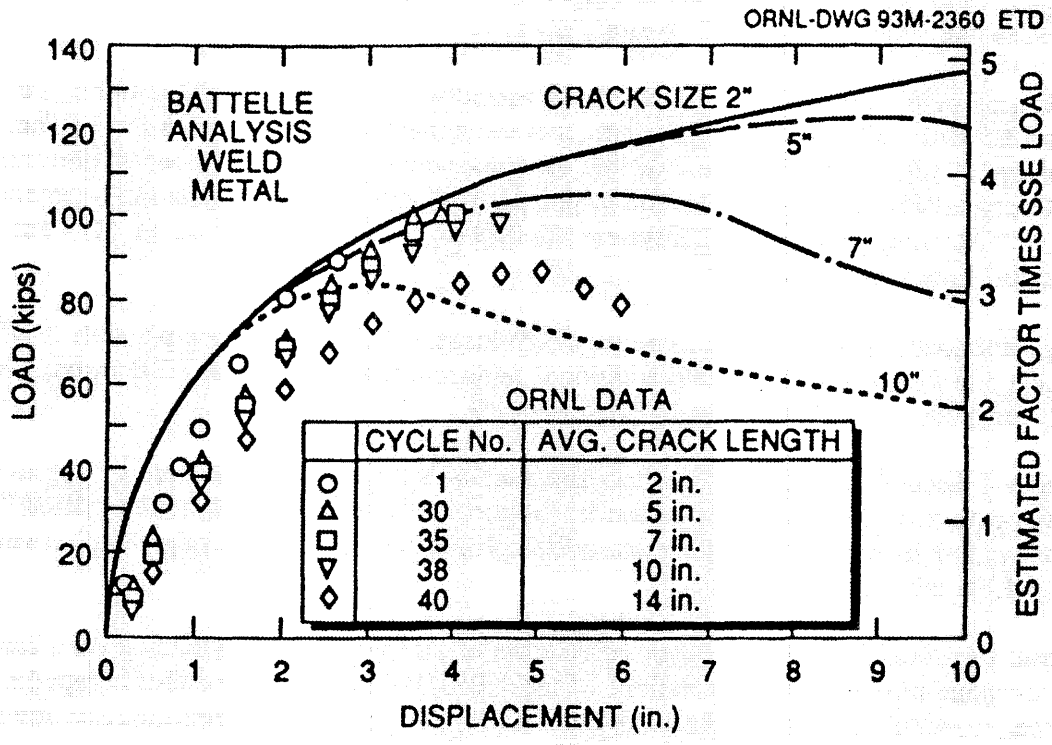

Fig. 7. - Battelle calculated load-displacement curve for cracked pipes loaded under four-point bending. The initial crack lengths assumed are indicated. The ORNL "C" pipe data are shown for various load cycles.

Using the measured load-displacement behavior of the C-pipe, ORNL calculated an estimate of deformation J for the C-pipe. The ORNL estimate of J is compared to the Battelle power-law fit J-estimation [3] on Fig. 8. These methods likewise correlate well.

The hydraulic ram loading fixture used in the C-pipe test is shown in Fig. 9. The C-pipe crack after 40 load cycles to high loads is shown in Figs. 10, 11, and 12. The crack length at the end of 40 cycles of large load was 16.5 in. (419 mm), or the crack grew a total of 14.5 in. (368 mm) during the test. At this crack length the pipe could support a load of approximately 85 kips (378 kN) without additional tearing. That load represents a factor of 3.1 times the previously employed L1 load of 27.5 kips (122 kN).

The C-pipe held the 100 kip (445 kN) load for between 38 and 39 cycles and could still support 85 kips (378 kN) after 40 cycles. It is clear, nevertheless, that if a mechanism for providing 100 kips (445 kN) were available, the pipe would have failed by separation during the 40th cycle. The necessary deflection to provide that separation is believed to be in excess of 30 in. (762 mm), while the PITF system's deflection capacity was but 4.5 in. (114 mm) as set up for the C-pipe failure test.

The C-pipe loads are considered to be very high loads, yet the degraded pipe, with 27 years of reactor service and considerable additional punishment to obtain the LBB through-wall crack, survived for 38-39 cycles at 100 kips (445 kN).

The above discussion of C-pipe test data together with the previous dynamic testing of the SS316L pipe provide a major data base in support of the hypothesis that the NPR-HWR primary piping provides high confidence of low probability of failure during a SSE covering the total life of the plant.

In order to establish a better analytic correlation of actual earthquake loading on a flawed pipe, dynamic pipe fracture calculations of the NPR-HWR system were also completed by Battelle (Appendix C). The analysis model was the cold-leg piping between the reactor vessel and heat exchanger. The approach was to determine an appropriate time history using a supplied floor response spectrum. The analysis was first completed for a pipe with no crack. From this first analysis the area of maximum stress was determined to be at the reactor vessel nozzle to elbow weld (see Fig. 13, node 1).

A second analysis was then completed in which a 10 in. (254 mm) long through wall crack was modeled as a nonlinear moment-rotation spring located at the highest stress location (node 1). The conditions for this analysis were for a 16 in. (406 mm) diameter schedule 40 [0.5-in. (13 mm) wall] reactor coolant pipe of Type 304 stainless steel material. The boundary condition at the reactor vessel was fixed and free lateral translations at the heat exchanger were assumed. The pipe fluid was at a temperature of 230°F (110°C) and pressure of 150 psig (1.03 MPa). The analysis included dead weight loading and seismic load in the Y direction. The analysis assumed 0.5 percent Rayleigh damping. At node 1, the linear elastic analysis had provided a von mises equivalent stress at SSE loading of 19.0 ksi (131 MPa). The design and analysis spectra is shown on Fig. 14 and the SSE spectrum compatible time history is shown on Fig. 15.

In order to show margin on crack stability, the 10 in. (254 mm) long crack model was loaded at 3 times the SSE loading. The analysis shows that portions of the piping will yield; however, the 3 SSE loading does not initiate crack instability. The analysis also shows the leak rate

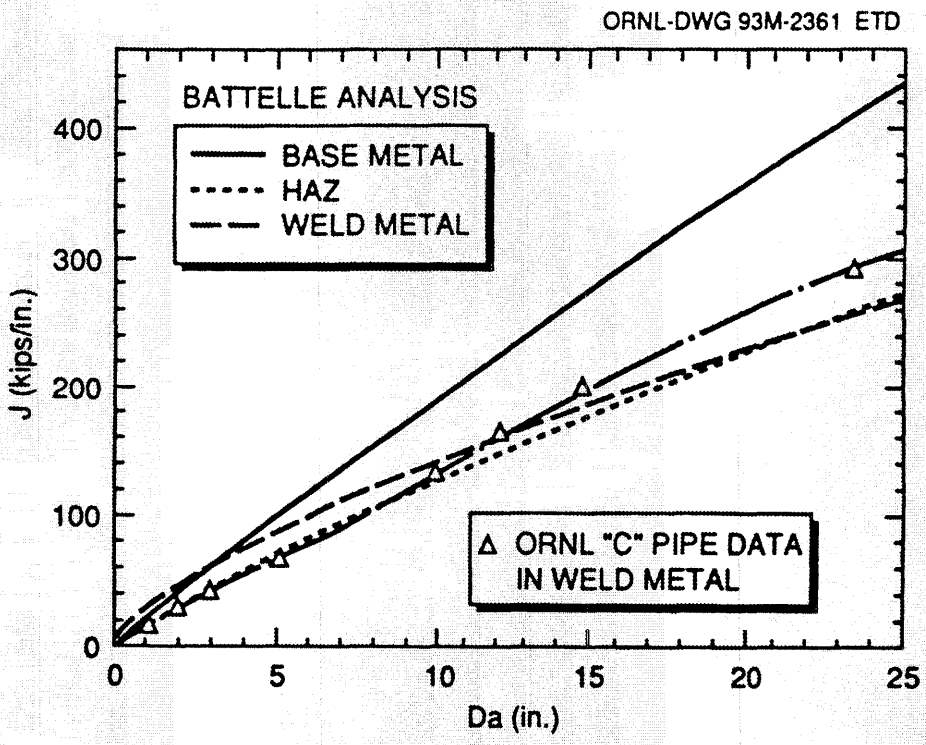

Fig. 8. - Battelle calculated power-law fit for crack growth resistance for the base metal, heat-affected zone, and weld metal. The data points shown on the graph are estimated J values developed by ORNL using "C" pipe test data.

ORNL-PHOTO 8500-91

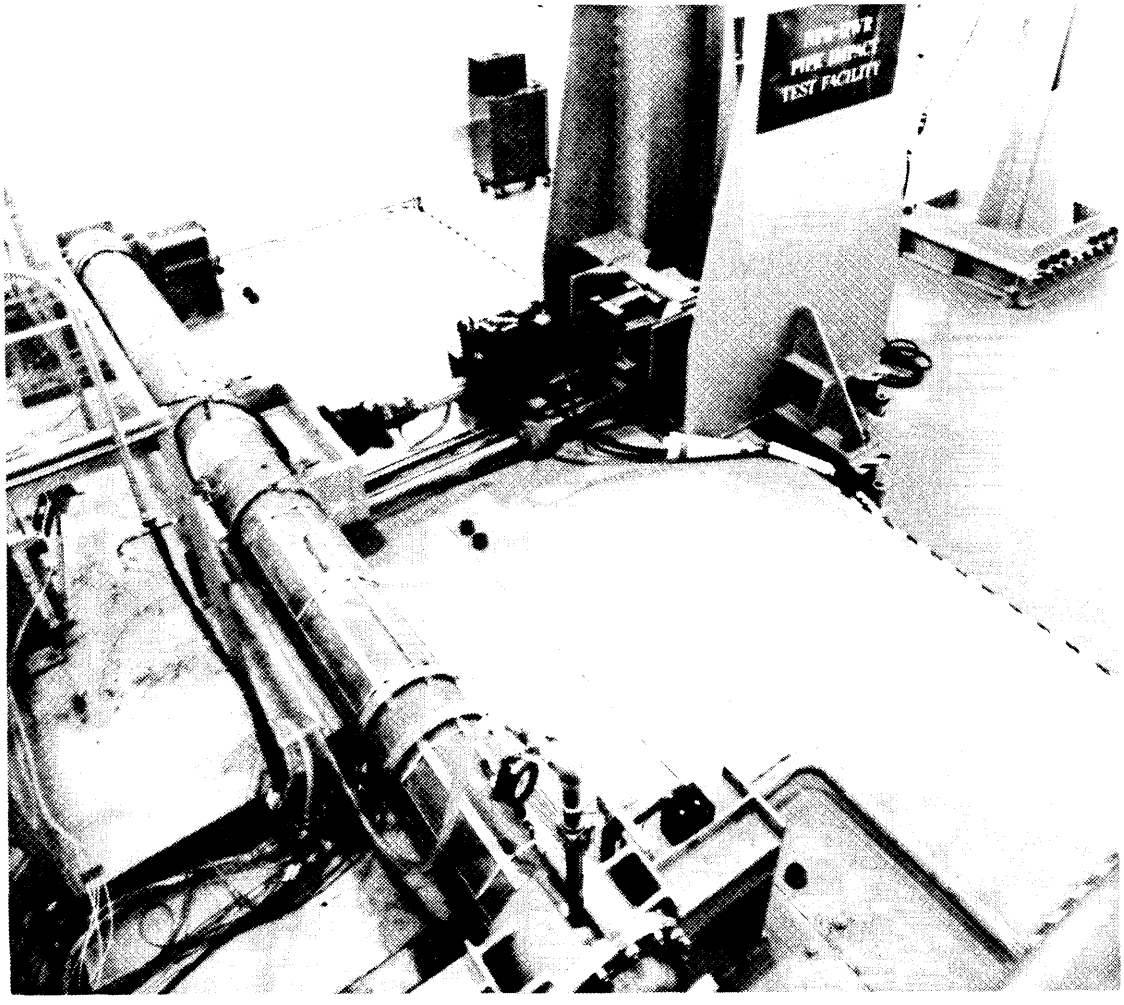

Fig. 9. - The ORNL test fixture is shown here with the hydraulic ram in position to load the pipe in four-point bending.

ORNL-PHOTO 8367-92

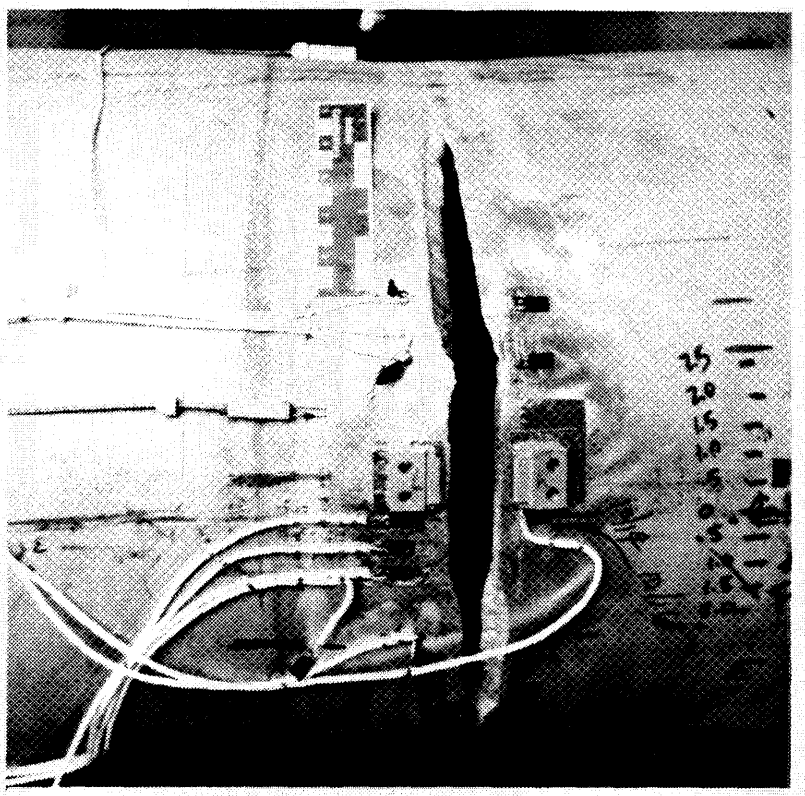

Fig. 10. - The "C" pipe shown here after 40 cycles of bending at +/- 400 ft-kips moment. The original 2 in. crack has grown to 16.5 inches in length.

ORNL-PHOTO 8369-92

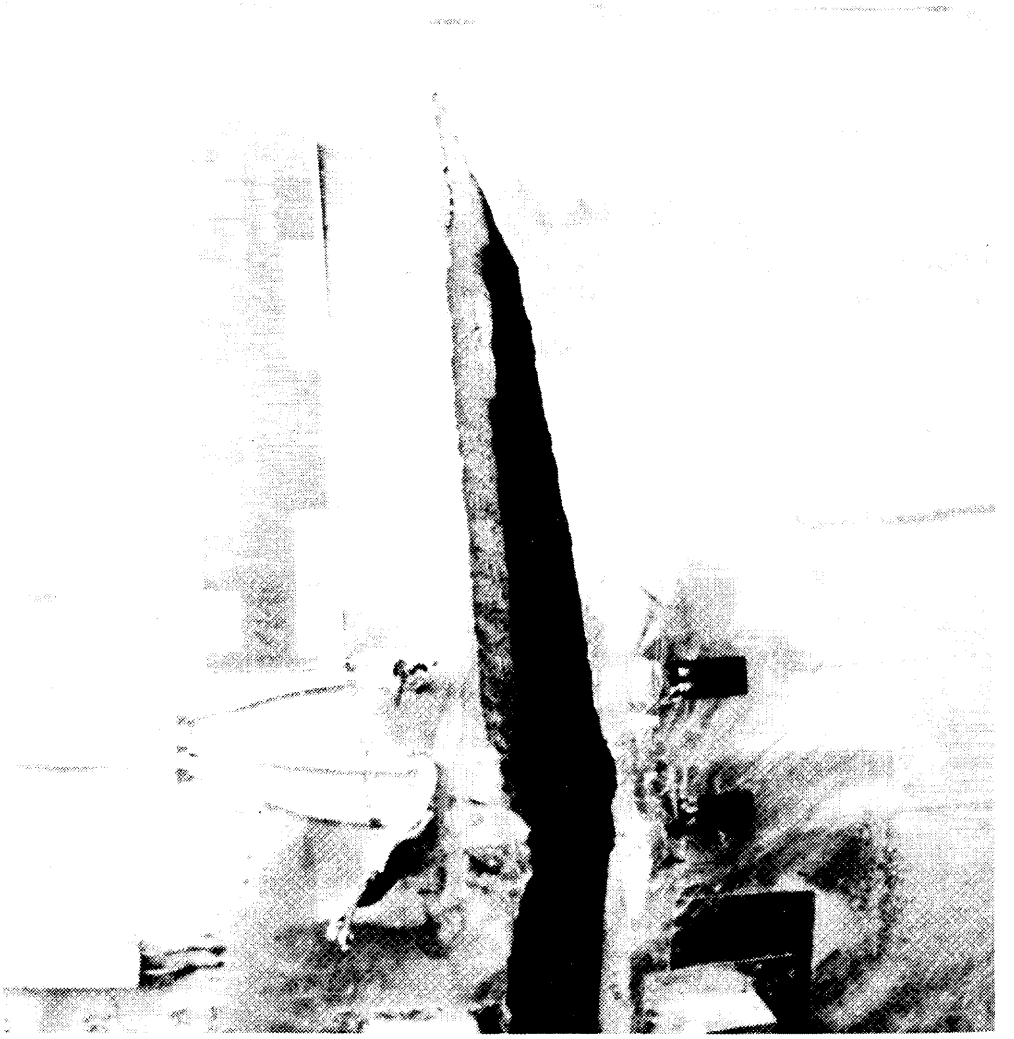

Fig. 11. - The top portion of the 16.5 in. crack is shown in this picture. The crack has twisted to the west (left side) and is tearing along the weld fusion-line.

ORNL-PHOTO 8368-92

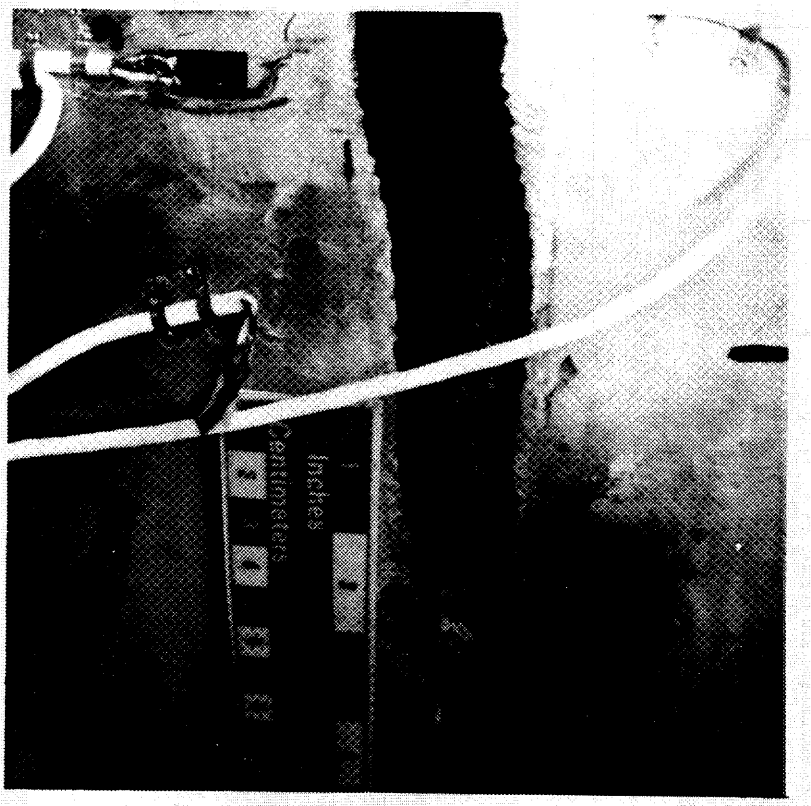

Fig. 12. - The bottom portion of the 16.5 in. crack is shown in this picture. The crack has twisted to the east (right side) and is tearing along the weld fusion-line.

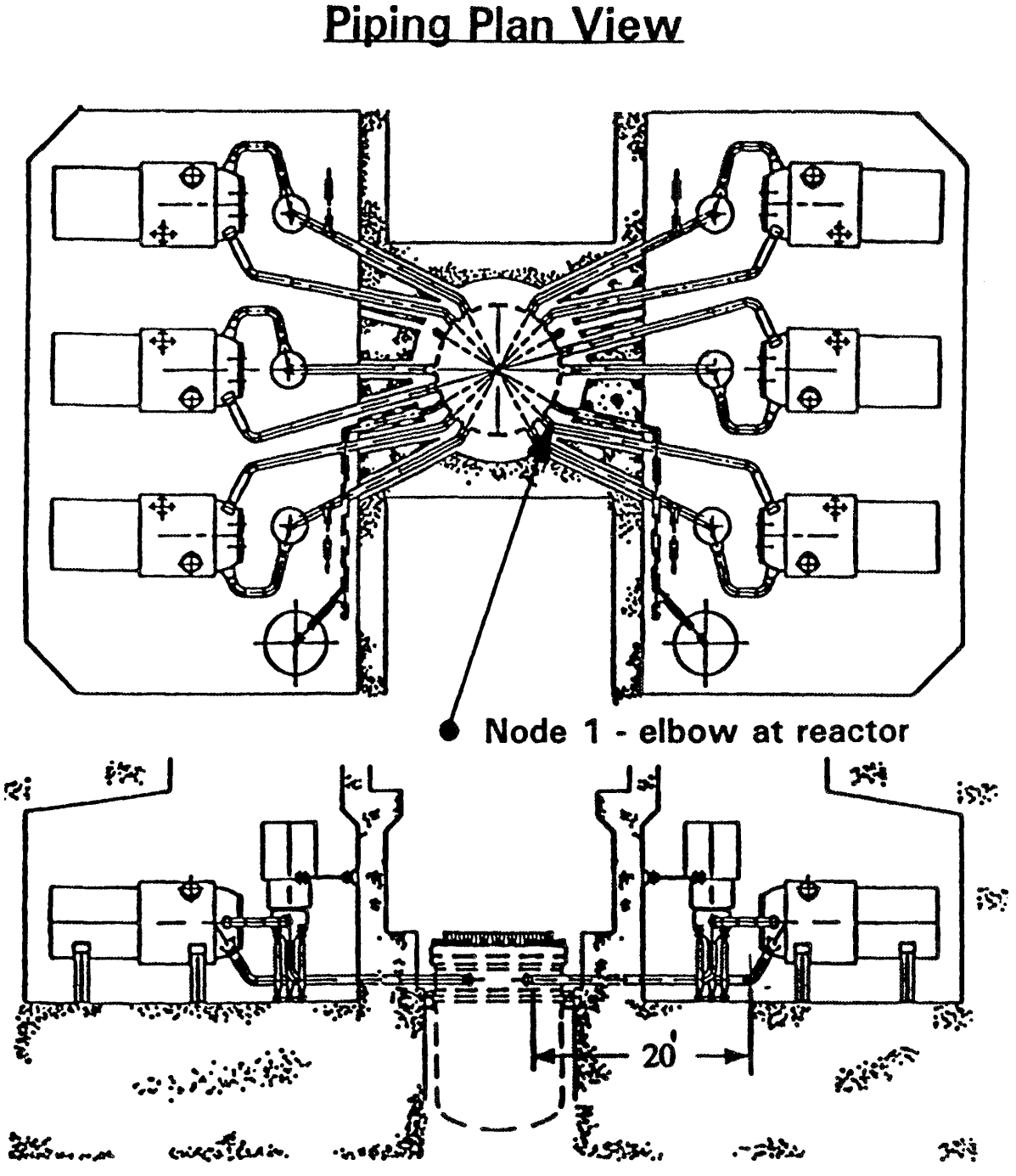

Fig. 13. - Preliminary NPR-HWR Coolant Piping.

Battelle Figure 5.21

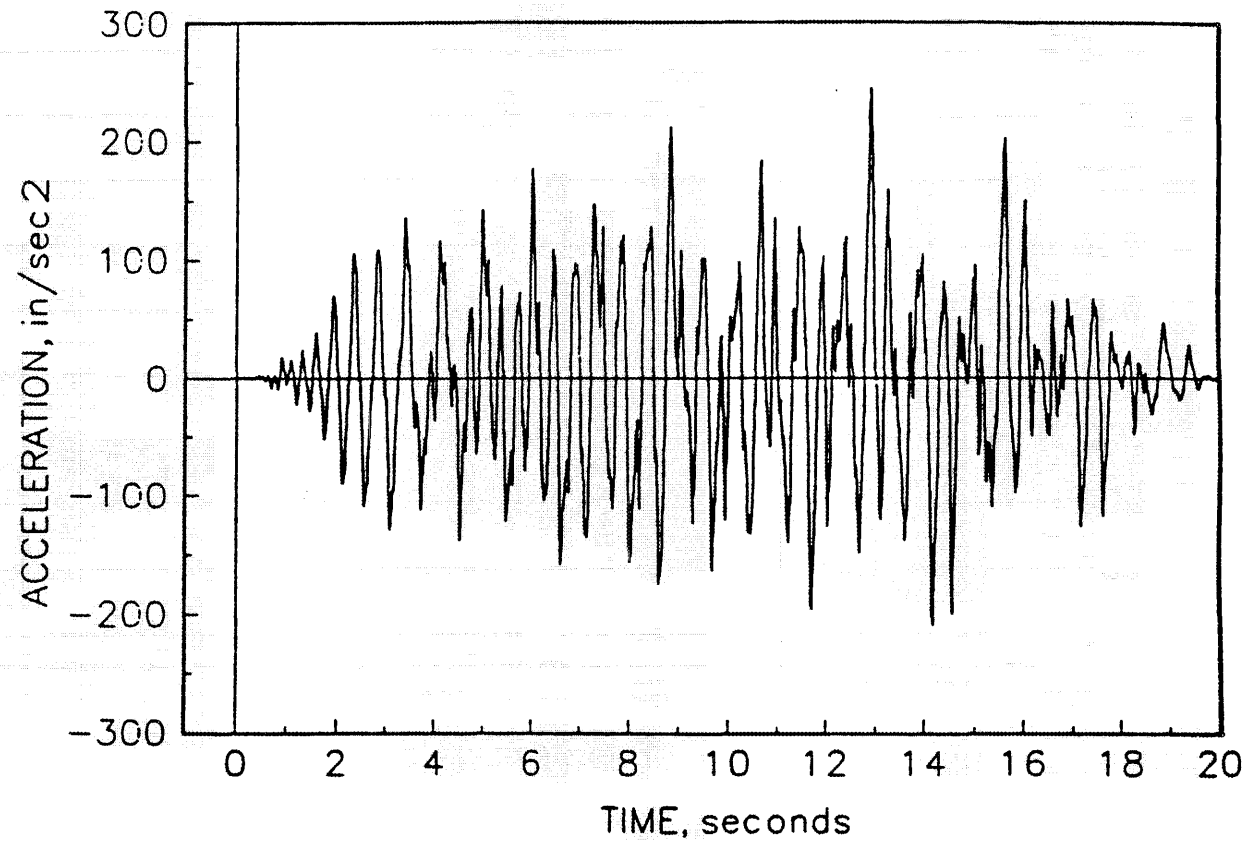

Fig. 15. - SSE Spectrum Compatible Time History used in the Piping Analysis.

Battelle Figure 5.20

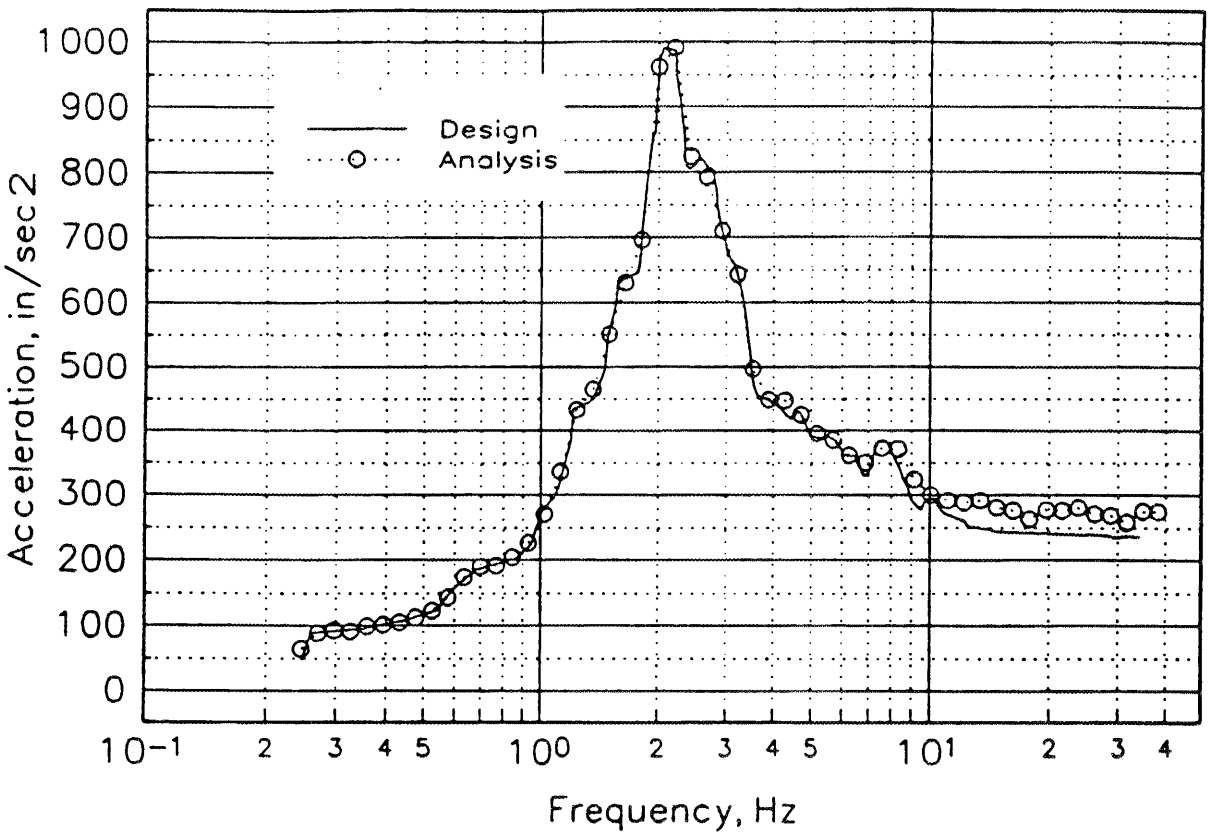

Fig. 14. - Design and Analysis Spectra Used in the Piping Analysis (Horizontal Floor Spectra at vessel for a 0.3 g ground motion SSE).

opening area to be small during the 3 SSE loading.

The final crack geometry considered was a complex crack that is consistent with a piping flaw at the Duane Arnold nuclear plant that was not discovered until it leaked; 40.6 percent of the circumference and 75 percent of the wall thickness deep. Compared to the 10 in. (254 mm) through-wall crack and a 40 percent deep complex crack, this complex-cracked-pipe section is much more severely degraded.

The predicted moment-rotation response at 3 SSE loading for the "Duane Arnold" complex crack showed that the crack reaches maximum moment and then tears stably. Compared to the 40 percent deep complex crack, the 75 percent deep complex crack does not tear significantly more, but it undergoes much more severe crack closure.

It is obvious from these data that the pipe remote from the crack undergoes very large deflections and that significant portions of the pipe would be well above yield. Combining the finite element crack rotations, J-estimation scheme crack length and crack-mouth-opening data, and assuming a diamond-shaped crack-opening area, the leak area as a function of time was established. The leak rate area reaches a maximum of 21 square inches (.013 m^2) during the seismic event with a very small residual crack opening after the seismic event. On the cycle when the crack reaches 21 square inches (.013 m^2), it takes 115 milliseconds to go from basically closed to the maximum opening.

The results from the complex-crack analysis support the contention that a large undetected surface flaw that breaks through and leaks under normal operating loads has enough integrity to sustain a 3 SSE loading. Because plasticity has been ignored, except at the crack, however, the results presented for the complex cracks cannot be relied upon as the sole basis for justifying removal of the instantaneous DEGB as the design basis event because the energy dissipated during yielding would alter the system dynamics. The uncracked pipe plasticity will effectively increase the damping which would reduce the loads on the pipe.

For the case of the 75 percent deep complex crack, the predicted maximum moment was only 27.1 ft·kips (36.7 kN·m). The elastic uncracked moment was a factor of 5.9 times larger than this, and amazingly the crack still survived with only a small amount of tearing. This demonstrates the large margins that may be realized from using nonlinear time-history analysis.

7. POST TEST EXAMINATION

After the C-pipe was separated into two pieces, the fatigue/fracture surface in the weld metal was examined. The through-wall fatigue crack that developed during 118K cycles was shown to have grown from a small lack of penetration area at the weld root. This lack-of-penetration (LOP) area was essentially located in the pipe wall thickness at an orientation which experienced the largest bending stress during the 118K cycles of fatigue. This bending stress essentially put the local pipe wall through thickness in tension. This tension stress caused the LOP to grow a fatigue crack from the inside surface to the outside surface as shown on Fig. 16. This growth pattern is nearly elliptical with a depth to length ratio of approximately 0.2. The initial LOP depth was approximately 0.03 in. (0.762 mm) which represented a wall defect of six percent at the inside surface.

ORNL-DWG 93M-2365 ETD

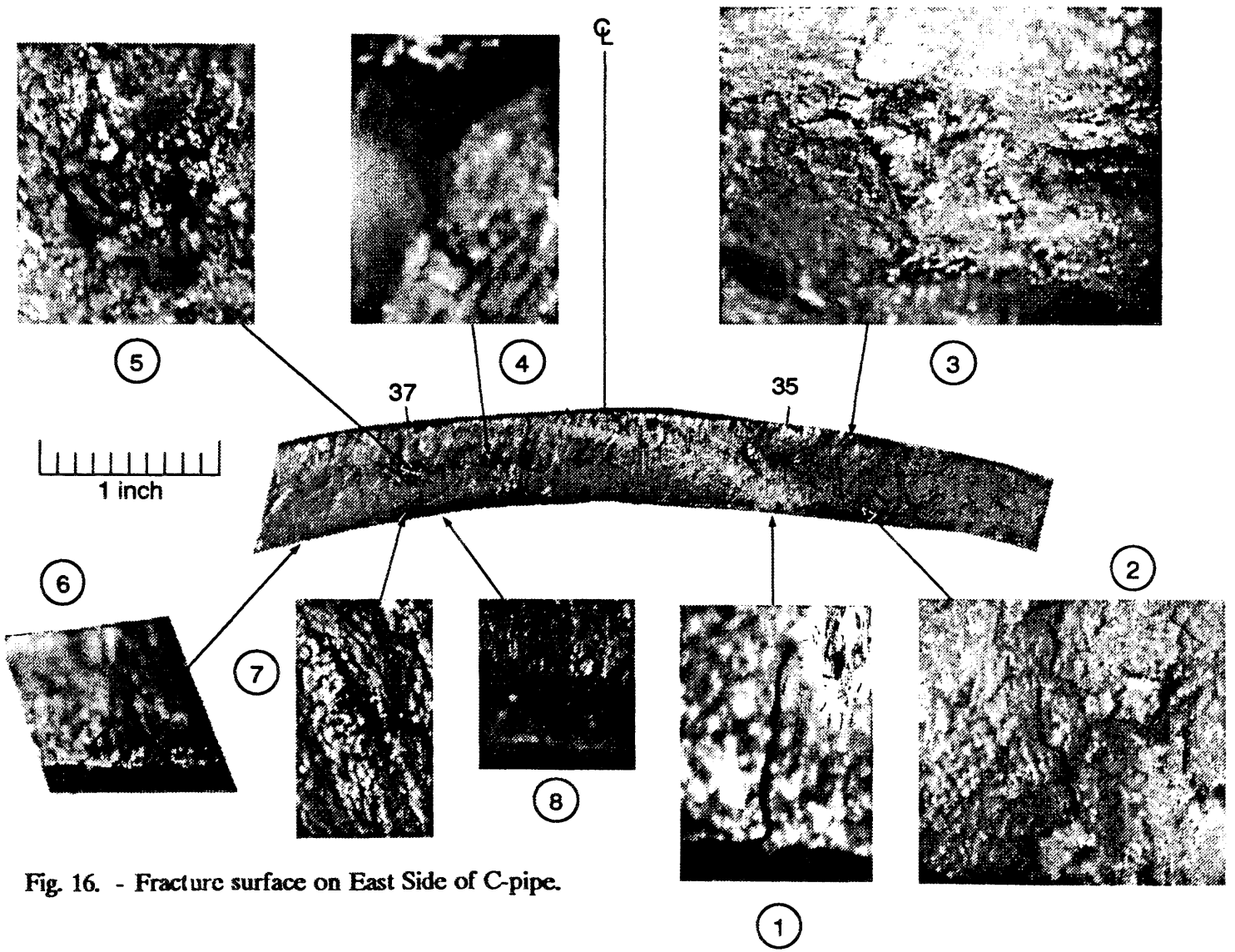

Fig. 16. - Fracture surface on East Side of C-pipe.

During in-plant ultrasonic (UT) inspections prior to C-pipe removal, two detectable indications areas had been identified by UT inspectors. These indications were at locations 19.5 - 20.4 in. and 35.2 - 36.1 in. relative to a permanent marker on the pipe weld. After the C-pipe section was removed and decontaminated, a visual examination could be completed at the same time as UT inspections. The UT indication at 19.5 - 20.4 in. was established to be a reflector from a grinding mark located on the inside surface. The UT indication at 35.2 - 36.1 in. was not associated with any pipe inside surface wall reflector. The initial UT examination in-plant sized the 35.2 - 36.1 in. indication at ten percent through-wall. The inside surface lack of penetration that grew through-wall during fatigue loading was located approximately between 36.2 - 37.0 in. relative to the UT marker location.

Examination of the C-pipe fracture surface provided several indications of IGSCC near the LOP. Fig. 16 provides pictures of the fracture surface and shows numerous locations by numbered enlargements. The number 1 enlargement is at the inside pipe surface approximately 1-1/2 in. below (to the right on the picture) the center of the lack of penetration. On Fig. 16, the side of the picture showing the 37 position is toward the top of the C-pipe as it was placed in the loading fixture. The centerline on Fig. 16 locates the position of maximum bending stress in the pipe during fatigue loading cycles. The depth of IGSCC in the number 1 enlargement is 0.07 in. (1.78 mm) from the inside wall surface. At the deepest part of the crack the IGSCC appears to extend in the longitudinal direction of the pipe toward the heat affected zone (HAZ). In the bottom of the IGSCC crevice brown stain can be seen on the material surface. It should be noted that this IGSCC crack is located at the 35 in. position relative to the UT marker. This puts it near the original in-plant UT call at the 35.2 - 36.1 in. location. The IGSCC depth is 14 percent through-wall relative to the initial UT call of 10 percent through-wall.

Slightly below (in the picture to the right of) the IGSCC indication (enlargement 1) there is seen a large area of brown stain almost completely across the pipe wall. Enlargements 2 and 3 show two sections of this stained area. In both of these enlargements, cracked areas can be seen. Near these cracked areas, patches of darker brown stain appear. This crack pattern and brown stain is indicative of IGSCC. These cracks are oriented radially and longitudinally along the pipe and have not been opened by the fatigue loading.

In the center of the C-pipe weld opposite from the LOP there are several areas that appear to be porosity in the weld. Enlargements 4 and 5 are of areas in the depressions of the porosity. Enlargements 4 and 5 show what appear to be cracking areas that have the dark brown stain located near the crack. Enlargements 6, 7 and 8 show areas near the inside surface LOP that may show indications of cracking.

It should be stated that the C-pipe was decontaminated prior to testing and during this decontamination the inside pipe surface was cleaned as follows:

a. Degrease with a solution of 50 volume percent Momar 800. This solution was heated to 50± 5°C for 5 minutes and stirred.

b. Rinse with room temperature water.

c. Clean in mixture of 3.5 M HN03 and 0.4 M HF at 50± 5°C for 30 minutes and stir.

d. Rinse with room temperature water.

e. Clean with mixture of 100 g/l oxalic acid. This solution was heated to boiling for one hour.

f. Final water rinse at room temperature and air dry.

The LOP areas were exposed to this decontamination process. Some of the cracking could have been enhanced by the decontamination process. However, of approximately seven lack of penetration areas observable around the fracture surface, the only area showing any evidence of IGSCC is that between markers 35 in. and 37 in. This location is near the original area identified in-plant as potential IGSCC indications.

After the C-pipe section had been load cycled to 100K cycles, WSR-NDE personnel traveled to ORNL to re-examine the C-pipe weld. All examinations were performed by WSRS/SSQ NDE examiners using P-scan and manual UT detection equipment. All the SSQ personnel had been qualified through the Electric Power Research Institute (EPRI), NDE center for detection and sizing of IGSCC with both manual and P-scan UT methods.

Manual and automated P-scan UT examinations were performed on C-pipe weld 3C-PW15-16 W15 at ORNL. The manually operated, weld scanner (MWS-2) was used for the P-scan examinations. The entire weld was scanned with 46° shear wave transducer. The area of interest, 34 - 38 in. from the marker location, was also scanned with a WSY70 flaw characterization/sizing transducer. A-scan data from the area of interest was stored from both transducers. The flaw areas were also sized manually using additional approved sizing methods.

The P-scan automated UT examination [5] revealed several high amplitude (> 100% DAC) indications in the weld area and one low amplitude indication in the HAZ. The HAZ indication (#3) had previously been evaluated and attributed to a grinding gouge. After 100K cycles this HAZ indication (#3) was still approximately 0.6 in. (15.2 mm) long, and still of low amplitude and did not appear to be a crack or have much of a through-wall dimension. The other six indications appear to be lack of fusion (LOF) and lack of penetration (LOP), both fabrication/welding imperfections. The 100K cyclic loading apparently had caused some of these indications to propagate. Table 2 provides the location of all the indications.

Indication #5 gave a response 224% DAC (over two times greater than the response from a 10% deep notch in the calibration standard). This indication (#5) was sized to a depth of 72% through-wall depth (TWD) and is located in the vicinity of the indication which was called during the previous examinations. No depth measurements were requested on any of the other locations.

Table 2

P-scan indication locations in weld 3C-PW15-16" W15	
Indication Number	Location from Marker
#1	5.28 - 6.60 in.
#2	7.48 - 9.68 in.
#3	13.20 - 14.08 in.
#4	29.44 - 30.81 in.
#5	34.33 - 37.85 in.
#6	41.37 - 42.28 in.
#7	47.54 - 49.30 in.

A visual examination of the C-pipe fracture surface showed that during pipe tearing a lack of penetration area had been broken into near each of these called indications with the exception of #3 which was in the vicinity of a large grinding mark.

The C-pipe fatigue data can provide three points of measured crack depth as shown in Table 3.

Table 3

C-pipe Fatigue Crack Data	
Crack Depth	Number of Cycles
0.03 in. (0.76 mm)	0 cycles
~ 0.36 in. (9.14 mm) Based upon UT	100K cycles
0.50 in. (12.7 mm) through-wall	118K cycles

Using Fatigue Crack Growth methods an estimation of crack growth though the wall was completed and is shown in Fig. 17. The Battelle EDEAC data for 304 stainless steel shown on Fig. 18 was used in this estimation. Provided on Fig. 18 are areas of fatigue crack growth representative of different pipe stress levels and crack sizes as establihsed by this testing and analysis program.

8. PIRG COMMENTS (Taken Directly from Appendix B)

Foreward. The Piping Integrity Review Group (PIRG) was established to provide a technical review of tests on wrought austenitic stainless steel piping subjected to repetitive loads simulating sixty years of operation of the heavy-water New Production Reactor. This end-of-life condition was followed by severe loads simulating greater than SSE seismic loading. The following is taken from the second and last PIRG report, with discussion limited to one

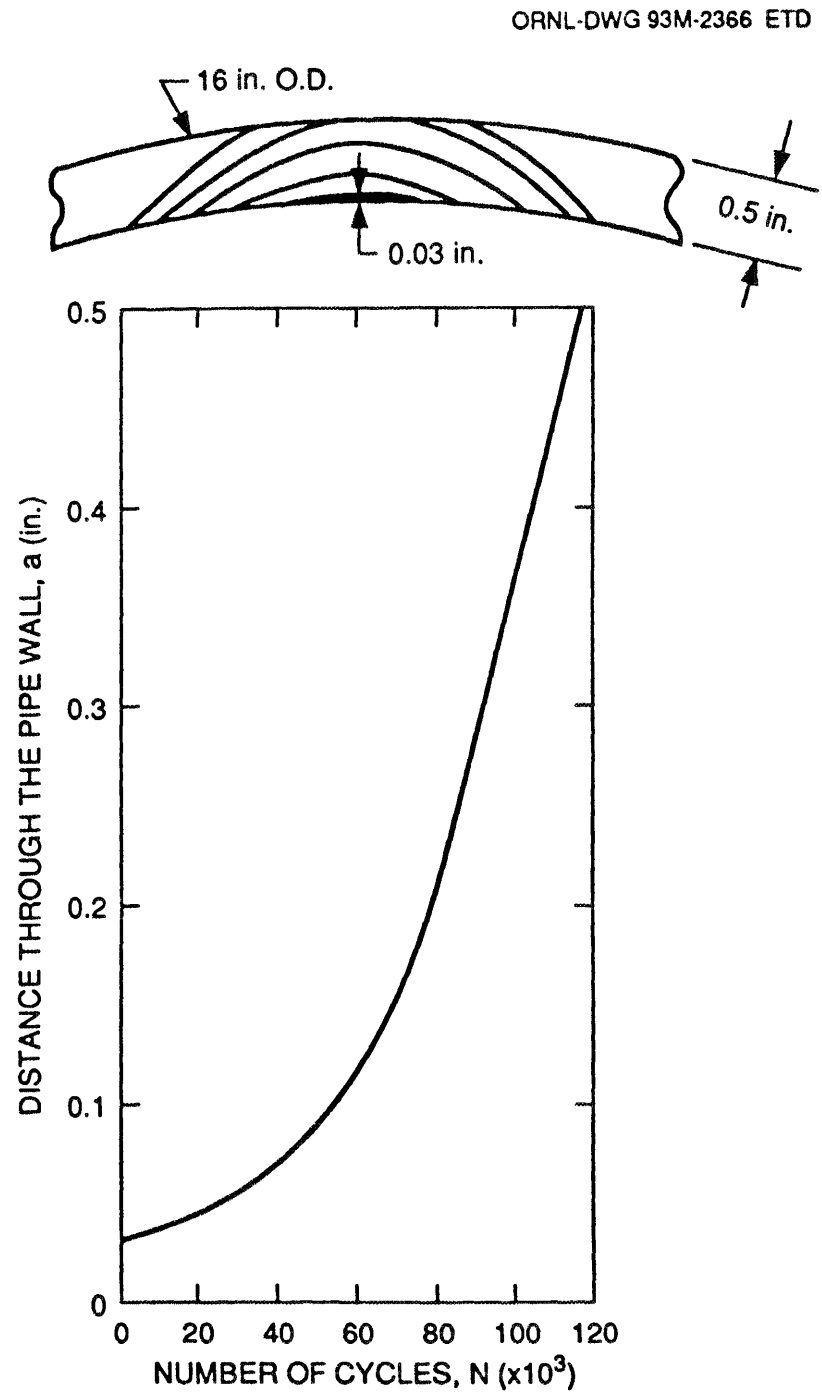

Fig. 17. - Fatigue crack growth through the SS304 pipe wall during fully reversed bending cycles at a bending moment of +/- 110 ft-kips.

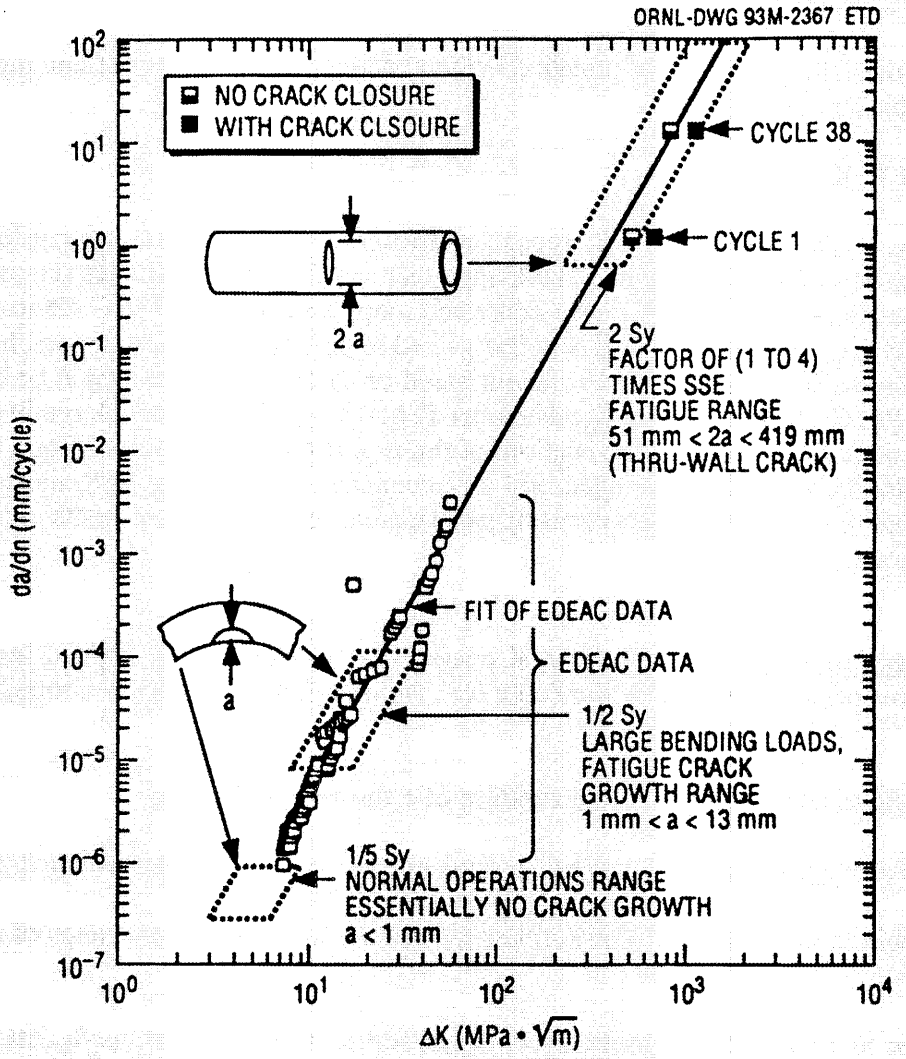

Fig. 18. - Fatigue crack growth data for 304 stainless steel in PWR water at 25°C, f=1Hz.

experiment (C-Pipe) and supporting analytic studies (See Appendix B for full report).

The following PIRG members participated actively in the development of this report:

Spencer H. Bush, Chairman
Robert J. Bosnak
Macintyre R. Louthan
Everett C. Rodabaugh
Gery M. Wilkowski

In addition, the following member provided written comments, but did not attend the review and discussion sessions:

Robert P. Kennedy

Introduction. The second PIRG report addresses the comments, conclusions and recommendations of PIRG related to the C-Pipe test and the analytic studies supporting or expanding on this test. The first report addressed scope issues in the PIRG Charter. The second report has, as its basis, the experience gained in preparing the first report; however, the second report is a "stand alone" document based on information provided at or before a meeting of PIRG held at Oak Ridge National Laboratory (ORNL) on December 16-17, 1992. The conclusions and recommendations of this report are based on this second meeting of PIRG, the information exchanged and the combined engineering judgement of the members cited in the Foreward who actively participated, or provided comments in the form of letter reports.

Experimental Program. The experimental program on C-Pipe can be divided into three distinct sectors presented in the "White Paper for the Piping Integrity Review Group," ORNL 12/7/92:

- The fatigue test leading to the generation of a through-wall crack;
- The severe cyclic loads attempting to simulate a seismic event greater than 1 SSE;
- A combination of load sequences ultimately leading to complete severance of the pipe weld;

PIRG agrees that cumulatively these three sectors represent very severe loads that confirm the high toughness of a wrought austenitic stainless steel such as AISI 304 and the resistance to double-ended guillotine break (DEGB) of this class of alloys; however, PIRG has specific reservations with regard to the test when taken in the context of an operating reactor piping system.

Analytic Programs. PIRG compliments Battelle Memorial Institute (BMI) [*sic*] on an excellent, albeit preliminary, analytic study simulating both a modeling of crack growth and realistic dynamic fracture assessment of a typical NPR-HWR primary pipe system. Other experiments and accompanying analyses have confirmed that the analytic technique used can predict observed experimental behavior with an acceptable degree of accuracy. These studies

confirmed which welds would see the highest loading conditions. As expected, they were in the welds attaching elbows to the reactor pressure vessel nozzles and the heat exchanger nozzles.

Direct DELTA J versus da/dN calculations were made using the EDEAC data base and comparing predictions to the ORNL C-Pipe tests, assuming the presence of a crack prior to the simulated seismic event and modeling the seismic event. The comparison of the C-Pipe test data was extremely close to the predicted EDEAC curve, even without crack closure. This modeled crack growth quite well. The analysis methodology verification covered:

- A comparison of J-estimation scheme prediction with NRCs degraded Piping Program cracked pipe quasi-static loading experimental data base.

- Comparison of dynamic cracked pipe analyses with International Piping Integrity Research Group (IPIRG-1) pipe system experiments.

The crack location was predicted to be at the weld attaching the elbow to the reactor nozzle. The summary statements are significant; namely:

- 3 SSE loading does not initiate (propagate) the crack;
- Portions of the piping will yield;
- The leak rate area is very small;

The above summary statements are sensitive to input assumptions (not surprising). Also, the model assumes the following:

- Only ductile tearing with no fatigue crack growth;
- No plasticity assumed in pipe;
- Analyses based on best information available;

The latter caveat covers the use of average properties not necessarily those of C-Pipe. A conclusion one can draw from these analyses is that the experimental results were more severe (and more conservative) than the analytic results simulating seismic loads. This could be due to load rates and times to load reversal where the analytic model had rapid reversals compared to the slow reversals in the experiment. PIRG recognizes that the approach used represents "advanced state-of-the-art" and will require validation. All seismic analyses conducted for this study utilize current regulatory guidance and were not based on proposed revisions now out for public comment; i.e., the new Appendix B to 10 CFR 100 and the new Appendix S to 10 CFR 50.

<u>Implications of Failure Probabilities</u>. If reactors are grouped loosely into three sets; namely:

- Operating DOE heavy or light-water reactors where T is about 100°C, maybe less and the primary system is austenitic stainless steel;

- Planned DOE reactors where T is about 100°C and P is < 1.72 MPa;

- The proposed ALWRs; [*sic*]

For the first group probability of a through-wall fatigue crack is very low; e.g., <E-7 during plant life. IGSCC will have a much higher probability; however, the probability of a potentially unstable crack such as 360° and nearly through-wall should be low because of bending moments during plant operation driving the crack through the wall so it is detected by leakage.

Failure (DEGB) due to fatigue cracking plus a severe seismic event has a very low probability (~E-13) so this scenario should be relegated to beyond DBE.

IGSCC can occur; however, IGSCC plus seismic to yield DEGB should have a low probability. The proposed analysis should clarify this scenario.

Set two is the same as the first part of Set 1 where IGSCC is not an issue. The scenario should be relegated to beyond DEGB.

Set three represents higher pressures and temperatures, more mechanisms such as thermal fatigue and stratification to fatigue the pipe. IGSCC should not be an issue. Therefore, one should anticipate a low probability of DEGB, but a higher overall probability of severe cracking. Also, axial cracking could be a problem. One can be cautiously optimistic that the overall probability of DEGB is <E-7, but more work would be necessary to arrive at a value accepted by Regulatory Authorities.

Restrictions Related to Conclusion One Below. Conclusion is based on a case where fatigue is the mechanism leading to cracking and the following restrictions also apply:

- Material is wrought austenitic stainless steel;
- Pipe is schedule 40 or no less than 0.5 in. (13 mm) wall for larger diameter piping;
- New materials selected essentially are immune to IGSCC;
- Reactors considered are essentially free from severe water hammer;
- Primary system temperatures not exceeding (~100°C) and pressures (< 1.72 MPa); therefore, thermal fatigue should not be an issue;
- Massive components such as pumps or heat exchangers are anchored so that a severe seismic event will not lead to gross movement of the component and overload failure of the pipe;
- For newer reactors ASME Section III Division 1 is used; for planned reactors the 1992 or later edition of the Code is used, provided that later editions are comparable to the 1992 edition;
- An Inservice Inspection program basically complying with IWB of Section XI (1992 edition) is in place;
- Technical Specifications define a leak detection system; this may be more difficult for low pressure light-water reactors;

9. PIRG CONCLUSIONS/RECOMMENDATIONS

Provided the restriction cited in the RESTRICTIONS RELATED TO CONCLUSION ONE section are in force, then the following conclusions are applicable:

(1) For DOE reactors at low pressure (≤ 1.72 MPa) and temperatures not exceeding (~100°C) with austenitic stainless steel piping, the DEGB should not be a DBE;

(2) For DOE low pressure low temperature reactors subject to IGSCC the analytic results with a 360° deep crack indicate that an instantaneous DEGB is highly improbable; PIRG believes further analyses would confirm that the instantaneous DEGB need not be a DBE used to evaluate core flow instability;

- For ALWRs, information is inadequate to justify relaxation of the current DEGB requirements other than that provided by 10 CFR 50 GDC-4 and 10 CFR 50.46 regarding leak-before-break;

With regard to recommendations PIRG suggests that further analytic studies could lead to relaxation of the instantaneous DEGB requirement as a DBE when the crack mechanism is IGSCC.

10. ACKNOWLEDGEMENTS

The authors wish to acknowledge the help and interest provided by J. J. Jicha, Jr. and W. A. Stringfield of the Office of New Production Reactors Program, Department of Energy and the help of many people at Westinghouse Savannah River Site for helping provide the C-Pipe, some of whom are as follows: J. M. Morrison, N. G. Awadalla, R. Lutz, R. Sindelar, and J. B. Elder. The authors also express their thanks to all the members of PIRG and R. Olson, S. Rahman, R. Mohan and R. Wolterman of Battelle Columbus who completed the excellent inelastic modeling and analysis work.

11. REFERENCES

1. Poole, A. B., Battiste, R. L., Clinard, J. A., and Hendrich, W. R., "Pipe Break Testing of Primary Loop Piping Similar to Department of Energy's New Production Reactor-Heavy Water Reactor," Oak Ridge National Laboratory Report, ORNL/NPR-92/8, January 1992.

2. Poole, A. B., Battiste, R. L., Clinard, J. A., and Hendrich, W. R., "Pipe Break Testing of Primary Loop Piping Similar to Department of Energy's New Production Reactor-Heavy Water Reactor," Pressure Vessel Fracture , Fatigue, and Life management, ASME-PVP-Vol. 233, June 1992, pp. 211-226.

3. Olson, R. J., "Cracked Pipe Analysis," working papers provided by Battelle Columbus for Piping Integrity Review Group, November 10, 1992, pp. 1-9.

4. Stoner, K. J., Sindelar, R. L. and Caskey, G. R., "Reactor Materials Program — Baseline Material Property Handbook — Mechanical Properties of 1950's Vintage Stainless Steel Weldment Components," Westinghouse Savannah River Company Report WSRC-TR-91-10, pp. 7-2 through 7-5, April 1991.

5. Elder, J. B., "Quality Control Condition Report SSQ/QC Job #C921241," WSRC Savannah River Site Report, SSD-QCM-920617, September 30, 1992.

APPENDIX A

Review & Synthesis Associates
Spencer H. Bush, P.E. • 630 Cedar / Richland, Washington 99352

October 7, 1992

Mr. David L. Moses
ORNL-NPR Project Manager
Oak Ridge National Laboratory
P.O. Box 2009
Oak Ridge, TN 37831-8051

Dear Mr. Moses:

Subject: First Report of the Piping Integrity Review Group (PIRG)

Attached is the first Piping Integrity Review Group (PIRG) report. The report addresses items a through g of the Scope of the Charter and represents compliance with item h of the Scope. Each issue is identified separately, PIRG member comments given, and a statement as to whether the comment represents a consensus, or is an identification of comments representing a departure from consensus.

While PIRG complies with the Scope as cited in the first paragraph, we feel that limiting the report to these issues alone is not adequate; therefore, we have addressed several ancillary items that we believe both amplify and strengthen the Scope issues. Each ancillary item is clearly identified in the report, followed by comments on the item.

The PIRG has the following membership:

Spencer H. Bush, Chairman
Robert J. Bosnak (Lawrence C. Shao as alternate)
Robert P. Kennedy
Donald F. Landers
Macintyre R. Louthan
Everett C. Rodabaugh
Gerald C. Slagis
Gery M. Wilkowski

Mr. Bosnak attended as did all other PIRG members except D. F. Landers.

RSA
Telephone: Business - (509) 375-2223 & 375-3749 / Home - (509) 943-0233

APPENDIX A

Review & Synthesis Associates
Spencer H. Bush, P.E. • 630 Cedar / Richland, Washington 99352

The report is an attachment rather than being combined with the comments in this letter as a letter report. We believe this permits greater flexibility. If, after reading the report, you believe specific items require clarification, please contact me and I will attempt to provide clarification with the caveat that such clarification cannot change the intent.

I suspect that this will be the only PIRG report because of the DOE action concerning NPR. Therefore, I have minimized deletions so that you obtain the collective opinions of all PIRG members. While this makes the report longer than intended, it does give you the various shadings of opinion in such a collective document.

On behalf of PIRG I thank ORNL for their hospitality.

Very truly yours,

Spencer H. Bush
President
REVIEW & SYNTHESIS ASSOCIATES
Chairman, PIRG

RSA
Telephone: Business - (509) 375-2223 & 375-3749 / Home - (509) 943-0233

APPENDIX A

FIRST REPORT OF THE PIPING INTEGRITY REVIEW GROUP BY MEMBERS OF PIRG

EXECUTIVE SUMMARY

This report contains the comments, conclusions and recommendations of PIRG in response to the specific issues cited in the Scope of the PIRG Charter. In addition, we have addressed ancillary issues impacting on the various Scope statements. Each of these ancillary issues are identified in the report.

Particular emphasis has been given to item b of the Scope because it represents a suggested redirection of the parameters in the proposed test program.

a. Review and Comment on the Merit of Present Test Methods and the Data Collected Merit of Test Method

The first test didn't seem to have a central theme, other than "let's put a lot of cycles on the pipe". More sensitivity studies to define the family of cracks that could cause problems at N+SSE loads is desired. A surface crack could be worse than the crack that has been tested. Pretest analysis would have shown that in the first test, the crack would have been very stable and that only subcritical crack growth should have been expected.

b. Evaluate the Testing Program being Conducted; Discuss Strengths, any Shortcoming and Recommend any Additional Testing Considered Necessary to Accomplish the Test Program Goals

One component of the modified test program is to select a through-wall pipe flaw sufficiently long so that the D_2O release during cyclic loading by reactor transients is roughly an order of magnitude higher than should be detected by redundant and diverse tritium detectors. This would place the flaw lengths well above the detection size of intermittent releases that would lead to shutdown and repair/replacement of the leaking section. This should be the flawed base line for the severe repetitive simulated seismic loads suggested by PIRG.

Impact Versus Slow Oscillatory Cyclic Tests

It is our understanding that the ORNL test fixture can either apply impact loads or slow-oscillatory-cyclic (SOC) loads laterally to the pipe specimen.

SOC loadings can be applied as either displacement or force controlled loadings. So long as the response remains nearly linear under multiple cycles of loading, it is immaterial whether the cyclic loadings are displacement or force controlled. However, if responses are highly nonlinear, substantial differences can result. Under highly nonlinear response, displacement

controlled SOC loading may understate the damage from an actual earthquake input; whereas an adequate number of force controlled SOC loadings will always conservatively replicate (often excessively so) the effects of earthquake induced responses. It is easy to show by an analytical comparison that 10 to 20 cycles of force controlled SOC loadings, each to the maximum earthquake-induced response overstate both the number and total duration of near-peak responses so long as SOC loadings are applied at a rate of two cycles per second, or slower.

Amplitude of Loading

Irrespective of whether future testing is conducted using impact or SOC loading, it is recommended that the response amplitude be significantly increased beyond that used in the previous test. Such an increase is necessary to find the largest response for which a given crack size remains reasonably stable (i.e., does not result in a LBLOCA) in about 40 cycles, which is more than sufficient to replicate earthquake responses.

Recommendations for Future Tests

To conservatively overstate earthquake-induced response effects, it is recommended that about 40 cycles of force-controlled SOC loading be applied in future tests. Ideally, the force level should be set as high as possible without resulting in a LBLOCA in less than about 40 cycles. Unfortunately, it may not be possible to achieve such a high force level. Because the test is force controlled and the oscillations are sufficiently slow to be essentially static loads, the force level should not exceed about 75% of that needed to induce plastic collapse under static load on an uncracked pipe.

The maximum force level which can be applied might also be limited by the test fixture. It is recommended that initially the applied force be set at a level 3 times that needed to produce the moment used in the previous test. After 40 cycles of applied force at this level, the force should be increased in about 30% increments until one of the following limits is reached:

1. 75% of the plastic collapse
2. limit of test fixture
3. load at which LBLOCA occurs in less than about 10 cycles

Application of Future Test Results

It is our understanding that the DBE for the NP-HWR will correspond to about a 10^{-4} annual probability of exceedance of ground motion level. Furthermore, to achieve a 10-fold reduction in the annual probability of exceedance requires a doubling of the DBE. Ground motion corresponding to three times the DBE are estimated to have an annual probability of exceedance of about 2.5×10^{-6}. Therefore, substantial margin is required between the design force level for the DBE and the maximum test force level applied for 40 cycles in the test program In order

to achieve an adequately low probability of a LBLOCA, the design force level should be set a factor of two to three below the maximum test force level.

Comments on Second Test

The focus of experiment 2 should be to examine crack opening for leak rates under normal operating conditions, and crack opening rates. This experiment would be a two part test; namely:

Experiment 2(a)

The initial objective is to assess the crack-opening geometry from a defect found in a similar plant. Significant parameters are the internal versus external crack lengths at a 0.1 and 1.0 gpm leak rate, and documentation of the surface roughness. This testing could be done at ASME Code maximum allowable normal operating stresses, i.e., Service Level A, or some fraction of it. This should be less severe than the actual plant stresses, but will provide a bounding limit for LBB analysis; i.e., the lower stresses will cause a longer crack for a given leak rate.

c. Comment on the Application of the Test Data toward Establishing a Best Estimate Bound to the NP-HWR Large Break Loss of Coolant Accident (LBLOCA)

One must recognize that the seismic simulation used is not an accurate representation of an actual seismic event. The approach will need to emphasize that the conditions causing crack growth represent upper bound loads and the initial flaw used is well above the size detectable by either RT or UT. Both represent substantial conservatisms in the size of the end-of-life flaw. Also, the through-wall flaw sizes should be detectable through leak detection or system walk downs. All of these factors represent cumulative conservatisms.

With regard to the end-of-life seismic loads greater than SSE, if the crack does not become unstable under these conditions, one may argue that the instantaneous DEGB is incredible and that it is difficult to postulate a DEGB over a finite time under these conditions. The suggested LBLOCA model is quite arbitrary and does not comply with the observed data. An ultimate position will depend on the proposed future tests to either confirm this is an incredible event, or indicate that it is conceivable if these upper bound conditions exist and a greater than SSE leads to failure.

d. Comment on the Consistency of the Approach with Recent Regulatory Policy Statements (SECY-88-325) and with Recent Changes to the ECCS Rule [10CFR50.46 (1988)]

One must recognize that 10 CFR 50.46 is for light water cooled plants and was not drafted with heavy water or liquid metal coolants in mind. There is nothing inherent in limiting LBB technology to establishing dynamic effects design bases only. All countries which accept LBB have this limitation nonetheless. The Commission and the ACRS recognize that LBB can in

concept be applied to establishing ECCS requirements. However, the proposal by DOE/ORNL would be breaking new ground. The major difficulty would be in defining a replacement breach of the reactor coolant pressure boundary which is sufficiently unlikely to be exceeded. Earlier discussion indicated vulnerabilities in other systems with potential effects on the reactor coolant pressure boundary. The NRC staff made the judgment for commercial light water nuclear power plants that safety would not be improved by allowing the use of LBB for establishing the ECCS requirement, and thus would not invest its resources to promote this use. However, the policy statement leaves open the door for commercial power plant owners to develop the technology (which primarily would be driven by economic concerns) with the understanding that the NRC would be disposed to review and accept this use if adequately justified.

e. Comment on the Consistency of the Approach with Previously Accepted Applications of Leak-Before-Break Technology and Rules Allowed in GDC-4

Conditions differ so markedly in the NP-HWR compared to a PWR that it is difficult to make a comparison. Certainly, each utility did not conduct tests on piping to justify LBB. The approach has depended on analyses and an accumulation of data. It is not applicable to some piping systems such as the feedwater where very severe failures can occur without LBB. Obvious examples of such failures are those due to erosion-corrosion. The best analogy is for the Class 1 PWR systems vis-a-vis the NP-HWR process water system. Loads and failure mechanisms (mechanical fatigue) are similar; however, piping materials differ; e.g., cast stainless or clad ferritic either A-533 or A-508. Certainly, the leak detection systems in the commercial reactors are much less sensitive.

The "bottom line" is that one can argue LBB for the NP-HWR, but one arrives at that conclusion for a different set of criteria.

f. Comment on Possibilities for Extrapolation of the NP-HWR LBLOCA to other Reactors such as the Savannah River K-Reactor HWR or to Specific ALWR Designs as Examples

The application and acceptance of the NP-HWR LBLOCA to ALWRs such as the AP-600 is doubtful. Conditions differ too greatly and the conditional acceptance of LBB by the USNRC doesn't warrant a shifting of the base. The data base is of limited use to the commercial reactors.

Basically, the possibility of extrapolating GDC-4 is limited to local dynamic effects; with other reactors it is dependent on precluding the material degradation conditions discussed in SRP 3.6.3. For ECCS applications, the core thermal hydraulics and reactivity response when a DEGB is postulated to occur also needs to be evaluated in addition to identifying the relevant degradation conditions.

g. State Consensus and note Dissenting Opinion among Panel Members in Conjunction with these Reviews and in Consideration of the Points of Scope Listed above

APPENDIX A

No dissenting opinions were expressed by the members of PIRG. We have used g to collect some items that do not fit well elsewhere. These are included here with the exception of an overall opinion under h.

h. Prepare and Submit a Written Report based on (g), which includes each Panel Member's Considered Opinion

The preceding complies with the requirements of h.

APPENDIX A

FIRST REPORT OF THE PIPING INTEGRITY REVIEW GROUP BY MEMBERS OF PIRG

INTRODUCTION

This report contains the comments, conclusions and recommendations of PIRG in response to the specific issues cited in the Scope of the PIRG Charter. In addition, we have addressed ancillary issues impacting on the various Scope statements. Each of these ancillary issues are identified in the report.

Particular emphasis has been given to item b of the Scope because it represents a suggested redirection of the parameters in the proposed test program.

SCOPE ISSUES

a. Review and Comment on the Merit of Present Test Methods and the Data Collected Merit of Test Method

The pipe impact loading demonstrates that a limited amount of crack growth can occur for single overload cycles. There is an extra margin over load-controlled loading. The difficulty in such an approach is to convince the reviewer that the test results are directly applicable to the NP-HWR. For instance, it is not certain that the pipe impact testing approach is as severe (i.e., same crack growth per cycle) as shaking the pipe with weights at both ends as was done by GE/EPRI (in report NP-2472), Battelle (in the IPIRG-1 program), and at JAERI. A pipe system test would be somewhere in between. The impact load experiments could be used to verify a dynamic model that, in turn, could be used to assess the actual plant design under high level SSE loading. Most people involved in seismic pipe testing will find it hard to believe that such pipe impact testing will simulate actual plant seismic loading. A significant redirection of the pipe test procedures may be in order to develop a defensible approach that will satisfy DNFSB.

The first test didn't seem to have a central theme, other than "let's put a lot of cycles on the pipe". More sensitivity studies to define the family of cracks that could cause problems at N+SSE loads is desired. A surface crack could be worse than the crack that has been tested. Pretest analysis would have shown that in the first test, the crack would have been very stable and that only subcritical crack growth should have been expected.

A pipe system test probably would have been more meaningful as a demonstration test. However, demonstration tests seldom cover all the cases of interest. For instance, there may be other locations in the piping that are worse than what is now assumed, i.e., the RHR piping system. Certainly, the elbow in the hot and cold legs would lower the natural frequency and

provide additional stored elastic energy in the system. The lower natural frequency tends to apply dynamic loads on the crack longer, hence there would be larger amounts of ductile tearing per large amplitude cycle. The higher amount of energy in the pipe system would tend to drive the crack further during ductile tearing.

Additionally, if the fusion line or HAZ is the low toughness region, then a critical reviewer may question the value of the first test where the crack was in the center of the weld. This would be hard to defend to the DNFSB if there are only a few demonstration tests. The lowest toughness direction needs to be determined prior to conducting the next two experiments.

It would be better to conduct experiments to verify a general analytical methodology that could be used for assessing any flaw geometry, pipe system, and load levels.

Data Collected

The data collected were quite good. Suggested improvements are:

(1) Add rotation devices to measure the rotation of the pipe on either side of the crack. This is desired since many of the elastic-plastic fracture analyses calculate moment versus rotation due to the crack.

(2) Add electric-potential measurements across the center of the crack. These data would help to detect the start of ductile tearing crack growth and the amount of crack growth during the experiments. The timing wire gages cannot detect the start of ductile tearing, and are susceptible to error due to plasticity causing the gage to debond, and the breaking of the wire may not correspond to the crack tip reaching it. The timing wires or a-c EP crack gages are good for subcritical crack growth, but they aren't good for ductile tearing in tough materials.

(3) There is some doubt whether a load cell was used or a strain gage at the bottom of the pipe opposite the center of the crack to determine the load. If a strain gage was used, the load calibration changes during the crack growth with any plasticity in the crack plane. Therefore, the strain gage output is not linearly related to the applied bending load during testing. As the crack grows, the strain output at this location increases for the same applied load. Alternatively, for the same strain level, as the crack grows, the load will be decreasing. If the strain gage at this location was used to determine the load on the test section, it is possible that the "calculated applied loads" were less than the actual bending loads that a load cell would have indicated. Low applied loads would result in a much more stable crack than would occur with true load-controlled loading. If so, this would explain why the crack remained stable even with "load-controlled loads" after the crack exceeded 50-percent of the circumference, see Figure 3 in ORNL/NPR-92/8. Another possible discrepancy in Figure 3 is the intermixing of code values of strength and actual strength, discussed later.

The impact tests do not replicate a seismic event. They are described as an "energy-controlled" loading. The impact imparts an initial velocity to the test specimen, which results in a certain

displacement. This is comparable to a displacement-controlled test. A conclusion from the IPIRG tests was that inertia-controlled loads are more severe than displacement-controlled loads for fracture.

The inertial load experiments in the IPIRG experiments showed markedly less fracture stability than those conducted under displacement-controlled loads. While the maximum load results for the two types of loading compare closely, inertial loading was shown to produce complete fracture instability in only a few cycles past maximum load, whereas there was only slow tearing in the displacement-controlled tests

The other major concern with the impact test is the introduction of higher frequency effects. The impact results in exciting the higher frequency modes of the test specimen as well as the fundamental bending mode. This is evident in the data and ORNL has suggested a breathing mode. The main question is -- what is the effect of these higher modes on crack stability? It is possible that the higher frequency effects reduce the flow rate and the crack growth.

Although the NP-HWR operating pressure is low, the maximum pressure should be applied during all crack stability testing.

In the context of ASME Section III the data when presented as SSE or 2SSE are misleading. The stress level for what is quoted as SSE is very low in comparison to the Code allowables for Level D. The tested stress level at SSE is only about 1/4 of the allowable of the lower of $3S_m$ or $2S_y$. The tested stress level at SSE is only about 1/2 of the Level B or OBE allowable. All discussion of the loading should be identified as a fraction of the Level D allowable not as 1SSE.

The calculations to establish the maximum 60 year crack are debatable.

The testing is very limited in scope--one size, one schedule, one material, and a crack in the center of a girth weld in straight pipe. How will this data be extended to other pipe fittings and the different pipe sizes in the other reactor coolant boundary piping. Apparently there is some test data that indicate the HAZ may be the critical area. Will there be dissimilar metal welds somewhere in the RCS boundary?

Figure 15 of ORNL/NPR-92/8 shows a significant reversal of the impact load. This does not seem possible. How does the hammer produce a tension load on the pipe? Is this due to dynamic springback of the pipe as the hammer recoils?

<u>Ancillary Issue a.1 - ANL Stress Corrosion Test Data</u>

The Argonne Slow Strain Rate Tests (SSRT), in particular those tests containing a crevice filled with a pin so that there is a limited annular area, represent very severe test conditions. The small annulus represents a stagnation condition accompanied by high strain rates. SSRT conditions may lead to substantial stress corrosion, either trans or intergranular, in days or weeks, whereas piping of the same alloy may require years before SCC is detected. A

reasonable conclusion is that SSRT may lead to SCC (IGSCC or TGSCC) while the pipe may not suffer SCC throughout reactor life. The opposite usually applies; namely, if no SCC is detected by the completion of SSRT runs, one would not expect SCC in the material when under reactor conditions of comparable temperature and water chemistry. A caveat is that SCC may occur after long periods under severe conditions in service whereas the SSRT would not indicate SCC; this may be due to the limited test time for SSRT.

Tests on 316NG (Nuclear Grade) with temperatures comparable to or somewhat higher than the NP-HWR, and water chemistry with species equal to or greater than those anticipated in the NP-HWR did not suffer SCC. A caveat is that chloride levels ≥ 1 ppm (much higher than expected) can lead to SCC under SSRT conditions at or greater than 150°C. There appears to be little or no SCC at 100°C at these chloride levels.

A justifiable conclusion is that SCC will not occur in 316NG piping under NP-HWR conditions throughout the projected plant life of 60 years.

b. Evaluate the Testing Program being Conducted; Discuss Strengths, any Shortcoming and Recommend any Additional Testing Considered Necessary to Accomplish the Test Program Goals

One component of the modified test program is to select a through-wall pipe flaw sufficiently long so that the D_2O release during cyclic loading by reactor transients is roughly an order of magnitude higher than should be detected by redundant and diverse tritium detectors. This would place the flaw lengths well above the detection size of intermittent releases that would lead to shutdown and repair/replacement of the leaking section. This should be the flawed base line for the severe repetitive simulated seismic loads suggested by PIRG.

Impact Versus Slow Oscillatory Cyclic Tests

It is our understanding that the ORNL test fixture can either apply impact loads or slow-oscillatory-cyclic (SOC) loads laterally to the pipe specimen.

An impact test applies a single cycle of the maximum moment with rapid decay in response of additional cycles during resultant free vibration. These free vibrations are at the natural frequency of the pipe. At least for small cracks, this pipe natural frequency is on the high end of the frequency spectrum (2 to 10 Hz) over which the predominant power of the DBE is input to the pipe. Both the rapid decay in response and the high frequency of such response from an impact load raise questions over whether such a loading can conservatively replicate the DBE response. An analytical comparison between the response from an impact load and the response from a typical earthquake input time-history is likely to show that 10 to 20 impact loads produce the same number of near-peak response excursions as is produced by the earthquake input time-history. However, because of its lower frequency of input the earthquake time-history is likely to produce a longer total duration at near-peak response levels than do 10 to 20 impact loads. If impact tests are to be continued, it is recommended that a simple analytical study be conducted

to determine how many impact loads must be applied to conservatively replicate both the number and total duration of near-peak responses from a typical earthquake input time-history. Even with such an analytical study, it might be difficult to overcome the perception that testing with a number of impact loads is a liberal surrogate for an actual earthquake input.

SOC loadings can be applied as either displacement or force controlled loadings. So long as the response remains nearly linear under multiple cycles of loading, it is immaterial whether the cyclic loadings are displacement or force controlled. However, if responses are highly nonlinear, substantial differences can result. Under highly nonlinear response, displacement controlled SOC loading may understate the damage from an actual earthquake input; whereas an adequate number of force controlled SOC loadings will always conservatively replicate (often excessively so) the effects of earthquake induced responses. It is easy to show by an analytical comparison that 10 to 20 cycles of force controlled SOC loadings, each to the maximum earthquake-induced response overstate both the number and total duration of near-peak responses so long as SOC loadings are applied at a rate of two cycles per second, or slower.

Amplitude of Loading

Irrespective of whether future testing is conducted using impact or SOC loading, it is recommended that the response amplitude be significantly increased beyond that used in the previous test. Such an increase is necessary to find the largest response for which a given crack size remains reasonably stable (i.e., does not result in a LBLOCA) in about 40 cycles, which is more than sufficient to replicate earthquake responses.

Recommendations for Future Tests

To conservatively overstate earthquake-induced response effects, it is recommended that about 40 cycles of force-controlled SOC loading be applied in future tests. Ideally, the force level should be set as high as possible without resulting in a LBLOCA in less than about 40 cycles. Unfortunately, it may not be possible to achieve such a high force level. Because the test is force controlled and the oscillations are sufficiently slow to be essentially static loads, the force level should not exceed about 75% of that needed to induce plastic collapse under static load on an uncracked pipe.

The maximum force level which can be applied might also be limited by the test fixture. It is recommended that initially the applied force be set at a level 3 times that needed to produce the moment used in the previous test. After 40 cycles of applied force at this level, the force should be increased in about 30% increments until one of the following limits is reached:

1. 75% of the plastic collapse

2. limit of test fixture

3. load at which LBLOCA occurs in less than about 10 cycles

APPENDIX A

Application of Future Test Results

It is our understanding that the DBE for the NP-HWR will correspond to about a 10^{-4} annual probability of exceedance of ground motion level. Furthermore, to achieve a 10-fold reduction in the annual probability of exceedance requires a doubling of the DBE. Ground motion corresponding to three times the DBE are estimated to have an annual probability of exceedance of about 2.5×10^{-6}. Therefore, substantial margin is required between the design force level for the DBE and the maximum test force level applied for 40 cycles in the test program In order to achieve an adequately low probability of a LBLOCA, the design force level should be set a factor of two to three below the maximum test force level.

Comparison to ASME Code Procedures

If one assumes that the NP-HWR piping is designed to ASME Section III, NP-3600 (Class 1 Piping), evaluation of an SSE (Level D event) will use the following Code equation:

$$B_1 * P * D_o + B_2 * M/Z \leq \text{lesser of } 3\,S_m \text{ or } 2S_y \qquad (1)$$

A comparison with ORNL's first pipe test:

$$0.5*250*16/2*0.5 + 1.0*M/91.5 = 2*45000 = 90000 \text{ psi} \qquad (2)$$

The data suggest that $S_y = 45000$, and actual properties should be used.

If equation (2) is solved for M:

$$M = (90000 - 2000)*91.5 = 8{,}052{,}000 \text{ in-lb} = 671 \text{ ft-kip} \qquad (3)$$

Where M is the maximum allowable moment due to weight and SSE.

If one uses the estimated maximum bending moment of 110 ft-kips given in the meeting handout sheet 12 (Facility Calculation 9/18/91 by A. B. Poole) in equation (3), the Deadweight is 4.85 ft-kip will yield a Code-allowable M(SSE) of 666 ft-kip. In passing it should be recognized that equation (1) does not include either thermal moments or seismic anchor moments. The significance of the 666 ft-kip is that the maximum moment applied by impact in the first test was 110 divided by 666 or 0.17 times that conceptually allowed by the Code.

The value of M = 110 ft-kip is questionable for other reasons. For example, the current conceptual design of NP-HWR would indicate that the process piping and important attached systems can be broken down as follows:

(a) from reactor vessel to pump
(b) from pump to heat exchanger
(c) from heat exchanger to reactor vessel
(d) between something and a pressurizer

APPENDIX A

(e) between something and an accumulator

It is highly improbable that the SSE response in each of these piping systems would be the same; therefore, to imply that M = 110 ft-kip is the SSE moment at the NP-HWR is misleading. One approach would be to identify the moment as M_1 as equal to 110 ft-kip and normalizing the results to M_1.

Most piping systems contain one or more elbows. In addition there usually are small branch connections for drains or vents and, possibly large branch connections if the pressurizer or accumulator is tied to the hot or cold leg. These not-just-straight-pipe portions usually control piping design, and the controlling location rarely is at the mid-span of a section of straight pipe. An example is for a normally-used elbow where the B_2 index matching the pipe is 3.8. Thus, if the allowable moment in a straight section is 110 ft-kip, the allowable moment at an elbow would be 110/3.8 or 29 ft-kip.

If the NP-HWR designer used the results of the first ORNL test, he would be required to design the piping for M(SSE) = 0.17 times Code allowable which could create problems because the load capacity of nozzles on the vessel and/or heat exchangers and/or pumps might control the allowable M(SSE); this could lead to restraint on the piping to limit nozzle loads.

The bottom line is that there is considerable incentive to apply higher loads in ORNL's second and third pipe tests. One incentive is that the first test, if interpreted as allowing M(SSE) = 0.17 times the Code allowable, does not have any margin to cover uncertainties in earthquake loadings, material responses, welds at elbows, torsional moments, etc. The other incentive is to see if it is possible to get a bit closer to the allowable per the present Code.

The first pipe test appears to be a test where there were a lot of fatigue cycles and impact tests conducted, but there was not a specific objective to the test plan other than putting on a lot of cycles. The desire to keep the load to 1SSE would force the crack growth to occur in fatigue, with little ductile tearing, and no ductile instability should occur. There did not seem to be a pretest analysis of what was anticipated from this test. A good pretest analysis would have shown that lots of cycles were needed, and that impact testing resulted in some low cycle fatigue cycles.

The fact that an instability did not occur in the first test is not surprising. There is a limited amount of energy which is being absorbed by the ductility of the material with each impact. Furthermore, with impact loading, the load to potentially cause ductile tearing is applied for only a short time and then unloads rapidly, hence the crack has to arrest.

After reviewing the impact testing and the plant design stresses, there may be some value to the impact testing, but it probably does not bound the actual behavior that might occur for plant piping. Therefore, for the remaining tests, growing the crack by fatigue at SSE loads isn't very productive.

APPENDIX A

Comments on Second Test

The focus of experiment 2 should be to examine crack opening for leak rates under normal operating conditions, and crack opening rates. This experiment would be a two part test; namely:

Experiment 2(a)

The initial objective is to assess the crack-opening geometry from a defect found in a similar plant. Significant parameters are the internal versus external crack lengths at a 0.1 and 1.0 gpm leak rate, and documentation of the surface roughness. This testing could be done at ASME Code maximum allowable normal operating stresses, i.e., Service Level A, or some fraction of it. This should be less severe than the actual plant stresses, but will provide a bounding limit for LBB analysis; i.e., the lower stresses will cause a longer crack for a given leak rate.

Experiment 2(b)-Option 1

Load the leaking cracked pipe to 3 or 4 times the SSE stress or alternatively the Code maximum allowable $2S_y$. Doing this for 40 cycles in load control would conservatively evaluate flaw stability under seismic loading. This should be reverse loading cycles. Since the leaking crack will be relatively short in length, the pipe may even buckle if just taken to the maximum load. It is strongly suggested that pretest calculations be conducted to evaluate the feasibility of such a test. This type of test will probably show that a leaking crack will be stable, and no crack velocity data will be generated.

Experiment 2(b)-Option 2

The second option is to stop the leaking test in Experiment 2a, and put a crack on the opposite side to generate crack velocity data. The current assumption is that there would be a through-wall crack prior to the SSE loading. It is possible that there is a surface crack of some geometry that could be stable at normal operating loads, but would be unstable at X*SSE. Sensitivity studies should be conducted to evaluate the family of surface crack geometries that may fail at various levels of SSE. One of these geometries could then be used in this test. The crack could be put at 180° from the existing crack without influencing this test objective. Loading of this "critical" surface crack may produce an instability. The velocity of the crack during the instability would be extremely useful data for the thermohydraulic analyses.

While Option 2 has a worth objective, the test facility may be a limit that diminishes the value of the experiment. If the test is conducted under load control, the surface crack could break through the thickness very rapidly, with a small crack opening area, then continue to propagate as a through-wall crack until the actuator reached its 6-inch stroke limit. This could result in a very small final crack opening area relative to the true DEGB area. If the test is conducted in displacement-control, the resulting through-wall crack will still propagate to the end of the initial surface crack very rapidly, but the through-wall crack would probably arrest once it

reached the end of the initial notch. A small amount of tearing past the initial surface crack may occur if there was sufficient stored energy in the pipe system and test machine; however, the ORNL test system could be limited so that the crack growth past the initial surface crack is minimal. Some instability calculations could be made to predict this behavior. The value of the data would be to check an analytical model that could be used in an analysis of the actual plant piping system with seismic loading dynamically applied.

The loading of this test could be monotonic until the surface crack failed, then cyclic with the displacement level for 40 cycles. The alternative is to start with a fixed cyclic load, perhaps at 3*SSE and cyclicly load for 40 cycles. The second loading option is preferred because it simulates some cyclic damage prior to fracture that may occur in a seismic event.

Experiment 3

The third experiment should demonstrate the USNRC LBB SRP 3.6.3 approach, especially if Experiment 2b-Option 2 has been exercised. After cyclic loading, the pipe should be loaded until large crack growth occurs to see the residual strength of the cracked pipe after cyclic loads. Load-controlled cyclic loading should be more conservative than impact loading, although the crack velocity and corresponding crack-opening-area rate probably is too high for thermohydraulic concerns.

The following steps are suggested to design and conduct the third experiment:

(1) Use the NRC safety factor of 10 on the leakage detection rate to give a leak rate for calculating the detectable crack; i.e., 10*(0.1 gpm) = 1 gpm.

(2) Calculate the circumferential crack length at the normal operating loads using mean data from the crack morphology variables for the crack growth mechanism anticipated. The mechanism would be fatigue crack growth where there may be a small amount of branching. IGSCC crack morphology variables (i.e., surface roughness, number of turns, actual path length/pipe thickness) may be overly conservative.

(3) Determine the lowest toughness location by conducting fusion line toughness tests with a slant notch that follows the fusion line. Conduct at least three tests without side grooves. Let the crack grow at least 30 percent of the ligament to see where it will grow. Metallographically section the specimens to see if the crack grows along the fusion line. Al Van der Sluys suggested that bend bar specimens may be better to use that C(T) specimens.

(4) Orient the pipe crack (internal surface crack and the through-wall crack) in the low toughness location. If the low toughness region is in the weld, ORNL already has the internal surface crack at the right spot. If the low toughness region is in the fusion line, HAZ, or in the base metal, then ORNL needs to redo the internal surface crack they have in the weld of this specimen. If the low toughness region is in the fusion line, check with Gery Wilkowski concerning how to do it based on his pipe weld crack tests.

(5) Calculate the displacement for the uncracked pipe equal to nominal elastic stresses equal to 3SSE. If SSE was $S_y/2$, then 3SSE is $1.5S_y$. To avoid criticism, use the actual yield strength of the ORNL test pipe, rather than the Section III Code value. The past Degraded Piping Program data base showed that for TP304 stainless steel at room temperature, several pipes had yield strengths of 40 ksi; however, several others were at 31 ksi, while the Code minimum was 30 ksi. Also, one of the pipes had a yield at room temperature of 36 ksi, well above the 30 ksi Code minimum, but at 550°F it was only 0.1 ksi above the Code value. The stainless steel pipe fracture data are being reviewed by the ASME Section XI Pipe Flaw Evaluation Task Group to see if the flow stress definition should be changed in IWB-3640. All of these pipes came from canceled nuclear power plants, and, hence, were typical materials. Therefore, use 1.5 times the actual yield in the elastic calculations to avoid falling into the trap of not knowing the margin between actual and Code values of the pipe strength to be used in the plant. If it is possible to go above 3SSE, the demonstration test will be more convincing.

(6) Apply the load corresponding to the displacement calculated in Step 5 to the test article as a load-controlled load. The hold time should be about 30 seconds to simulate a load-controlled cycle without excessive primary creep crack growth at the crack tips.

(7) Repeat the cyclic loading from Step 6 under load-control for 39 more cycles using the load from the first cycle. Ideally, use a load cell to measure this load. As an option strain gages on the pipe could be used, as long as the strain gages are remote from the crack plane and that section of the pipe remains elastic. Don't use strain gages in the plane of the crack as a load cell due to plasticity and crack length increases changing the elastic response of the pipe.

(8) After 40 cycles, load the pipe monotonically until there is large crack growth and a maximum load is surpassed. This will show the remaining margin based on load.

PIRG recognizes that the fabrication used to produce the pipe section represents technology about 40 years ago, and that the pipe section has operated for several years which would translate to a large number of operating cycles. Apparently the pipe does not contain IGSCC although it may have weld root defects. While one can say that a "degraded" pipe is being tested, its not apparent what is expected or will be obtained from this test, or what correlations can be made with the first and third tests. One approach would be to test it at higher loads than used in the first test. If the yield strength is about 45000 psi, then the perfectly plastic limit load is about:

$$M(L) = 1.3S_y*Z = 1.3*45000*91.5 = 446 \text{ ft-kip}$$

This load could be applied with the ram, if the ram capacity is > 112 kip. Impact loading might be used to get a calculated moment of 446 ft-kip, but that might have the principal effect of pushing the pipe out-of-round.

Because of the strain-hardening of stainless steel, the displacement could be applied that is above the limit moment displacement and, after a few cycles of +/- displacements, the load might

build up to about 600 ft-kip; if the ram capacity is
> 150 kip. The approach would be to apply the displacement some 20 to 40 times. After this sufficient cycles should be applied to fatigue-grow the existing "defects" to some size of crack where it could be reasonably claimed that it would be detected by leakage. After this apply the initially-set displacement another 20 or so times to (hopefully) demonstrate that the crack is stable.

ORNL's "time-delay" concept appears to be intriguing; however, it is difficult to tie it to the first test. Apparently it assumes that NP-HWR will have severe earthquake detectors which will (a) trip the reactor in a couple of seconds and (b) start the ECCS in a couple of seconds. This could lead to problems for both designer and plant operator.

The preferred test is cyclic, fully reversed load. The best approach would be to impose a sine load of a certain frequency (2 to 10 Hz) for different test specimens. If not, then the duration of the loading needs to be controlled in some manner. To apply the load for a "long" time is unnecessarily conservative. If the load/displacement is nonlinear, then the longer the load is applied the more the displacement. The duration of the maximum earthquake load should be simulated as close as possible. The load/displacement cyclic history should be recorded. There should be significant strain hardening effects.

The initial crack size should be based on realistic estimates of the maximum 60 year flaw. There is no benefit in using an unrealistically large initial crack size.

The simulated earthquake loadings for the initial tests should be based on the Code Level D allowables, not predicted stress levels. Subsequent tests should be run a factor of (3?) times the Level D allowable to establish margins.

The uncertainties need to be addressed. There are a number of variables that cannot be simulated--the cracking mechanism, plant loadings, aging and environmental effects, design or operational errors, the earthquake magnitude.

Crack stability data on cracks in parent material and the HAZ should be tested. The fabrication of the RCS boundary on the NP-HWR should be consistent with Section III Class 1 practices. The inner diameter would be counterbored to control mismatch. This weld geometry should be tested with a crack in the "corner" of the counterbore.

<u>Ancillary Item b.1 :Probabilistic Fracture Mechanics Calculations on 316NG under NP-HWR Conditions using the PRAISE Code</u>

PRAISE (Piping Reliability Analysis Including Seismic Events) is a computer code developed for USNRC that has been applied to fatigue failure probabilities of PWR primary piping and to stress corrosion cracking failures of BWR piping. We recommend completion of the ANL effort to determine NP-HWR process piping failure probabilities due to fatigue. Recognizing that PRAISE is quite sensitive to inputs, the model should closely represent anticipated NP-HWR

operating conditions.

The general trend in the nuclear industry is toward a risk-based approach, where risk is the product of the failure probability at a specific location and the consequences of the failure at that location. ASME Section XI is considering the risk-based approach to optimize locations selected for nondestructive examination. Therefore, the NP-HWR PRAISE study is in line with similar activities related to commercial nuclear reactors.

Ancillary Item b.2 :Complementary Information on Probabilistic Fracture Mechanics, Documentation of Value to the NP-HWR

Access to the Federal Republic of Germany Biblis B probabilistic fracture mechanics study using a modification of the PRAISE Code will yield a stratified approach that gives a spectrum of probabilities as functions of break size. A report by Helmut Schulz indicates the range of values used and represents an earlier approach than the Biblis B study.

Ancillary Item b.3 :Complementary Information on Simulated Response of Piping under Simulated Seismic Loads

Several test programs have been carried out on piping simulating nuclear reactor systems. The PIRG believes that citation of these programs should strengthen your test program because of closer simulation of seismic loads. Examples are the ETEC uncracked pipe program funded by EPRI and USNRC; NRC's International Piping Integrity Research Group (IPIRG) program on cracked pipe; Japanese tests on defected piping; and the HDR uncracked pipe tests (NUREG/CR-5646). These are available and served as bases for predicting low probabilities of failure unless there were multiple simulated earthquakes at high accelerations. Other such tests also exist.

Ancillary Item b.4 :Complementary Information on Failure Mechanisms expected in 316NG under NP-HWR Conditions

An extensive examination of Licensing Event Reports for piping larger than two inches diameter disclosed no severe failures in reactor primary systems where severe covers severance, major fishmouth failures approaching the DEGB area, and large splits. Table 1 compiled from these data cover the various failure mechanisms. Stress corrosion is not on this list because there have been no major failures in more than 2000 reported cases of SCC. An examination of the failure mechanisms in Table 1 confirms that several do not apply to 316NG process piping. This includes erosion-corrosion because austenitics are not susceptible. Bellows are not an issue, and it is highly improbable that any water hammer, if such occurred, would be sufficiently energetic to rupture an austenitic stainless steel line. The recorded failures due to water hammer have been splits in A-106 feedwater lines, or breaks of small (about 1-in. D.) lines attached to a larger line that moved due to a water hammer. Thermal fatigue has a very limited potential; while there could be leak-through at a valve, the valved off liquid should not be at a temperature, either higher or lower, sufficiently different to lead to thermal fatigue. A ΔT of

at least 50°C is necessary and this usually leads to no more than a leaking crack with limited width.

Basically, that leaves design/fabrication defects which usually are found during preservice examination or may lead to failure during hot functional testing. The other mechanism is by mechanical fatigue, provided the operating loads throughout life are high enough.

Ancillary Item b.5: Resolution of Uncertainties

To deal with uncertainties particularly involving loadings for design, and uncertainties in other aspects of the test program, DOE/ORNL should (must) do a probabilistic margin analysis to determine conditional probabilities of accident sequences initiated by seismic events larger than the design basis SSE which could lead to pipe rupture. These sequences can and should include pipe ruptures caused indirectly by seismic events, such as failure of the RHR system and its accumulator (briefly flashed on the screen raising more questions than answers). The conditional probability results can be used to calculate high confidence of low probability of failure (HCLPF) values for the primary system given various accident sequences, and to calculate which components and systems limit the plant seismic capability. This should include the previously mentioned RHR system to determine its vulnerability with regard to seismic events. For example, has the RHR system components and supports been designed with sufficient HCLPF values to be comfortable with the statement that the design operates in a non-isolable fashion.

c. Comment on the Application of the Test Data toward Establishing a Best Estimate Bound to the NP-HWR Large Break Loss of Coolant Accident (LBLOCA)

The impact test data are of little, if any, use in determining an appropriate large break LOCA or break opening time for the NP-HWR. There appears to be some question about the limiting consideration, break size versus break opening time. If break size is the limiting consideration, then ORNL could use existing pipe fracture methods, and the USNRC's leak-before-break methodology in the draft SRP 3.6.3 to show that the LBLOCA was extremely unlikely under earthquake loadings larger than SSE. On the other hand, if break opening time is the limiting consideration, then approximations could be made using existing formulations and engineering judgment. This would work for those situations where the crack remained stable and should reliably establish a best estimate bound for the NP-HWR LBLOCA.

If a compliant instability were to occur, the crack extension rate could increase significantly, and there is no data base that could be used to estimate that rate. Pipe fracture experiments can be, and have been, designed to produce a compliant instability, and the test specimen could be instrumented to get the necessary crack extension and crack opening data.

Depending upon the limiting consideration, and the need to experimentally validate the analytical procedures, pipe fracture experiments could be designed to provide the appropriate test data. The USNRC has funded similar work both at Battelle and at the U. S. Navy's David Taylor Research Center. The Battelle work has been more sophisticated, involving larger diameter

pipe, and pipe system tests. The relatively simple compliant instability tests conducted by the Navy, if scaled appropriately, could be used to provide the crack opening rate data. However, the pipe system test approach provides equally valid data, with the added advantage of correctly reflecting system compliance and other design considerations, and would be a more convincing test.

One must recognize that the seismic simulation used is not an accurate representation of an actual seismic event. The approach will need to emphasize that the conditions causing crack growth represent upper bound loads and the initial flaw used is well above the size detectable by either RT or UT. Both represent substantial conservatisms in the size of the end-of-life flaw. Also, the through-wall flaw sizes should be detectable through leak detection or system walk downs. All of these factors represent cumulative conservatisms.

With regard to the end-of-life seismic loads greater than SSE, if the crack does not become unstable under these conditions, one may argue that the instantaneous DEGB is incredible and that it is difficult to postulate a DEGB over a finite time under these conditions. The suggested LBLOCA model is quite arbitrary and does not comply with the observed data. An ultimate position will depend on the proposed future tests to either confirm this is an incredible event, or indicate that it is conceivable if these upper bound conditions exist and a greater than SSE leads to failure.

The work that was done to establish the crack opening rate by ORNL for B&W's thermohydraulic calculations used what was available from the experimental results with some elastic analyses. However, it is subject to criticism. For instance the crack growth rates of 0.5 to 1.0 inch per cycle imply significant ductile tearing; however, the Paris/Tada elastic crack opening functions were used. If this amount of tearing was to occur, then plasticity would occur and the crack opening area would be much larger than the elastically calculated values. More elaborate J-estimation scheme analyses exist to make this type of calculation.

The IPIRG inertial cracked pipe experiments prove that once the maximum load is attained, then the crack growth becomes much more rapid, and for 6-inch diameter pipe only 2 to 4 cycles were needed after reaching maximum load to cause a DEGB. On the other hand, the pure inertial experiments allowed free rotation at the ends. In a piping system, the rotation is limited by the nozzles which may make the crack more stable.

The actual crack opening rate of the plant piping under seismic loading may be significantly different than the current ORNL calculations. It probably would take detailed calculations to make such an assessment.

If a cyclic load test that simulates the earthquake can be achieved, then it should be possible to develop and justify a best estimate bound to the LBLOCA. Analytical correlation together with correlations with other test programs are essential.

d. Comment on the Consistency of the Approach with Recent Regulatory Policy Statements

APPENDIX A

(SECY-88-325) and with Recent Changes to the ECCS Rule [10CFR50.46 (1988)]

One must recognize that 10 CFR 50.46 is for light water cooled plants and was not drafted with heavy water or liquid metal coolants in mind. There is nothing inherent in limiting LBB technology to establishing dynamic effects design bases only. All countries which accept LBB have this limitation nonetheless. The Commission and the ACRS recognize that LBB can in concept be applied to establishing ECCS requirements. However, the proposal by DOE/ORNL would be breaking new ground. The major difficulty would be in defining a replacement breach of the reactor coolant pressure boundary which is sufficiently unlikely to be exceeded. Earlier discussion indicated vulnerabilities in other systems with potential effects on the reactor coolant pressure boundary. The NRC staff made the judgment for commercial light water nuclear power plants that safety would not be improved by allowing the use of LBB for establishing the ECCS requirement, and thus would not invest its resources to promote this use. However, the policy statement leaves open the door for commercial power plant owners to develop the technology (which primarily would be driven by economic concerns) with the understanding that the NRC would be disposed to review and accept this use if adequately justified.

The proposal to go beyond the current use of LBB technology (elimination of local dynamic effects) will be a precedent setting application and must focus on the thermal hydraulic and reactivity responses of a heavy water cooled core to postulated pipe breaks.

A historic perspective of LBB is of value to put it into perspective. Significant development occurred in response to the resolution of USI A-2, Asymmetric Blowdown where the motivation was to demonstrate that a pipe rupture at a PWR reactor nozzle was extremely unlikely and that the dynamic effects need not be considered in the design. Generic Letter 84-04 accepted LBB formally and allowed the removal of pipe whip restraints using the exemption process. The NRC Piping Review Committee in 1985 recommended rulemaking as a necessary action to permit widespread use of LBB. This appeared in NUREG-1061.

Both the limited scope rulemaking amendment to GDC-4 in 1986 and the broader rulemaking in 1987 specifically excluded applications of LBB technology to modify functional and performance requirements for containments and ECCS of LWRs. Only the dynamic effects of pipe ruptures could be eliminated from the design basis when LBB is demonstrated. The broad scope amendment allowed application of LBB to all piping which met rigorous acceptance criteria which included the submittal and acceptance of analyses.

In publishing the final broad scope rule, the Commission indicated that, in the interim, only dynamic effects design bases would be modified; however, the Commission recognized that justifications can be developed for alternative requirements for other aspects of facility design. (See 52 FR 41290, Issue 4). In a Staff Requirements Memorandum dated October 9, 1987 relating to the broad scope rule the Commissioners stated:

> There are possibly other areas which could benefit from expanding the leak before break concept and simplification of requirements such as environmental qualification and

> ECCS. The staff should review other areas for possible modifications and solicit public input through a Federal Register Notice requesting detailed suggestions on changes which could be made to Commission regulations to enhance safety by application of this concept.

The application of LBB to both EQ and ECCS were explored by NRC through public notices in 1988. The upshot was a decision not to expand LBB to cover EQ and ECCS, but rather to revise the ECCS rule. A major factor was selection of a replacement for the instantaneous DEGB. Such a replacement would need to explore all potential breaches in the RCPB such as failures in manways, rupture disks, bellows, flanged connections, pump seals, valve bonnets, branch connections and multiple steam generator tube ruptures. This would need to be done on a plant-specific basis. While the DEGB was considered to be a very remote event <E-6/yr, a decision would be needed as to what the frequency of the more realistic criterion should be; e.g., E-6/yr or E-5/yr.

The ACRS in its March 14, 1989 letter dealing with the expanded use of LBB to EQ and ECCS agreed with the staff's conclusion not to undertake rulemaking to allow the use of LBB to EQ and ECCS at that time. However, the ACRS recommended that an avenue be left open which would allow the use of LBB for EQ and ECCS when technical justification supports the feasibility and benefits of this use.

e. Comment on the Consistency of the Approach with Previously Accepted Applications of Leak-Before-Break Technology and Rules Allowed in GDC-4

Several commercial nuclear power plants have applied for the application of LBB. While the LBB and intermediate break positions were well defined, it took several years to obtain approval of the current version of General Design Criterion 4 of 10 CFR 50 Appendix A. GDC-4 as currently worded follows:

> Criterion 4-Environmental and dynamic effects design bases. Structures, systems, and components important to safety shall be designed to accommodate the effects of and to be compatible with the environmental conditions associated with normal operation, maintenance, testing, and postulated accidents, including loss-of-coolant accidents. These structures, systems, and components shall be appropriately protected against dynamic effects, including the effects of missiles, pipe whipping, and discharging fluids, that may result from equipment failures and from events and conditions outside the nuclear power unit. However, dynamic effects associated with postulated pipe ruptures in nuclear power units may be excluded from the design basis when analyses reviewed and approved by the Commission demonstrate that the probability of fluid system piping rupture is extremely low under conditions consistent with the design basis for the piping.

All such requests have been on a case-by-case basis using plant-specific information or through

owners groups using bounding values.

Conditions differ so markedly in the NP-HWR compared to a PWR that it is difficult to make a comparison. Certainly, each utility did not conduct tests on piping to justify LBB. The approach has depended on analyses and an accumulation of data. It is not applicable to some piping systems such as the feedwater where very severe failures can occur without LBB. Obvious examples of such failures are those due to erosion-corrosion. The best analogy is for the Class 1 PWR systems vis-a-vis the NP-HWR process water system. Loads and failure mechanisms (mechanical fatigue) are similar; however, piping materials differ; e.g., cast stainless or clad ferritic either A-533 or A-508. Certainly, the leak detection systems in the commercial reactors are much less sensitive.

The "bottom line" is that one can argue LBB for the NP-HWR, but one arrives at that conclusion for a different set of criteria.

The tests to validate this approach should be conducted in the lowest toughness region. Use the slant notch fusion line tests suggested in (b) prior to any fracture tests.

The PRAISE code work provides technical arguments that the crack will never get to the size of concern. There are some aspects of that work that need refining; i.e., the criteria for linking of multiple cracks. A limitation is the time required with a Monte Carlo method. Another approach is to use another probabilistic technique where the computational time is very short. A code such as FORM/SORM calculates the probability of failure, assuming a crack with a given leak rate. The subcritical crack growth calculations need to be programmed. It would be a good investment for DOE to have a modern probabilistic code if they are to make calculations in a realistic time frame.

The white paper on eliminating the instantaneous double-ended guillotine break (IDEGB) seems to place heavy emphasis on the moderate (or low) energy characteristics of the system. The low versus high energy argument is applicable for considerations of pipe whip and jet impingement effects. It isn't apparent how the energy argument is applicable to ECCS design. From the documentation it isn't possible to determine whether the IDEGB considerations are for ECCS, or pipe whip, or compartment pressurization, or environmental effects.

Because stress corrosion cracking and other degradation mechanisms leading to 360° effects have been effectively ruled out for the material and service conditions, and because of excellent leak detection capabilities, this proposal is consistent with GDC-4, particularly with respect to local dynamic effects.

DOE/ORNL's statements on LBB and ECCS for FFTF and CNBRP are misleading and should be revised. In these two situations, not requiring ECCS did not result because a DEGB was ruled out by LBB technology. ECCS was not required for these plants because of core physics and the fact that any significant loss of coolant could not be tolerated. To make the consequences of the event less severe, guard pipes and guard vessels were used and this was

irrespective of LBB technology.

Ancillary Item e.1 :Suggestion that you Review the Latest Draft of USNRC Standard Review Plan 3.6.3

In conjunction with the USNRC leak-before-break position, 3.6.3 of the SRP was modified to provide guidance on applying General Design Criterion 4. Again, this may help strengthen your overall position even where DOE has not yet accepted LBB.

f. Comment on Possibilities for Extrapolation of the NP-HWR LBLOCA to other Reactors such as the Savannah River K-Reactor HWR or to Specific ALWR Designs as Examples

The application and acceptance of the NP-HWR LBLOCA to ALWRs such as the AP-600 is doubtful. Conditions differ too greatly and the conditional acceptance of LBB by the USNRC doesn't warrant a shifting of the base. The data base is of limited use to the commercial reactors.

Basically, the possibility of extrapolating GDC-4 is limited to local dynamic effects; with other reactors it is dependent on precluding the material degradation conditions discussed in SRP 3.6.3. For ECCS applications, the core thermal hydraulics and reactivity response when a DEGB is postulated to occur also needs to be evaluated in addition to identifying the relevant degradation conditions.

g. State Consensus and note Dissenting Opinion among Panel Members in Conjunction with these Reviews and in Consideration of the Points of Scope Listed above

No dissenting opinions were expressed by the members of PIRG. We have used g to collect some items that do not fit well elsewhere. These are included here with the exception of an overall opinion under h.

Ancillary Item g.1 : Concern with Regard to the RHR Line

As we understand the proposed layout of the RHR line, it is un-isolable from the reactor in the event of a break inside containment. An obvious concern is the accumulator feeding the RHR line where the high center of gravity of the accumulator with respect to the RHR line means that particular emphasis is required to ensure support of the accumulator so that it is not affected by a severe seismic event. While PIRG believes this problem is recognized, we cite it because the failure probability of the RHR may prove to be higher than the Process line.

h. Prepare and Submit a Written Report based on (g), which includes each Panel Member's Considered Opinion

The preceding complies with the requirements of h.

APPENDIX A

Ancillary Item h.1 :Suggestion that a Comprehensive Internally Consistent Report be Developed

The PIRG believes that a comprehensive, internally consistent report is essential to "sell" the Defense Nuclear Facilities Safety Board on the concept of either a DEGB occurring over a finite time or the justification of leak-before-break preceding or applying during a severe seismic event. Essential components of such a report are the following:

- A clear presentation of the ORNL tests, including the modifications suggested by PIRG;
- Presentation of relevant simulated seismic tests on piping that complement the ORNL tests;
- Analytic verification/confirmation of the behavior of 316NG piping under severe seismic loads when containing a through-wall flaw long enough to release D_2O at rates well above the detection thresholds of the tritium detectors; a geometry simulating the process water system from vessel to heat exchanger is reasonable; the seismic input should consider the potential site;
- All of the above components should be combined into a defensible definitive report;

General comments intended to strengthen DOE presentation to the DNFSB

In general presentations should not be made to the board that have questionable viewpoints or involved discussions that don't directly get to the point. Examples of things that should not be included in a DNFSB presentation are:

> Don't talk about the South Texas piping system used to estimate the loads for the NP-HWR. At this presentation, you should have the system defined enough so that actual design values are available.
>
> Don't talk about hardness methods to determine the strain-hardening of the material when actual tensile test data are available.
>
> The impact testing concept to simulate seismic loading is difficult to accept. A very long explanation is necessary to demonstrate similitude with seismic loading, and even then, it is necessary to conduct some detailed dynamic calculations for the actual plant to have confidence in the impact test results. It was apparent from the Blue Ribbon Panel's reactions of not being enamored with the impact testing, that a similar response would come from the DNFSB and their consultants. You should think hard about basing your technical arguments for non-instantaneous break DEGB on impact test results.

APPENDIX A

Some other detailed technical aspects that conflict with information in the open literature are:

(1) For the complex (or compound) crack geometry there is a constraint condition that reduces the material toughness significantly. T_{mat} values from TP304 stainless steel complex-cracked pipe experiments have been determined to be as low as 10 to 15 instead of the C(T) specimen values of 100 to 150.

(2) The J solution in ORNL/NPR-9218 report lacks certain factors. The elastic term is missing the shell stress-intensity magnification factor, $F(\theta)$, which has been developed by Erdogan, Folias, and more recently by Sanders for different shell thicknesses. There are a half dozen J plastic solutions for circumferentially cracked pipe, but the solution used in this report isn't available so it isn't possible to know how it compares to past experimental pipe fracture data or these other analyses.

TABLE 1 - FAILURES BY MECHANISM FOR PIPING $\geq$2-IN. D.
PERIOD 1964-91

MECHANISM	NO.	CL.1	CL.2/3	BOP
VIBRATORY FATIGUE	5	0	2	3
WATER HAMMER	9	0	4	5
THERMAL FATIGUE	0	0	0	0
MAINTENANCE ERROR	0	0	0	0
EROSION&CORROSION (36)				
GENERAL/MIC	4	0	3	1
CAVITATION	2	0	2	0
EROSION-CORROSION (30)				
SINGLE PHASE	11	0	7	4
WET STEAM	19	0	0	19
MISCELLANEOUS (37)				
DESIGN/FAB.ERROR	4	0	2	2
OVER-PRESSURE/OP. ERROR	4	0	2	2
PUMP SEIZURE	1	0	0	1
GASKET FAILURE	2	0	1	1
CONSTRUCTION	4	0	4	0
VALVE PULLOUT	2	0	0	2
EXPANSION JOINTS	14	0	1	13
OTHER/UNKNOWN	5	0	3	2
VALVE RUPTURE	1	0	1	0
	87	0	32	55

FAILURES ARE DEFINED AS SEVERANCE, MAJOR SPLITS, FISH MOUTH.

APPENDIX B

Review & Synthesis Associates
Spencer H. Bush, P.E. • 630 Cedar / Richland, Washington 99352

January 18, 1993

Mr. David L. Moses
ORNL-NPR Project Manager
Oak Ridge National Laboratory
P.O. Box 2009
Oak Ridge, TN 37831-8051

Dear Mr. Moses:

Subject: Final Report of the Piping Integrity Review Group (PIRG)

Attached is the final report of PIRG. I believe that the report is responsive to the approach suggested in the first report of PIRG. You will note that we have expanded the coverage to cover a spectrum of reactors of interest to DOE.

Unless I hear from you to the contrary, I believe that the submittal of this report is the final activity of PIRG and the group now is dissolved.

Very truly yours,

Spencer H. Bush
Chairman, PIRG

RSA
Telephone: Business - (509) 375-2223 & 375-3749 / Home - (509) 943-0233

APPENDIX B

SECOND REPORT OF THE PIPING INTEGRITY REVIEW GROUP BY MEMBERS OF PIRG

FOREWORD

The Piping Integrity Review Group (PIRG) was established to provide a technical review of tests on wrought austenitic stainless steel piping subjected to repetitive loads simulating sixty years of operation of the heavy-water New Production Reactor. This end-of-life condition was followed by severe loads simulating greater than SSE seismic loading. This report is the second and last, with discussion limited to one experiment (C-Pipe) and supporting analytic studies.

The following PIRG members participated actively in the development of this report:

Spencer H. Bush, Chairman
Robert J. Bosnak
Macintyre R. Louthan
Everett C. Rodabaugh
Gery M. Wilkowski

In addition, the following member provided written comments, but did not attend the review and discussion sessions:

Robert P. Kennedy

INTRODUCTION

This report addresses the comments, conclusions and recommendations of PIRG related to the C-Pipe test and the analytic studies supporting or expanding on this test. The first report[1] addressed scope issues in the PIRG Charter. This report has, as its basis, the experience gained in preparing the first report; however, the second report is a "stand alone" document based on information provided at or before a meeting of PIRG on December 16-17. The conclusions and recommendations of this report are based on this second meeting of PIRG, the information exchanged and the combined engineering judgment of the members cited in the Foreword who actively participated, or provided comments in the form of letter reports.

APPENDIX B

EXPERIMENTAL PROGRAM

The experimental program on C-Pipe can be divided into three distinct sectors presented in the "White Paper for the Piping Integrity Review Group", ORNL 12/7/92:

- The fatigue test leading to the generation of a through-wall crack;
- The severe cyclic loads attempting to simulate a seismic event greater than 1 SSE;
- A combination of load sequences ultimately leading to complete severance of the pipe weld;

PIRG agrees that cumulatively these three sectors represent very severe loads that confirm the high toughness of a wrought austenitic stainless steel such as AISI 304 and the resistance to double-ended guillotine break (DEGB) of this class of alloys; however, PIRG has specific reservations with regard to the test when taken in the context of an operating reactor piping system.

We will address the following classes of reactors:

- The heavy-water New Production Reactor;
- Westinghouse Savannah River Reactors such as K;
- Other DOE Test Reactors using Austenitic Stainless Steel Piping and operating at relatively low pressures and temperatures;
- Planned DOE Reactors such as the Advanced Neutron Source;
- Advanced Light Water Reactors such as SBWR and AP-600 where DOE sponsors work in such reactors;

C-Pipe was selected because it was believed to contain IGSCC. Examination did not detect IGSCC; however, a substantial lack-of-penetration at the weld root was detected. Such a fabrication defect would lead to a stress intensification factor substantially greater (~1.65) than the 1.0 typical of a high-quality girth butt weld. Although the number of cycles to leakage was less than Section III (Figure I-9.2.1) would allow, the number was far more SSE level cycles than would occur.

The fatigue test intended to simulate behavior after sixty years of operation is unduly severe for all of the above classes of reactors; namely:

Fatigue Test: applied 118000 cycles of nominal stress (M/Z) of +/- 14.4 ksi, which produced a through-wall circumferential fatigue crack about 2-inches long;

Crack Growth Test: applied 39 cycles of a nominal bending stress (M/Z) of +/- 52.5 ksi, which grew the initial circumferential crack from about 2-inches to about 16-inches length;

The first four classes of reactors have limited thermal gradients so thermal fatigue should be a minor contributor to cracking. Mechanical or vibrational fatigue in larger diameter piping also should not be a major contributor unless there is excessive vibration from sources such as pumps. Our engineering judgment is that the Cumulative Usage Factor (CUF) during reactor operation should be no more than 0.1, whereas the fatigue test probably reached a condition comparable to a CUF=1 after fatigue cycles simulating a few years of operation. The fifth class of reactors, SBWR and AP-600, should reach higher CUF values than 0.1 in the nozzle regions after 60 years, but much less than the condition represented by the 118,000 fatigue cycles provided by the fatigue program. A CUF in current BWRs and PWRs in the nozzle regions should be well below 1.0 at forty years and, probably, below 1.0 at sixty years. An ASME Section III analysis which gave a CUF below 1.0 would predict no cracking at end-of-life, or, at most, limited onset of cracking.

The above arguments apply to fatigue and corrosion-fatigue processes. They do not apply to stress corrosion cracking in austenitic stainless steels with sensitized heat-affected zones such as are present in the Savannah River Reactors or in other DOE Reactors containing sensitized stainless steel piping. PIRG has suggested an analytic study simulating the behavior of a pipe which contains a crack similar to that found in a boiling water reactor (Duane Arnold) where 360° IGSCC occurred to depths at or greater than 70%t. We hope that BMI can simulate this condition using the approach discussed under ANALYTIC PROGRAMS.

Stress corrosion should be a minor issue in future DOE reactors or in the ALWRs because the materials selected will be quite resistant to IGSCC; therefore, the IGSCC problem is limited to the existing DOE Reactors containing a sensitized HAZ.

The second sector covered cyclic loading conditions intended to simulate 3 SSE loads with a probability $\leq$E-6. PIRG agrees that the 40 cycles represent a very severe cyclic loading sequence where the through-wall crack grew from 2-inches to 16.5-inches. While the cyclic loading was very severe, we doubt that it truly simulates a 3 SSE earthquake. Loading rates and stress reversal times differed markedly from those expected in an earthquake. From the point-of-view of material response we believe the crack growth observed was much greater than in a 1 SSE earthquake; however, we do not believe it is possible to draw a direct comparison with the behavior in an 3 SSE quake. In any event this slow loading should be much more conservative than the loading in an actual quake.

The third sector confirms an opinion cited earlier; namely, austenitic stainless steels are very tough and, even after generating a 16.5-inch crack representing about one-third of the piping circumference, it required a substantial number of high-load cycles before total severance occurred. In essence, this confirmed the resistance to severance of the material even after a condition simulating a very severe earthquake.

ANALYTIC PROGRAMS

PIRG compliments BMI on an excellent, albeit preliminary, analytic study simulating both a modelling of crack growth and a realistic dynamic fracture assessment of a typical NPR-HWR primary pipe system. Other experiments and accompanying analyses have confirmed that the analytic technique used can predict observed experimental behavior with an acceptable degree of accuracy. These studies confirmed which welds would see the highest loading conditions. As expected, they were in the welds attaching elbows to the reactor pressure vessel nozzles and the heat exchanger nozzles.

Direct ΔJ versus da/dN values from the ORNL C-Pipe test were compared to the EDEAC data base values for TP304 stainless steel. The comparison of the C-Pipe test data was extremely close to the extrapolated EDEAC curve, even without crack closure. This modelled crack growth quite well. The analysis methodology verification covered:

- A comparison of J-estimation scheme prediction with NRCs Degraded Piping Program cracked pipe quasi-static loading experimental data base.

- Comparison of dynamic cracked pipe analyses with International Piping Integrity Research Group (IPIRG-1) pipe system experiments.

The crack location was predicted to be at the weld attaching the elbow to the reactor nozzle. The summary statements are significant; namely:

- 3 SSE loading does not initiate (propagate) the 10-inch long crack:
- Portions of the piping will yield;
- The leak rate area is very small;

The above summary statements are sensitive to input assumptions (not surprising). Also, the dynamic model assumes the following:

- Only ductile tearing with no fatigue crack growth;
- No plasticity assumed in uncracked pipe (Ramberg-Osgood materials behavior);
- Analyses based on best information available;

APPENDIX B

The latter caveat covers the use of nominal properties not necessarily those of C-Pipe as well as knowledge of the actual boundary conditions and pipe loop dimensions. A conclusion one can draw from these analyses is that the experimental results were more severe (and more conservative) than the analytic results simulating seismic loads for this crack length. This could be due to load rates and times to load reversal where the analytic model had rapid reversals compared to the slow reversals in the experiment. PIRG recognizes that the approach used represents "advanced state-of-the-art" and will require validation and refinement once actual pipe system design conditions are finalized.

All seismic analyses conducted for this study utilize current regulatory guidance and were not based on proposed revisions now out for public comment; i.e., the new Appendix B to 10 CFR 100 and the new Appendix S to 10 CFR 50.

REAL PIPING SYSTEMS

Nuclear plant piping systems designed to ASME Section III with a fatigue analysis for Class 1 systems and Category I seismic should display no, or, at most, very limited cracking, even after life extension to sixty years. This assumes the transients used in the design analysis reasonably simulate actual operating conditions, or that operating conditions are less severe than design conditions. System design conditions are presumed to preclude thermal stratification and other unpredicted and unreviewed thermal cycling events. Inherent in these assumptions is the additional assumption that failure mechanisms other than fatigue do not occur. For IGSCC, the assumption probably isn't valid for older plants such as the Savannah River Reactors; therefore, this condition must be considered outside the design envelope. Our experience is such that we should be able to select materials and fabrication/joining processes to minimize or eliminate SCC in plants yet to be constructed.

Another potential failure mechanism is water hammer. The low pressure/low temperature reactors without valves or bellows in the Class 1 systems should have few or no water hammers and, if they occur, the energy content should be low enough so that austenitic stainless steel pipes should suffer little or no damage. This position applies to Class 1 systems, not necessarily to Class 2/3 systems or balance-of-plant. This is particularly true for BWRs and PWRs and the ALWRs. While we can conclude that Class 1 systems will be relatively unaffected by water hammer, this cannot be extrapolated to other systems.

Inherent in the above comments is a position PIRG believes should apply to future reactors or to replacement piping in existing DOE reactors. We believe piping should not be less than Schedule 40 for diameters leading to wall thicknesses less than 0.5-inches and larger diameter pipes should have at least 0.5-inch wall thickness.

There are benefits in construction, resistance to transients, ISI crack detection, and to overall reliability. The bottom line with piping systems in operating or planned reactors is that the CUF should be well below 1.0 and fatigue cracking should not be an issue even at end-of-life.

FAILURE MECHANISM

For Class 1 austenitic stainless steel piping systems in reactors operating near or below 100°C, fatigue should not be a problem. IGSCC can be an issue in older plants, but should not be one in new plants. This should apply to both reactors operating at low temperatures and to those operating at conditions typical of commercial BWRs and PWRs. Water hammer should be a minor issue in Class 1 systems, particularly if the new EPRI guidelines are used. The above applies to Class 1 systems. These criteria should not be applied to Class 2/3 or BOP without appropriate analyses.

CRACK/FAILURE PROBABILITIES

The following discussion is intended to apply to DOE reactors having Class 1 systems fabricated of wrought austenitic stainless steel and operating near or below 100°C with appropriate pressures for these temperatures. The generation of a through-wall crack of 2-inches, comparable to the ORNL C-Pipe test should have a very low probability of development by a fatigue-controlled mechanism. Calculations using the PRAISE computer code in this country and in Germany for PWRs yield annual failure probabilities substantially below E-7 (E-9 to E-14). Since the crack driving forces should be less in a low temperature system than in a PWR, the probabilities for fatigue cracks to develop should be even lower. PIRG arbitrarily accepts a value of E-7 at end-of-life for through-wall cracking. We believe a definitive PRAISE calculation would confirm that the cumulative value throughout life is less than E-7 for the low temperature classes of reactors. We suggest that the existing PRAISE results, particularly those for Biblis-B be used for PWRs.

It is possible to use PRAISE-CC for IGSCC. This has been done for BWRs; however, PIRG believes a probability cannot be assigned for generation of long through-wall IGSCC cracks without appropriate analysis. We prefer the analytic approach using a 360° crack simulating the crack found in Duane Arnold, then analytically applying a severe (3 SSE) seismic event to a pipe containing that crack.

The probability of a 3 SSE seismic event at a site such as Savannah River will have a probability of about E-6/year. Therefore, we have two conditional probabilities, that of a through-wall crack at end-of-life and the 3 SSE seismic event assuming there is no repair of the crack. The combined probability will be about E-13 assuming the seismic event occurs at end-of-life. This value is far below

the probabilities accepted by USNRC; therefore, we conclude that a break even larger than predicted experimentally and analytically (namely, the DEGB) should not be a Design Basis Event (DBE) for these low temperature/pressure reactors.

While this probabilistic approach can be applied to ALWRs, PIRG is unwilling to accept similar values without rigorous analysis.

ACTIONS TO REDUCE FAILURE PROBABILITIES

Inherent in the PRAISE Code are assumptions that cracks may be detected by Inservice Inspection, leak detection, or other techniques such as Acoustic Emission. In addition, optimum material selection for Class 1 systems and incorporation of a seismic trip represent items that reduce failure/accident probabilities and core damage significantly. Materials selection, Inservice Inspection and leak detection will be addressed to illustrate how each can assure that severe cracking/failure probability is very low.

MATERIAL SELECTION

For existing low temperature/pressure DOE reactors using austenitic stainless steel piping, the prior arguments apply to the very low probability of fatigue crack growth. IGSCC is still an issue in older reactors; however, it should be controlled in future DOE reactors. We assume that future reactors will use the 1992 or later edition of Sections III and XI.

INSERVICE INSPECTION

The 1992 version of ASME Section XI will be used as a reference condition to indicate the reduction in failure probability. Class 1 systems require at least 25% of the welds be examined using either Plan A or Plan B of IWB-2411 or IWB-2412. An example problem is used that can be applied to an HWR-NPR. If one assumes ten welds in each hot leg and cold leg (high), there will be 60 welds in the six hot legs and 60 welds in the six cold legs. A 25% sample would require at least 15 welds be examined in both systems. Analysis should confirm that the welds adjacent to the pressure vessel and heat exchanger nozzles will have the highest CUFs. The preservice ultrasonic examination on 100% of the welds will serve as a baseline. If only 25% of the welds are examined for either Plan A or Plan B Intervals, emphasis should be given to welds at or near nozzles per IWB-2500 B-J and welds between straight pipe and elbows. With two such welds at each nozzle, not all nozzle welds would be examined per interval with a 25% sample. An obvious solution is to be sure that all critical welds are examined in any two sequential intervals. If one uses the A Plan (no domestic reactor does), the probability of picking up gross design/installation errors early in life is maximized. If there is a concern with "wearout" in the last 20 years of a 60 year life

(improbable), reversing the first 20 year intervals of the A Plan will optimize the inspection intervals as the plant ages and should enhance the probability of detection of cracks.

If the weld joint is optimized for UT, and Section XI, including Appendix VIII is used, the probability of detection of a 50% through-wall fatigue crack, when accessible from both sides of the weld, should be 0.8 to 0.9, even for wrought austenitic stainless steel piping which is more difficult to examine ultrasonically than is carbon steel piping. Stress corrosion cracks are more difficult to detect; however, 50% through-wall crack should have 0.7 to 0.8 probability of detection. The inspection problem for IGSCC is the determination of which weldments to inspect. It does not follow that those having the highest probability of failure by fatigue will be most likely to crack by IGSCC.

LEAK DETECTION

The tritium content of the moderator/coolant in heavy water reactors provides the capability for very sensitive, on-line leak detection. Application of this capability to the NPR-HWR will reduce the probability of a large break failure by increasing the assurance that any flaw that may develop in the piping and grow through-wall will be detected when the leakage rates are very low. For example, the sensitivity for leak detection in the SRS reactors (moderator/coolant loss of 0.0001 gallons per minute) far exceeds the performance of leak detection systems in commercial nuclear reactors (approximately 1 to 5 gallons per minute)[2].

The NPR-HWR may have been slightly less sensitive to leakage than the current SRS reactors because of moderator detridiation. However, even with detridiation, the leak rate sensitivity for the NPR-HWR would far exceed that of commercial nuclear reactors. The tritium content in the SRS reactor moderator is approximately $3\text{-}5 \times 10^{(-2)}$ Curies per cubic centimeter. Detridiation was anticipated to maintain the tritium content in the moderator/coolant of the NPR-HWR at approximately $1 \times 10^{(-2)}$ Curies per cubic centimeter. This reduction in the tritium content of the moderator/coolant may reduce the leak detection sensitivity. The magnitude of that reduction would depend on the plant design, but, in any event, the leak detection system would be capable of detecting very small (tens of pounds per day) amounts of leakage.

The ability to detect small amounts of leakage will provide significant assurance that through-wall cracks are detected before they approach a critical size. Application of this leak detection capability to detect small through-wall cracks, combined with the materials selection and the in-service inspection programs, to provide additional margins of safety against large-break loss-of-coolant accidents.

While the leak-detection in a D_2O cooled/moderated low-pressure

reactor should provide more than adequate LBB margin, the same may not be true for a low-pressure reactor cooled with H_2O. In such a reactor one depends on the detection of water losses of 2-5 gpm often requiring several hours before these losses are noted. This may be critical in systems susceptible to IGSCC because one may generate 360° cracks at low applied stresses and the leak detection would be the same as for a relatively short simple crack, with the major difference that the 360° crack would require substantially lower seismic loads to cause failure. If such a condition is anticipated, a more intensive NDE program may be required to detect cracks before they reach critical size. Of course the problem will be to select the correct welds to inspect.

IMPLICATIONS OF FAILURE PROBABILITIES

If reactors are grouped loosely into three sets; namely:

- Operating DOE heavy or light-water reactors where the temperature T is about 100°C, maybe less and the primary system is austenitic stainless steel;
- Planned DOE reactors where T is about 100°C and P is <250psi;
- The proposed ALWRs;

For the first group probability of a through-wall fatigue crack is very low; e.g., ≤E-7 during plant life. IGSCC will have a much higher probability; however, the probability of a potentially unstable crack such as 360° and nearly through-wall should be low because of bending moments during plant operation driving the crack through the wall so it is detected by leakage.

Failure (DEGB) due to fatigue cracking plus a severe seismic event has a very low probability (~E-13) so this scenario should be relegated to beyond DBE.

IGSCC can occur; however, IGSCC plus seismic to yield DEGB should have a low probability. The proposed analysis should clarify this scenario.

Set two is the same as the first part of Set 1 where IGSCC is not an issue. The scenario should be relegated to beyond DEGB.

Set three represents higher pressures and temperatures, more mechanisms such as thermal fatigue and stratification to fatigue the pipe. IGSCC should not be an issue. Therefore, one should anticipate a low probability of DEGB, but a higher overall probability of severe cracking. Also, axial cracking could be a problem. One can be cautiously optimistic that the overall probability of DEGB is <E-7, but more work would be necessary to

arrive at a value accepted by Regulatory Authorities.

RESTRICTIONS RELATED TO CONCLUSION ONE BELOW

For fatigue as the mechanism leading to cracking and applying the following restriction:

- Material is wrought austenitic stainless steel;
- Pipe is schedule 40 or no less than 0.5-inch wall for larger diameter piping;
- New materials selected essentially are immune to IGSCC;
- Reactors considered are essentially free from severe water hammer;
- Primary system temperatures not exceeding (~100°C) and pressures (≤250psi); therefore, thermal fatigue should not be an issue;
- Massive components such as pumps or heat exchangers are anchored so that a severe seismic event will not lead to gross movement of the component and overload failure of the pipe;
- For newer reactors ASME Section III Division 1 is used; for planned reactors the 1992 or later edition of the Code is used, provided that later editions are comparable to the 1992 edition;
- An Inservice Inspection program basically complying with IWB of Section XI (1992 edition) is in place;
- Technical Specifications define a leak detection system; this may be more difficult for low pressure light-water reactors;

CONCLUSIONS/RECOMMENDATIONS

Provided the restriction cited in the RESTRICTIONS RELATED TO CONCLUSION ONE section are in force, then the following conclusions are applicable:

(1) For DOE reactors at low pressure (≤250psi) and temperatures not exceeding (~100°C) with austenitic stainless steel piping, the DEGB should not be a DBE;

(2) For DOE low pressure low temperature reactors subject to IGSCC the analytic results with a 360° deep crack indicate that an instantaneous DEGB is highly improbable; PIRG believes further analyses would confirm that the instantaneous DEGB need not be a DBE used to evaluate core flow instability;

- For ALWRs, information is inadequate to justify relaxation of the current DEGB requirements other than that provided by 10CFR50 GDC-4 and 10 CFR 50.46 regarding leak-before-break;

With regard to recommendations, PIRG suggests that further

analytic studies could lead to relaxation of the instantaneous DEGB requirement as a DBE when the crack mechanism is IGSCC.

REFERENCES

(1) First Report of the Piping Integrity Review Group by Members of (PIRG)

(2) R. L Sindelar and W. L. Daugherty, WSRC-RP-90-99, Savannah River Laboratory, Aiken, SC 29808 (March 9, 1990)

APPENDIX C

FINAL REPORT

on

Battelle NP-HWR Analytical Assistance Program

to

Martin Marietta
Energy Systems, Incorporated

by

G. M. Wilkowski
R. Olson
S. Rahman
R. Mohan
R. Wolterman

January 29, 1993

Battelle
505 King Avenue
Columbus, Ohio 43201

APPENDIX C

CONTENTS

Page

EXECUTIVE SUMMARY 1

4.0 COMPARISON OF CYCLIC CRACK GROWTH DATA FROM THE ORNL C-PIPE TEST WITH EXTRAPOLATION OF FATIGUE CRACK GROWTH DATA 43

4.1 Objective 43
4.2 Method of Analysis 43
4.3 Results 44
4.4 References 45

5.0 DYNAMIC PIPE FRACTURE ANALYSIS OF A PROTOTYPICAL NP-HWR PIPE SYSTEM SUBJECTED TO SEISMIC LOADING 48

5.1 Objective
5.2 Leak-rate Analysis for Sizing of the Through-wall Crack 48
5.3 Moment-rotatin Predictions for Complex-cracked Pipe 49
5.4 Dynamic Pipe Fracture Calculations of NP-HWR Pipe System 51

5.4.1 Analysis Tools and Methodologies 53
5.4.2 Analysis of NP-HWR Pipe System 59

5.5 Results 63

5.6 References 64

6.0 CONCLUSIONS 110

APPENDIX C

EXECUTIVE SUMMARY

Battelle was commissioned by ORNL to perform analyses to assist in the design and analysis of experiments and evaluations of actual behavior of postulated cracks in a pipe system representative of the proposed DOE New Production Heavy Water Reactor (NP-HWR). The project lasted from August 1992 to the end of January 1993. There were four analytical efforts undertaken.

- The first effort was a sensitivity study to analytically determine the family of surface crack geometries that could fail at various normal plus safe shutdown earthquake (N+SSE) stress levels. The subsequent work in this report and the work done by ORNL all dealt with through-wall-cracked pipe where leak-before-break (LBB) behavior can occur. From the work in this effort, we would like to point out that there is a potential for a surface-crack failure without detection of leakage that may be more challenging to the structural integrity of the pressure boundary of the reactor. The analysis in this effort were a first step in the structural integrity assessment of a surface crack causing a pipe failure, and additional surface-cracked pipe evaluations under dynamic loading are needed to complete this assessment.

- The second effort provided pretest predictions of the C-pipe experimental load, load-line displacement, crack growth, center-crack-opening displacement and the resulting crack-opening area. These results were used by ORNL to assess the C-pipe test. Considering that typical, not actual, values of the material strength and toughness were used in these calculations, the agreement was quite good.

- The third effort was to determine if the cyclic crack growth in the low cycle fatigue tests on the C-pipe agreed with an extrapolation of high-cycle fatigue data on TP304 stainless steel from the EPRI Database on Environmentally Assisted Cracking (EDEAC). This agreement was extremely good, implying that in principle, one could make slightly conservative, yet reasonably accurate, predictions of such crack growth.

- The final effort was to conduct nonlinear time-history seismic analyses of one design of the NP-HWR pipe loop with a crack in it subjected to 3SSE loading. Although the exact dimensions and boundary conditions of the pipe loop modelled probably differ from what would be the final design configuration, this time-history nonlinear cracked-pipe analysis showed that there is considerable margin over conducting typical response-spectrum uncracked pipe elastic stress analysis for the fracture evaluations. The nonlinear time-history analysis of several very severe cracks showed that there was margin of over a factor of 5 compared with predictions using elastic uncracked pipe analyses typically used. This margin comes from the short duration of the large amplitude cycles in the seismic event and the nonlinear behavior of the crack. Furthermore, the nonlinear time-history analysis, even with a crack more severe than the Duane Arnold safe-end intergranular stress corrosion cracks, showed only a small amount of ductile tearing after the 3SSE loading.

The key findings of this work are that the occurrence of a double-ended guillotine break (DEGB) for the conditions examined are highly unlikely, even with the most severe crack geometry that occurred in a commercial power plant. Furthermore, the results to date show that the peak dynamic crack

opening for this worst case crack was less than 22 in^2, which is less than 10 percent of the area ot a double-ended break, with an even smaller residual crack-opening after the seismic event was completed. This relatively small crack-opening area should preclude thermohydraulic problems that Babcock and Wilcox predicted using the RELAP code assuming an instantaneous DEGB.

Should the NP-HWR program restart, these analyses should be repeated with the precise boundary conditions and geometry of the final design of the plant piping. The analyses should be extended to include the effects of low cycle fatigue crack growth during the seismic event, as well as the ductile tearing calculations that were done to date. Effects such as reverse cyclic loading on decreasing the toughness were not included at this time, since they involve evolving technology and interactive time-history analyses that were beyond the limitations of the level of effort funded. Finally, analyses should be conducted to assess the propensity of fracture for a surface crack to propagate under dynamic loading, since all the work to date was on through-wall-cracked pipe. This would provide guidance for the maximum allowable surface-crack length for in-service inspection criteria.

APPENDIX C

4.0 COMPARISON OF CYCLIC CRACK GROWTH DATA FROM THE ORNL C-PIPE TEST WITH EXTRAPOLATION OF FATIGUE CRACK GROWTH DATA

4.1 Objective

The objective of this effort was to assess if the cyclic crack growth in the C-pipe experiment is consistent with extrapolation of high cycle fatigue data crack growth data. If so, then it may be possible to calculate low cycle fatigue crack growth, for a loading such as that conducted in the C-pipe test in a totally predictive manner. Hence, this approach would be independent of the prediction of ductile tearing by J-R curve methods, such as discussed in the last section.

4.2 Method of Analysis

The analysis of cyclic crack growth classically involves the use of the linear elastic stress intensity factor, K. In the presence of plasticity at the crack tip, Dowling (Ref. 4.1) used the J-integral parameter. In our report, the cyclic J, ΔJ, is calculated by integrating the load-displacement test record on a cycle by cycle basis. This is illustrated in Figure 4.1. This is a relatively straight-forward procedure, except when the reverse loading is negative. With negative load ratios[2], the area used for calculating the energy for ΔJ is more complicated. For fully reversed loading, it has been suggested that a negative load level be used that would correspond to the crack, Ref. 4.2. This is sometimes estimated to be at 30 percent of the tensile load, but it can also be determined from the experimental test record.

The calculation of J for a through-wall-cracked pipe experiment where the load and load-line displacement are known is best done using an analysis known as and η-factor analysis, Ref. 4.3. Here,

$$J = J_e + J_p \tag{3.1}$$

and J_e is the elastic contribution of J taken from the elastic solution by Sanders as given in Ref. 4.4. The J_p term is the plastic contribution of J, and requires the η-factor solution in Equation 3.2.

$$J_p = 2\int \eta P d\delta p + (2/R)\int_{a_0}^{a} \gamma J_p da \tag{3.2}$$

---

[2] The load ratio or R-ratio is the ratio of the minimum to the maximum load.

where:

η	=	$-h'(\theta)/(Rth(\theta))$
$h(\theta)$	=	$\cos(\theta/4) - 0.5 \sin(\theta/2)$
γ	=	$h''(\theta)/h'(\theta)$
P	=	half of total load from four-point bending
t	=	thickness
δ_p	=	plastic displacement
θ	=	half crack angle
a	=	crack length at mean radius
R	=	mean radius

The important consideration in analyzing the data is that the displacement is only the plastic component of the displacement. Hence, elastic displacements from the uncracked pipe, elastic displacements from the crack, and displacements for the compliance of the test machine need to be subtracted from the experimental displacements.

Moreover, to account for the effects of crack closure, the data need to be examined to determine the crack closure loads. On examining the ORNL C-pipe experimental data, it appeared that crack closure occurred on Cycle 1 at a load of 50,000 pounds and on Cycle 38 at a load of 54,400 pounds.

The calculation of J using the η-factor equations and accounting for the elastic displacements is done automatically in a program developed at Battelle called IETAPIPE. This program was used to determine the compliance of the test machine, and calculate the elastic and plastic contributions of J.

4.3 Results

ΔJ values were calculated with and without crack closure load corrections. Since this was not a totally automated procedure, the ΔJ values were calculated only for Cycle 1 and Cycle 38. This represents the extremes, where crack growth was the smallest and the largest in the C-pipe experiment.

In hindsight, it may have been better to use Cycle 2 instead of Cycle 1, since Cycle 1 may contain some plasticity in the uncracked pipe which will add to the energy calculations and give a higher J value. In Cycle 2, the uncracked pipe has been strain-hardened to take this load elastically, and the uncracked pipe plasticity is no longer a concern.

The ΔJ values were converted to ΔK values using

$$K = (JE)^{0.5} \tag{4.3}$$

where E is the elastic modulus, and was assumed to be 29,000,000 psi from a handbook.

APPENDIX C

The calculated ΔK versus da/dn values from the C-pipe experiment were compared to an extrapolated curve of data available from the EPRI Database on Environmentally Assisted Cracking (EDEAC) operated by Battelle for EPRI, Ref. 4.5. The C-pipe test values are compared to the EDEAC data and a linear regression line through only the EDEAC data in Figure 4.2. The C-pipe data points fall remarkable close to the EDEAC extrapolated curve.

Two observations can be made from Figure 4.2. The first is that the data without crack-closure-load corrections was as good or better than that with the crack-closure load correction. Secondly, the data from Cycle 1 had a higher ΔK value relative to the corresponding EDEAC curve da/dn value than the ΔK value from Cycle 38. This may be due to plasticity of the uncracked pipe on the first loading cycle as previously mentioned. Nevertheless, the agreement with the EDEAC extrapolated curve is extremely good, and this result shows that in principle, one could use the EDEAC curve as a design basis to predict the C-pipe test.

4.4 References

4.1 Dowling, N. E., and Begley, J. A., "Fatigue Crack Growth during Gross Plasticity and the J-Integral", Mechanics of Crack Growth, ASTM STP 590, 1976, pp. 82-103.

4.2 Joyce, J. A. and Hackett, E. M., "Elastic-Plastic Characterization of a Cast Stainless Steel Pipe Elbow Material," NUREG/CR-5774, January 1992.

4.3 "The Development of a Plan for the Assessment of Degraded Nuclear Piping by Experimentation and Tearing Instability Analysis," Prepared for NRC by Battelle, Final Report, NUREG/CR-3142, June 1983.

4.4 Klecker, R., and others, "NRC Leak-Before-Break (LBB.NRC) Analysis Method for Circumferentially Through-Wall-Cracked Pipes Under Axial Plus Bending Loads", NUREG/CR-4572, May 1986.

4.5 Agrawal, A., Chandler, K., Hopper, A., and Mindlin H., "EPRI Database for Environmentally Assisted Cracking (EDEAC) - Revision 1", Battelle interim report to EPRI on Project C102-9, July 1992.

APPENDIX C

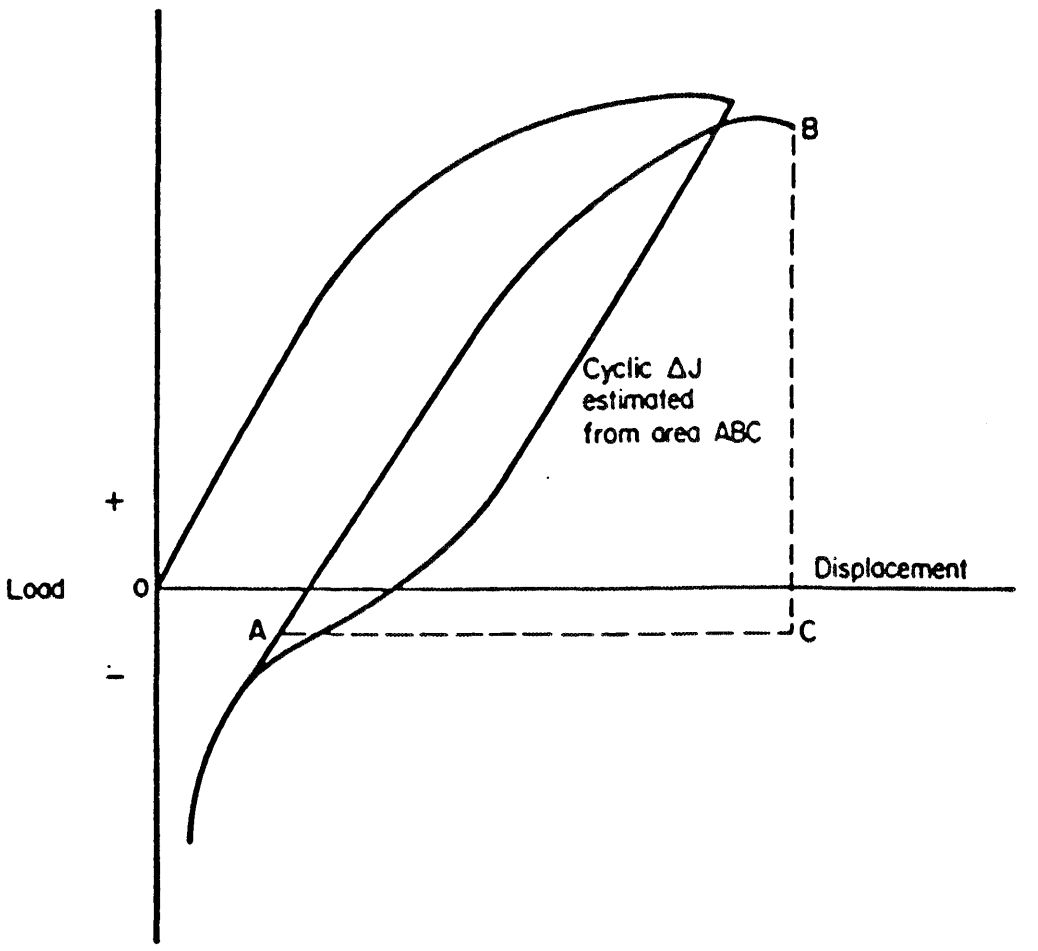

Figure 4.1 **Dowling analysis of area used in J calculations for crack growth in the presence of plasticity**

APPENDIX C

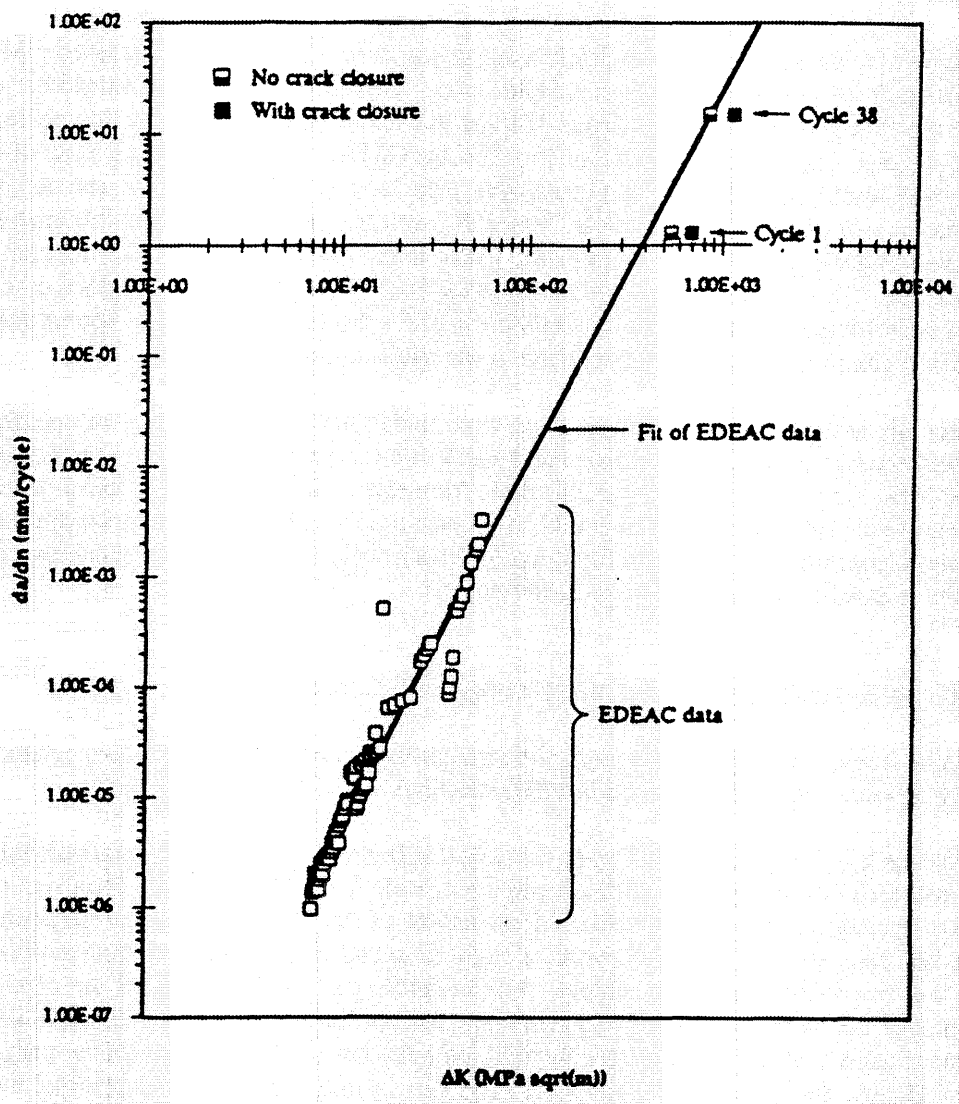

Figure 4.2 Comparison of C-pipe experiment cyclic crack growth values to extrapolation of EDEAC data for TP304 stainless steel at ambient temperature

APPENDIX C

5.0 DYNAMIC PIPE FRACTURE ANALYSIS OF A PROTOTYPICAL NP-HWR PIPE SYSTEM SUBJECTED TO SEISMIC LOADING

5.1 Objective

The objective of this effort was to analytically evaluate the dynamic stability of a cracked pipe system representative of the NP-HWR pipe heat transfer loop. This effort came about to address concern raised by the Pipe Integrity Review Group (PIRG) that DOE assembled, as to the representative nature of the pipe impact tests initially undertaken by ORNL. Consequently, a state-of-the art, nonlinear time-history analysis of a representative pipe loop containing a crack and subjected to seismic loading was undertaken by Battelle. The PIRG wanted Battelle to conduct this analysis with a very severe crack that was similar to the worst case crack found due to IGSCC in a commercial LWR, Ref. 5.1. This was a circumferential complex-crack where there was a surface crack of 75 percent of the thickness all around the circumference, and a through-wall crack of approximately 20 percent of the circumference in the same plane as the surface crack, see Figure 5.1.

To conduct this analysis, three analytical steps were undertaken. The first was to determine the through-wall crack-length that corresponded to the leak rate currently thought to be used for detection at the HW-NPR. The second step was to calculate, from elastic-plastic fracture mechanics analyses, the moment versus rotation due to the crack. This was a necessary step to calibrate the nonlinear cracked pipe element to be used in the final step of the dynamic pipe fracture calculations. Each of these analyses is described in the following subsections.

5.2 Leak-rate Analysis for Sizing of the Through-wall Crack

In this effort, it was necessary to determine the through-wall-crack length that would correspond to a desired leak rate. The leak rate cited in PIRG meetings was 2.0 gallons per minute.

To calculate the leak rate, the SQUIRT code developed at Battelle for the NRC's International Piping Integrity Research Group program (IPIRG) was used, Ref. 5.2. This leak-rate code was recently enhanced to account for a more sophisticated evaluation of the crack morphology parameters that affect the leak rate, Ref. 5.3. In that work, a study of actual cracks removed from service found that past leak-rate models were too simple. For instance, past models assumed the cracks grow straight through the thickness. In reality, some may follow the fusion line of a weld, while others have tortuous paths that are much longer than the pipe thickness. The effective flow path length, surface roughness, and number of turns a crack takes may also differ as a function of the crack opening. For instance, if the crack is very tight, then there may be a large number of turns, but the surface roughness for an IGSCC crack would be the microscopic roughness of the grain boundary, i.e., a local surface roughness. However, if the crack opening is large, then the number of turns is significantly reduced, but the surface roughness increases to a much larger macroscopic value, i.e., a global surface roughness.

Statistics of the local and global surface roughness, number of turns, and effective flow path lengths were developed in Reference 5.3 for intergranular stress corrosion cracks in stainless steels, and

corrosion fatigue cracks in ferritic steels. Additionally, a probabilistic version of the SQUIRT code was developed to calculate the distribution of crack sizes for a given leak rate.

Other critical inputs to the leak-rate analysis are the applied loads, and the selection of the appropriate cracking mechanism. For this analysis, it was assumed that a large crack, such as the Duane Arnold crack, could only occur in the NP-HWR plant with a mechanism such as IGSCC, Ref. 5.1. Thermal fatigue was ruled out due to the low operating temperature of the plant.

Other critical parameters are the normal operating loads. These loads were taken from an ANSYS analysis, conducted by Battelle, of an early version of the NP-HWR pipe loop. The details of this analysis are given in Section 5.4 of this report. One of the key aspect of determining the appropriate loads, was that the normal operating bending moments were small, i.e., 504 in-lb, in the direction that would open a crack under seismic loading, but were much larger at 90-degrees to that orientation, i.e., 55,517 in-lb. The 90-degree direction moments were sufficiently larger, that the crack would have to first form in this bending plane. To be conservative, we used the 55,517 in-lb bending moment, but assumed that the crack would be in the same plane as the applied seismic loading. The applied tension load from the ANSYS run was 26,507 pounds and was also included in the leak-rate calculations.

The final critical information for the leak-rate analysis is the water condition. Here, the water was assumed to be at 230 F and 150 psi. Hence, two-phase flow effects are minimal in these calculations, but are nevertheless accounted for automatically in the SQUIRT code.

The results of the probabilistic analyses of the 2 gpm crack are shown in Figure 5.2. These results were generated by Monte Carlo simulations using 1,000 calculations. The mean total through-wall crack length was 18.38 inches, and the standard deviation was 1.014 inches. To be slightly on the conservative side, we assumed that the through-wall-crack length was the mean length plus two standard deviation lengths, 20.408 inches. This length is 40.6-percent around the circumference, which is longer than the worst case Duane Arnold IGSCC safe-end cracks that were around 25 percent of the circumference.

5.3 Moment-rotation Predictions for Complex-cracked Pipe

The next step in the analysis was to calculate the moment versus rotation due to the crack response of a complex crack with various surface-crack depths and a length of 40.6 percent of the circumference. The analysis to predict the behavior of complex-cracked pipe is more difficult than for a simple circumferential through-wall-cracked pipe. Two different corrections are needed to the simple through-wall crack analyses.

The first correction is one for constraint on the toughness by the complex-crack geometry. Past work in References 5.4 to 5.6 has shown that for a complex crack, the presence of the internal surface crack significantly reduces the apparent toughness of the material. This is due to the physical limitation of the plasticity in the axial direction on either side of the surface crack. The resulting plasticity resembles a strip yield model where it is contained only in the surface-crack ligament. In Reference 5.5, it was shown that the reduction of the toughness is a simple function of the depth of

the surface crack. This is illustrated in Figure 5.3. These data were generated from pipe experiments on TP304 stainless steel base metal, A106 B base metal, Inconel 600 base metal, as well as stainless steel TIG welded pipe.

The second correction is an analytical consideration. The current NRCPIPE code developed at Battelle treats complex-cracked pipe in a very idealistic manner. It assumes that the presence of the surface crack effectively reduces the thickness of the pipe, and the material J-R curve is reduced by the appropriate value from the upper-bound curve in Figure 5.2. However, a complex-cracked pipe can transmit compressive loads across the crack faces which raises the load-carrying capacity compared to a simple through-wall crack analysis. To make a first-order correction for the compressive loads across the crack faces, we developed a correction based on a net-section-collapse analysis. This was done by rederiving the net-section-collapse equations to account for crack closure loads on the maximum moment for a complex-cracked pipe (M_{cc}) as noted below.

$$M_{cc} = 2\sigma_t R^{*2} t^* (\sin\beta - \sin\theta) + 2\sigma_f R^2 t \sin\beta \tag{5.1}$$

where,

$$\beta = \frac{(\pi - \theta) R^* t^*}{(R^* t^*)} - \frac{\pi R_i^2 p}{2(R^* t^* + Rt)\sigma_t} \tag{5.2}$$

and,

R^* = mean radius of complex-cracked pipe = $(R_o + R_i - d)/2$
R_o = outside radius
R_i = inside radius
t^* = reduced thickness = t-d
t = actual pipe thickness
d = depth of surface crack
σ_f = flow stress = $(\sigma_y + \sigma_u)/2$
p = internal pressure.

The ratio of the complex-crack net-section-collapse load to the net-section collapse load for a simple though-wall-crack formulation (Equations 2.1 and 2.2), where t is just replaced by t^* and R is replaced by R^*, is illustrated in Figure 5.4. Hence, if the through-wall-crack length, θ, is less than 70 percent of the circumference, then the load-carrying capacity of the complex-cracked pipe is greater than the simple through-wall-crack analogy.

This complex-crack net-section-collapse analysis was validated using Battelle data from TP304 stainless steel and Inconel 600 complex-cracked pipe experiments, both with through-wall cracks of 37-percent of the circumference and surface-crack depths of nominally 60-percent of the thickness (Experiments 4113-2 and -4) from Reference 5.5. These comparisons are shown in Figures 5.5a and 5.5b. There is better agreement with the experimental maximum loads with the crack-closure correction than without it. Hence, the crack-closure-load correction was employed in the following calculations.

The next step was to conduct the elastic-plastic fracture mechanics analysis using the LBB.ENG2 method in Battelle's NRCPIPE code using the toughness correction for complex-crack constraint and the crack-closure-load corrections. The predicted moment-rotation response for complex cracks with through-wall lengths of 40.6-percent of the circumference, and depths of 0-, 20-, 40-, 60-, 75-, and 80-percent of the thickness are shown in Figure 5.6. Results with and without the crack-closure-load correction are shown. For the purpose of the calibration of the nonlinear cracked-pipe element in the dynamic calculations, the curves with the crack-closure-load correction were used.

5.4 Dynamic Pipe Fracture Calculations of NP-HWR Pipe System

The previous analyses, and the ORNL pipe impact experiments conducted in support of eliminating the instantaneous DEGB as the design basis event for the NP-HWR, have not provided data that can be used as a convincing argument that such an event should not be considered. Rather, the experiments have provided data that suggest that the stainless steel pipe material is very tough, i.e., it is tolerant of large circumferential defects, and that break areas for cracks with large circumferential lengths are small. The analyses have shown that analytical techniques, which agree well with the experimental data, are available to assist in predicting the behavior of the piping. Neither the experiments nor the analyses have, however, generated any information regarding the loads that may actually be applied to the pipe during a seismic event, the occurrence and magnitude of large unstable ductile tearing episodes, or the timing for such instabilities. Because these issues are crucial to the arguments for removing the instantaneous DEGB as the design basis event, dynamic pipe fracture analyses were undertaken by Battelle, using state-of-the-art analysis techniques, to develop some data in these areas to ascertain whether elimination of the instantaneous DEGB is reasonable.

The focus of the analyses to be presented is to directly relate, through dynamic pipe fracture system analyses, the expected earthquake-induced motions of the plant from SSE level and greater loadings to the crack driving force, i.e., bending moment at the crack location, and consequent crack opening and crack stability. These analyses thereby incorporate plant-specific loading, flaw growth behavior under realistic loading, and, because the analyses are conducted in the time domain, timing estimates for break opening area. The key elements in the analyses include:

- Finite element time-history analysis
- Crack behavior modeled as a nonlinear spring element at the highest stress location

- Piping model consisting of the cold-leg piping from the reactor pressure vessel to the heat exchanger

- Loads based on a 0.3 g earthquake being equal to a one SSE loading.

The results are presented in the format of:

- Moment at the assumed crack location as a function of time

- Crack length and crack opening area as a function of time

- Peak stresses and deflections in the piping system at key locations.

With these data, one can then begin to construct the arguments necessary to remove the instantaneous DEGB as the design basis event.

The dynamic pipe fracture analyses done in support of the NP-HWR project have, of necessity, been limited in scope. The time and funding constraints have precluded the extensive parametric studies needed to fully justify removal of the instantaneous DEGB. In most cases, the analyses have been conducted with less than perfect knowledge of the system configuration, due to continuous evolution of the design. Where data have been lacking, engineering assumptions have been made which, strictly speaking, cannot always be justified as being conservative or unconservative. Rather, the assumptions can only be suggested to be not outrageous. With an acknowledgement of these limitations, the results of the analyses, can be summarized as follows:

- The results are sensitive to the boundary conditions and crack location material properties. To build a more credible case for eliminating the instantaneous DEGB as the design basis, more and better data are essential.

- Only ductile tearing from a monotonic J-R curve is assumed in these analyses. No cyclic effects on the J-R curve were included. Past experience shows that interrupted ductile tearing with a negative load can significantly lower the fracture resistance of TP304 stainless steel as well as carbon steels, Refs. 5.7 and 5.8. Fatigue crack growth, which is ignored, will certainly reduce the load carrying capacity of flaws.

- Under SSE loading with no flaw, the whole piping system remains elastic.

- With a postulated 10-inch long through-wall flaw at the highest stress location, 3 SSE loading is not sufficient to cause the crack to initiate and grow.

- 3 SSE loading will induce plasticity in the piping system and this will have an influence on the integrity of flaws under dynamic loading.

- Postulated 360-degree, 40-percent and 75-percent deep internal surface cracks with a 2-gpm leak rate through-wall crack initiate and grow under 3 SSE loading. The cracks are predicted

to grow stably and arrest just past maximum moment. The maximum crack-opening area during the complex-crack seismic events is estimated to be 21 square inches, with a 115 millisecond time to reach that opening.

5.4.1 Analysis Tools and Methodologies

Typical seismic piping analysis generally follows the flow chart shown in Figure 5.7, from a prescribed input free field ground acceleration spectrum, to soil-structure interaction analysis, to building dynamic analysis, and finishing with piping response spectra analysis. In the case of the present NP-HWR analysis, however, the time-history branch for analysis of the piping must be followed because of the nonlinearity of the crack. Furthermore, considering the availability of data and time and funding constraints, the present analysis begins with a prescribed floor response spectra.

The tools and methods used for analysis of the NP-HWR system are state-of-the-art. Because of this, they have not been adopted for routine seismic analysis of piping systems and are thus, probably not familiar to most people. Therefore, to provide background information and to more completely document the NP-HWR analysis effort, a presentation of some of the theoretical basis of the analysis tools and justification for their use is warranted.

Earthquake Time-History Analysis

Time-history analysis is generally considered necessary to either qualify or design systems and components that exhibit highly nonlinear behavior. The cracked section in the NP-HWR pipe system is an example of such a "component". Because there are no recorded building motions that exhibit the uniform frequency distributions of a typical floor response spectrum, it is necessary to generate a floor response spectrum-consistent time history of motion whose response spectrum matches the design spectrum for a given damping value.

There are a number of methods for developing a time history from a response spectrum. For the present study, the time history of floor response has been synthesized using a superposition of continuous waves. In particular, the procedure advocated by Levy and Wilkinson, Ref. 5.9, has been adopted.

The Levy and Wilkinson procedure for synthesizing a floor-response time history uses a superposition of a large number of sine waves whose amplitudes are iteratively adjusted to match the prescribed design spectrum. To achieve frequency richness, closely-spaced frequencies are selected so that the half-power points of adjacent frequencies overlap. In equation form, the Levy and Wilkinson procedure can be summarized as:

Number of Frequencies from f_1 to f_n:

$$n = \frac{\ln\left[\frac{f_n}{f_1}\right]}{\ln\left[1 + \frac{2c}{c_c}\right]} \tag{5.3}$$

Frequency Spacing:

$$\Delta f_i < 2 f_i \left[\frac{c}{c_c}\right] \tag{5.4}$$

Time History:

$$\ddot{X}(t) = F(t)\sum_{i=1}^{n}(-1)^i A_i \sin(2\pi f_i t) + B t^2 + C t \tag{5.5}$$

where F(t) is an envelope function to account for time severity of the earthquake, i.e., buildup, stationary portion, and motion decay, B and C are coefficients that can be used to adjust the response to bring residual velocities and displacements to zero when the shaking stops, and (c/c_c) is the damping ratio.

The coefficients A_i, are adjusted iteratively according to the following scheme:

Iteration 1:

$$A_i^1 = k\, SRS_{ref}|_{f_i} \tag{5.6}$$

where k is some proportionality constant, SRS_{ref} is the value of the design response spectrum at frequency f_i

Subsequent Iteration j:

where SRS_i^{j-1} is the response computed in the previous iteration.

$$A_i^j = A_i^{j-1}\left[\frac{SRS_{ref}}{SRS_i^{j-1}}\right] \tag{5.7}$$

B and C coefficients are assumed zero at first iteration, adjusted iteratively to make residual velocity and acceleration zero. Iterations are continued until the computed response matches the reference design spectrum to a desired degree.

The determination of the response at each iteration involves calculating the maximum absolute acceleration of single degree-of-freedom oscillators at each of the frequencies, $\omega_i = 2\pi f_i$. This computation is done using a numerical time-integration procedure. For each oscillator, the equation

$$\frac{d^2y_i}{dt^2} + 2\xi\omega_i\frac{dy_i}{dt} + \omega_i^2 y_i = -\ddot{X}(t) \tag{5.8}$$

where y_i is the displacement of the ith mass relative to the ground, and ξ is the damping ratio, (c/c_c), is solved in time to find the maximum response. The acceleration of interest to be compared with the design spectrum is

$$SRS_i^{j-1} = \ddot{y}_i + \ddot{X} \tag{5.9}$$

which can be shown to be approximately equivalent to the maximum absolute value of $\omega_i^2 y_i$ for low values of damping.

The spectrum-consistent floor-response time history consists of floor acceleration versus time. In general, one would apply base-motion acceleration to the pipe fixed ends and calculate pipe internal forces, reactions, and stresses due to relative motion of the pipe system and the floor. In a practical sense, however, the desired pipe system response is obtained where the fixed ends are held rigidly, and body forces due to the acceleration are applied.

Dynamic Pipe Fracture Analysis

There are at least three different categories of cracked pipe dynamic analyses. These are:

- Complete three-dimensional finite element modeling.
- Substructuring, using beam elements for the uncracked pipe and three-dimensional elements at the crack location.

- Using beam elements for the uncracked pipe and a nonlinear spring element to simulate the crack response.

Complete three-dimensional, elastic-plastic, dynamic analysis is extremely costly, time consuming, and is not a practical engineering tool. Substructuring with beam elements and three-dimensional elements at the crack is more practical, but the computer time for such analyses, if crack growth is considered, makes such an approach very expensive. The final approach is the one used to analyze the NP-HWR system and involves the most economical, and possibly the most accurate approach. In this approach, the crack response is represented by a nonlinear spring placed at the crack location. This spring is defined by experimental data or J-estimation scheme analyses such as those discussed in References 5.10 and 5.11.

Crack Modeling. The response of a crack in a pipe system is established as shown in Figure 5.8. Basically, the response is characterized as a nonlinear moment-rotation (stiffness) in the plane of the crack at a point in the piping system. Although experimental data (i.e., results from a quasi-static pipe fracture experiment with the same material and flaw size) may be available, the J-estimation scheme approach for predicting the moment-rotation response is more fundamental. In calculating the stiffness of a cracked section using a J-estimation scheme, the material properties (i.e., stress-strain and J-R curve) and crack-section geometry (i.e., pipe diameter, thickness, crack length, and crack depth) need to be defined. In addition, several assumptions are made in generating the crack stiffness:

- For low-cycle high amplitude loading, the cyclic load effects on the circumferential crack growth are assumed to be small; crack growth is dominated by ductile tearing under increasing load amplitude.

- High strain rate effects on crack growth and on the constitutive relationship are typically ignored, even though they may tend to influence crack growth and the plastic flow for some materials. Rarely will one have access to dynamic material property data (i.e., dynamic tensile or J-R curve data).

- Only a separation mode (Mode I) of crack propagation under bending is assumed. This implies that the crack section is considered to be rigid in all degrees of freedom except the rotation corresponding to the crack opening.

- Cyclic effects on the material properties are ignored. Past work has shown that cyclic unloading during ductile tearing with negative loads can significantly lower the apparent toughness of TP304 stainless steel. However, such cyclic effects are barely being understood at this time, and methods to predict the magnitude of the effect are the subject of current evaluations at Battelle. Consequently these effects are not included at this time.

- The rotational deformation due to the crack and relevant plastic deformations are confined to the crack section.

The nonlinear-spring model of piping cracks is applicable to both surface and through-wall cracks. As currently implemented, surface cracks are modeled as a series of spring-slider elements. The

spring-slider element is a two node, two degree-of-freedom element with a linear spring and a friction slider in series. At low loads, the slider is locked and the two nodes behave as if they have a linear spring between them. When the spring load reaches a magnitude of $\pm F_{slide}$, the force between nodes I and J remains constant. If the spring-slider reaches the limiting force and then is unloaded, a permanent displacement will remain when the load is brought back to zero. Putting two or more spring-slider elements in parallel with different stiffnesses and F_{slide} values allows one to model a multi-linear load-deflection curve. Figure 5.9 illustrates the modeling of a 3 segment spring-slider curve.

The nonlinear-spring model of through-wall cracks is implemented as shown in Figure 5.10. Using the rigid offset kinematic relationships and the prescribed moment-rotation relationship from the J-estimation scheme analysis, a stress-strain curve is derived for the nonlinear truss that gives the desired moment-rotation response. Unlike the surface-crack spring sliders, the through-wall-crack implementation is applicable past maximum load.

There are two important features of the nonlinear-spring model that need to be mentioned. First, both the spring-slider and nonlinear-truss elements described above model the Baushinger effect, i.e., kinematic hardening in a plasticity analysis. The implication of using models like this is that energy is absorbed at the crack under cyclic loading. This is especially important for dynamic analyses, because the crack will appear, effectively, as damping in the pipe system. The second important feature is that the surface-crack and through-wall crack nonlinear springs can be, with some manipulation, combined (see Figure 5.11) so that surface-crack to through-wall-crack transitions can be modeled. This is important for determining stability of a crack under dynamic loads. If enough strain energy is stored in a surface-cracked pipe system under load, when the surface crack breaks through, the resulting through-wall crack may not arrest if the dynamic load is sustained. The present nonlinear-spring analysis is currently the only methodology that can make such stability assessments.

In application, the multi-linear spring-sliders and/or nonlinear truss are attached to a pair of coincident nodes at the crack location in the pipe model, coupling the two nodes together in the relative rotation bending degree-of-freedom of the attached pipe elements. The remaining five degrees-of-freedom; the two shears, the torsion, the tension, and the remaining bending degree-of-freedom, are rigidly coupled with constraint equations. To accommodate crack closure in the nonlinear-spring model, a very stiff spring is inserted that is "activated" when the relative rotations try to become negative.

Pipe System Modeling. The remainder of the piping system in a dynamic cracked-pipe system analysis uses standard finite element analysis capabilities. Straight pipe and elbow elements model the piping, direct time-history integration of the equations of motion is used, standard finite element loading is available (temperature, pressure, forces, displacements, accelerations), and features such as general plasticity in the pipe can be invoked.

Analysis Validation. The crack simulation by the nonlinear-spring approach has been used to analyze dynamic inertially loaded through-wall-cracked pipe experiments, compliant instability through-wall-cracked pipe experiments, surface-cracked-pipe water-hammer experiments, and a series of simulated seismic pipe system experiments at PWR conditions in which a surface-crack transitions

to a through-wall crack. As a means of demonstrating the efficacy of the nonlinear-spring methodology, the results of a comparison between an experiment and a prediction for one of the latter experiments will be presented.

The nonlinear-spring method of modeling cracked pipe was used in the design and analysis of the results from the IPIRG-1 pipe system experiments, Refs 5.12 and 5.13. The IPIRG pipe system was fabricated from 16-inch nominal diameter Schedule 100 pipe and is configured as an expansion loop with 100 feet of pipe and 5 long radius elbows. Figure 5.12 is an artist's concept of the pipe system while Figure 5.13 shows the pipe system dimensions. The pipe loop had internal pressure (2,250 psi), dead-weight, thermal expansion (550 F), and dynamic displacement induced loads. A surface crack, nominally 50-percent of the pipe circumference in length and 66-percent of the pipe wall thickness in depth, was introduced into the pipe loop at a critical high stress location. The response of a crack to dynamic excitation in a number of different materials was evaluated during the course of the five IPIRG-1 cracked pipe system experiments. The materials evaluated were:

- An A106 Grade B carbon steel which had shown signs of being susceptible to dynamic strain aging effects in laboratory scale tests, i.e., tensile and fracture toughness tests. The toughness of this material was low enough that contained plasticity conditions should exist for this pipe diameter and hence, elastic-plastic fracture conditions should govern.

- A high toughness SA358 Type 304 stainless steel for which fully plastic (i.e., limit load) conditions should exist.

- A low toughness submerged-arc weld (SAW) in both the A106 Grade B carbon steel and the Type 304 stainless steel.

- A section of CF8M cast stainless steel which had been artificially aged at 750 F for 700 hours to simulate 9 years of service for a cold leg or 2 years for a hot leg.

The calculated moment-rotation response due to the crack for the various crack size/material combinations (i.e., the stiffness of the nonlinear-spring crack element) was established using the SC.TNP finite length surface-cracked pipe J-estimation scheme, Ref. 5.11, and the LBB.ENG2 J-estimation scheme for the through-wall cracks, Ref. 5.10, both developed as part of the Degraded Piping Program, 5.14. These calculations use a Ramberg-Osgood representation of the stress-strain curve and a power-law extrapolation of the J_D-R curve for the materials of interest.

Focussing on the aged-cast-stainless experiment, IPIRG-1 Experiment 1.3-7, the forcing function, and input moment-rotation responses are shown in Figures 5.14 and 5.15. The finite element prediction compared with the experimental result for the crack-section moment is shown in Figure 5.16. The comparison is outstanding. Maximum moments, time phasing of the dynamic response, and the surface-crack to through-wall-crack transition all are predicted very well. Equally good comparisons have been made for the other IPIRG-1 pipe system experiments and the other types of experiments mentioned above.

Although the data presented do not necessarily constitute a fully documented validation of the cracked-pipe dynamic analysis methodology, when coupled with other results, Refs. 5.15 and 5.16,

the data suggest that the J-estimation scheme accurately predicts the moment-rotation behavior of both surface and through-wall cracks, and the dynamic analysis results indicate that the essential features of system loads, performance, and crack-driving force are captured in the analysis. Thus, there is a reasonable basis for using the nonlinear-spring cracked-pipe analysis to help make the supporting arguments for eliminating the instantaneous DEGB as the design basis event for the NP-HWR.

5.4.2 Analysis of NP-HWR Pipe System

The structural analysis of the NP-HWR system consisted of four distinct activities: model development, static analyses, a dynamic uncracked-pipe system analysis, and dynamic cracked-pipe system analyses. The activities were sequential, with results from one activity providing input for the succeeding activities. As indicated previously, assumptions frequently had to be made that have an impact on the results. Because there was no opportunity to explore the consequences of any particular assumption, the results presented here must be viewed as a demonstration of potential, rather than a definitive case for eliminating the instantaneous DEGB as the design basis.

Model Development

The information available for developing the NP-HWR analysis model is summarized in Table 5.1 and Figures 5.17 through 5.18. Although these data represent a significant fraction of what is needed to perform a cracked-pipe analysis, it is obvious that there are some deficiencies: detailed dimensions of the piping geometry are required, elbow radii should be specified, all boundary conditions must be defined, and seismic excitation should be in three orthogonal directions. Because these data were not available, due to the NP-HWR design not being fixed at the time of these analyses, engineering assumptions were made about the missing data. Where initially reasonable assumptions appeared to have an obviously large and unfavorable impact on the results, modest parameter studies were performed to find a more reasonable set of assumptions.

Given only the one dimension shown in Figure 5.17, a model of Leg A was developed by scaling. In developing the model, it was assumed that the elbows are long-radius type. Figure 5.19 shows the 18-node, 17-element model geometry. Comparing the corresponding plan and elevation views from Figure 5.17, provided that the 20-foot dimension in Figure 5.17 is accurate, the model faithfully reproduces the geometry.

The prescribed seismic horizontal floor-response spectrum at an SSE loading level is shown in Figure 5.18. Using the procedures previously discussed, a spectrum-compatible time history of floor motion horizontal acceleration was developed. In developing the time history, it was assumed that the envelope function, F(t), ramps linearly from zero to one in five seconds, remains fixed at one for 10 seconds, and then linearly ramps to zero in another five seconds. Figure 5.29 shows the match between the design spectrum and spectrum from the time history. The match is very good. Figure 5.21 is a plot of the time history. In the analyses to be discussed, the time history of acceleration was applied in the Y direction of Figure 5.19 because it was felt that this would induce the largest possible bending moments in the pipe. The validity of this assumption was, however, never checked. For analyses performed at a 3 SSE level, the time-history amplitudes were simply multiplied by 3.

Static Analysis

Given the basic model geometry, some static and eigenvalue analyses were performed to establish the boundary conditions at the heat exchanger. Table 5.2 summarizes the results of assuming three reasonable boundary conditions. In this analysis and all subsequent ones, ASME elbow flexibility factors and stress indices were used.

Although fixity at the heat exchanger seems nominally correct, the pipe is much too constrained, developing excessively large static stresses. In fact, the static bending moment is sufficient to yield the pipe and/or cause almost any hypothetical crack at the highest stress location to reach maximum moment. The moment-free condition, although more reasonable in terms of stresses, is hard to reconcile relative to the structure shown supporting the heat exchanger, i.e., a moment-free condition could only be achieved with some sort of ball joint at the heat exchanger. The free lateral translation condition relieves the static thermal stresses and may be physically possible due to the heat exchanger being up on "stilts", even though it is almost certain that a designer would not permit the heat exchanger to move significantly.

In all likelihood, the pipe geometry would be changed so that the thermal expansion could be accommodated with a fixed boundary condition. However, because of constraints on this program, one of the three candidate boundary conditions had to be selected for use in the dynamic analyses. The free translation condition was chosen because: 1) It has static stresses that are in line with what would be judged acceptable, and 2) It probably will respond more to dynamic loading due to its lower natural frequency.

With the free translation boundary condition, the first five modes of the NP-HWR pipe system are shown in Figures 5.22 through 5.26. From these data, it is obvious that the piping system will respond almost exclusively in the X-Y plane, with limited participation in any of the higher modes.

Dynamic Uncracked-Pipe Analysis

The first dynamic analysis performed was for uncracked pipe at SSE level loading to determine where to put the crack and what orientation the crack should have. For this analysis and all subsequent dynamic analyses, the dynamic excitation was assumed to be in the Y direction (perpendicular to the long straight run of pipe, see Figure 5.19) and damping was assumed to be 0.5 percent Rayleigh (mass and stiffness) damping in the first and fourth modes. This low value of damping is justified on the basis that there are no pipe hangers or other energy dissipating features in the pipe system. A summary of the deflections and stresses from the linear elastic analysis is presented in Tables 5.3 and 5.4.

From these results, it is clear that the highest stress location is at the reactor pressure vessel nozzle. Looking at the bending moment versus time at this location, Figure 5.27, it is clear that the largest elastic bending moment occurs in the negative direction, implying that the crack should be oriented so that it is on the positive Y side of the elbow, the intrados. The maximum dynamic bending moments at the reactor pressure vessel, as expected, are in the X-Y plane, so the crack needs to have its centerline in the X-Y plane. At N+1SSE loading, the maximum dynamic moment is -643,000 in -lb. At N+3SSE the maximum dynamic moment can be linearly proportioned, and is -1,928,000

in -lb. (The negative sign reflects the location around the circumference that was chosen. At 180-degrees around the circumference the moment is a positive value.

Although no analyses were performed to demonstrate that the free translation boundary condition dynamic response provides an upper bound for crack driving force, common sense suggests that it probably does.

Dynamic Cracked-Pipe Analyses

Three dynamic cracked-pipe analyses were performed. The first analysis had a through-wall crack, while the second and third analyses had complex cracks (combined internal surface and through-wall crack). All cracks were assumed to occur at the reactor pressure vessel nozzle girthweld. The through-wall crack was analyzed because of its similarity to one of the cracks that was loaded in the ORNL experimental program. The complex cracks were analyzed because they represent worst case flaws that could go undetected. In the cracked-pipe analyses, a 3 SSE loading was applied, see Figure 5.28. Since the maximum moment in the uncracked pipe analysis was a negative value, the crack was located at 180-degrees from the location of the Figure 5.27 results.

Through-Wall Crack Analysis. The through-wall crack selected for analysis was 10 inches long. Using the procedures described previously, a nonlinear spring to represent the crack moment-rotation response was developed, see Figure 5.29. Subjecting the pipe system with the non-linear spring (crack) element 3 SSE loading, the moment generated at the crack location is predicted to reach approximately 1,750,000 inch-pounds, per Figure 5.30. Comparing this moment to Figure 5.29, it is obvious that the crack did not reach maximum moment and hence, did not propagate in ductile tearing. This assertion is confirmed when the cracked-section response is viewed in moment-rotation space (Figure 5.31); the crack was loaded and unloaded elastically. (In Figure 5.31, one can see that significant crack closure occurred).

Tables 5.5 and 5.6 summarize the highlights of the system response. It is interesting to note that although the pipe is highly stressed under 3 SSE loading with the through-wall crack, the compliance of the crack keeps the crack-opening moments from getting large enough to tear the crack. The magnitude of the Von Mises stress at the crack location, 60.5 ksi, suggests, however, that torsional stresses are large at this location. If crack-opening area is assumed to be diamond shaped, the finite element crack rotations and J-estimation scheme crack length and crack-mouth-opening displacement data can be combined to predict the crack-opening area as a function of time, Figure 5.32. The leak-rate area is very small.

Another interesting aspect is that the maximum moment with the crack behaving elastically is lower than for the elastic uncracked pipe. This is due to the compliance of the through-wall crack in tension changing the dynamic characters slightly.

Complex-Crack Analyses. A complex crack is one in which a portion of a 360-degree internal surface crack is assumed to have penetrated the pipe wall. For these analyses, it was assumed that there is a through-wall crack that leaks at 2-gpm (20.408-inch long crack). Two different depths were investigated for the surface-crack portion of the complex crack, 40-percent deep and 75-percent deep. These two cracks represent cracks that could go undetected until they leak, and because they

so significantly degrade the moment-carrying capacity of the pipe, they may represent bounding cases of pipe system response.

The first complex crack analyzed had a 40-percent deep surface crack and a 2-gpm leaking through-wall crack. The moment-rotation response from the J-estimation scheme analysis of this crack is shown in Figure 5.6 (the curve used include crack-closure-load correction). The predicted moment-carrying capacity of this crack is significantly less than for the 10-inch through-wall crack.

The predicted crack-section response to 3 SSE loading for the 40-percent deep complex crack is shown in Figures 5.33 and 5.34. The crack initiates, reaches maximum moment after about 13 cycles of loading, tears slightly, and then arrests. It subsequently is subjected to something less than 30 cycles of loading, some of which reinitiate and grow the crack slightly. The corresponding predicted crack-opening area for this flaw is shown in Figure 5.35. The maximum dynamic leak area is about 17 square inches with a residual opening of less than 1 in^2 at the end of the seismic event.

Global system response for the 40-percent deep complex crack is summarized in Tables 5.7 and 5.8. The displacements are very large, particularly at the heat exchanger end. Remote stresses from the crack, in general, are well beyond yield. Because extensive yielding would change the energy dissipation behavior of the pipe system, the crack response would probably be altered significantly if general plasticity was permitted. This would increase the effective damping which would reduce the dynamic loads applied to the crack.

An interesting finding from this analysis, is that the 40-percent deep complex crack survived the loading and it's maximum moment capacity was 843,000 in-lb. The elastic uncracked pipe maximum moment was therefore, a factor of 2.38 larger than the nonlinear dynamic maximum moment of the surviving cracked pipe.

The final crack geometry considered was a complex crack that is consistent with a piping flaw at the Duane Arnold nuclear plant that was not discovered until it leaked; 40.6-percent of the circumference long (20.408-inches), and 75-percent of the wall thickness deep. The J-estimation scheme prediction of the moment-rotation response for this crack is shown in Figure 5.6. Compared to the 10-inch through-wall crack and 40-percent deep complex crack, this complex-cracked-pipe section is much more severely degraded.

Figure 5.36 shows a plot of the crack-section moment as a function of time, while Figure 5.37 shows the predicted moment-rotation response at 3 SSE loading for the "Duane Arnold" complex crack. The crack reaches maximum moment and then tears stably. Compared to the 40-percent deep complex crack, the 75-percent deep complex crack does not tear significantly more, but it undergoes much more severe crack closure.

Tables 5.9 and 5.10 are highlights of the system response. It is obvious from these data that the pipe remote for the crack undergoes very large deflections and that significant portions of the pipe would be well above yield. Combining the finite element crack rotations, J-estimation scheme crack length and crack-mouth-opening data, and assuming a diamond-shaped crack-opening area, the leak area as a function of time is as shown in Figure 5.38. The leak rate area reaches a maximum of 21

square inches during the seismic event with a very small residual crack opening after the seismic event. On the cycle when the crack reaches 21 square inches, it takes 115 milliseconds to go from basically closed to the maximum opening.

The results presented for both complex-crack analysis support the contention that a large undetected surface flaw that breaks through and leaks under normal operating loads has enough integrity to sustain a 3 SSE loading. Because plasticity has been ignored, except at the crack, however, the results presented for the complex cracks cannot be relied upon as the sole basis for justifying removal of the instantaneous DEGB as the design basis event because the energy dissipated during yielding would alter the system dynamics. The uncracked pipe plasticity will effectively increase the damping which would reduce the loads on the pipe.

For the case of the 75-percent deep complex crack, the predicted maximum moment was only 325,000 in-lb. The elastic uncracked moment was a factor of 5.9 times larger than this, and amazingly the crack still survived with only a small amount of tearing. This demonstrates the large margins that may be realized from using nonlinear time-history analysis.

5.5 Results

The dynamic cracked-pipe analyses conducted in support of the NP-HWR design suggest that it is probably reasonable to consider eliminating the instantaneous DEGB as the design basis for the plant. The analyses show that within the limitations imposed by the program duration and level of effort, the NP-HWR pipe system is very tolerant of large cracks at large seismic load levels.

Summarizing the findings of the analyses,

- The results are sensitive to the boundary conditions and material properties at the crack location. To build a more credible case for totally eliminating the DEGB as the design basis, more and better data are essential.

- Only ductile tearing is assumed in these analyses. Fatigue crack growth, which is ignored, will certainly reduce the load-carrying capacity of flaws. Reverse cyclic loads are also known to reduce the J-R curve of the material, which would also cause more tearing to occur. This aspect was not included due to time and funding constraints.

- Under SSE loading with no flaw, the whole piping system remains elastic.

- With a postulated 10-inch long through-wall flaw at the highest stress location, 3 SSE loading is not sufficient to cause the crack to initiate and grow. Leak opening areas for this flaw are very small.

- A 3 SSE loading will induce plasticity in the piping system remote from the crack and this will have an influence on the integrity of flaws under dynamic loading. This plasticity will probably lower the applied loads due to effectively increasing the damping.

- Postulated 360-degree, 40-percent and 75-percent deep internal surface cracks with a 2-gpm leak-rate through-wall crack initiate and grow under 3 SSE loading. The cracks are predicted to grow stably and arrest just past maximum moment. The maximum crack-opening area during the complex-crack seismic events is estimated to be 21 square inches, with a 115 millisecond time to open and close on the next cycle, The residual opening at the end of the seismic event is much smaller.

- The accuracy of the complex-crack analysis results must be viewed with some caution because the pipe system is predicted to yield extensively. Because this plasticity effect has been ignored, more energy will be dissipated during the seismic load cycles, and this would increase the damping and thus, lower the dynamic loads.

- One of the key observations is that the complex cracks were predicted to survive even though the elastic uncracked pipe moments were 2.3 to 5.9 times larger than the maximum moment of the complex-cracked pipe. This illustrated the large potential margins that can be realized from non-linear time-history calculations over using conventional linear-elastic peak dynamic stress in a fracture analysis.

Although there are obvious limitations to the analyses presented here, the results are certainly tantalizing enough to warrant further studies due to the large margins that can be realized over using conventional peak elastic stresses in fracture calculations. None of the analyses conducted suggest that an instantaneous DEGB is possible, and a DEGB may not occur even at "acceptably" slow rates. Clearly, any consideration of totally eliminating the DEGB as the design basis, however, must consider other flaw geometries, loading scenarios, material variability, general plasticity, inspection capabilities to preclude the existence of a bigger than "Duane Arnold" undetected flaw, and degradation mechanisms that are still unknown.

5.6 References

5.1 "Investigation and Evaluation of Stress-Corrosion Cracking in Piping of Light Water Reactor Plants", by NRC Pipe Crack Study Group, NUREG-0531, February 1979.

5.2 Paul, D. D., Ahmad, J., Scott, P. M., Flanigan, L. F., and Wilkowski, G. M., "Evaluation and Refinement of Leak-Rate Estimation Models", NUREG/CR-5128, April 1991.

5.3 Rahman, S., Ghadiali, N., Paul, D., and Wilkowski, G., "Probabilistic Pipe Fracture Evaluations for Leak-Rate Detection Applications", NUREG/CR-6004, to be published in 1993.

5.4 Wilkowski, G. M., Pan, J., and Kanninen, K. F., "Effect of Flaw Shape on J-Resistance Curve of a Circumferentially Cracked Pipe," Proceedings of the 4th ASME National Congress on Pressure Vessel and Piping Technology, Portland, Oregon, June 1983.

5.5 Kramer, G. and Papaspyropoulos, V., "An Assessment of Circumferentially Complex-Cracked Pipe Subjected to Bending", NUREG/CR-4687, October 1986.

5.6 Hays, R. A., Vassilarious, M. G., and Gudas, J. P., "Fracture Analysis of Welded Type 304 Stainless Steel Pipe", prepared by David Taylor Naval Ship R&D Center for the NRC, NUREG/CR-4538, Vol. 1.

5.7 Wilkowski, G., Vieth, P., Kramer, G., Marschall, C., and Landow, M., "Results of Separate-Effects Pipe Fracture Experiments", Post-SMiRT-11 Conference, August 1991, Paper 4.2.

5.8 Olson, R., Scott, P., Marschall, C., and Wilkowski, G., "Comparison of Fracture Toughness Values from Large-Scale Pipe System Tests and C(T) Specimens", in proceedings of IAEA/CSNI Specialists Meeting on Fracture Mechanics Verification by Large Scale Testing, editor Dr. Claud Pugh ORNL, Oak Ridge, Tenn., October 1992.

5.9 Levy, S. and Wilkinson, J.P.D., "Generation of Artificial Time-Histories Rich in All Frequencies, From Given Response Spectra", Transactions of 3rd SMiRT Conference, Paper K 1/7, September 1975.

5.10 Brust, F. W., "Approximate Methods for Fracture Analyses of Through-Wall-Cracked Pipes", NUREG/CR-4853, February 1987.

5.11 Scott, P. and Ahmad, J., "Experimental and Analytical Assessment of Circumferentially Surface-Cracked Pipes Under Bending", NUREG/CR-4872, April 1987.

5.12 Schmidt, R. A., Wilkowski, G. M.,and Mayfield, M. E., "The International Piping Integrity Research Group (IPIRG) Program -- An Overview", Transactions of 11th SMiRT, Paper G23/1, August 1991.

5.13 Olson, R. J., Darlaston, B. J., Mayfield, M. E., and Schmidt, R. A., "The IPIRG Dynamic Pipe Loop Test Facility", 17th MPA-Seminar, Paper 26, October 1991.

5.14 Wilkowski, G. M., and others, "Degraded Piping Program - Phase II", Summary of Technical Results and Their Significance to Leak-Before-Break and In-Service Flaw Acceptance Criteria, March 1984-January 1989, by Battelle Columbus Division, NUREG/CR-4082, Vol. 8, March 1989.

5.15 Olson, R., Scott, P., and Wilkowski, G., "Application of a Nonlinear-Spring Element to Analysis of Circumferentially Cracked Pipe Under Dynamic Loading", ASME PVP Conference, New Orleans, March 1992.

5.16 Olson, R., Wolterman, R., and Wilkowski, G. M., "Dynamic Analysis of HDR E31 Cracked Pipe System Experiments", SMiRT-12, August 15-20, 1993, Stuttgart, Germany, Paper G12/1.

APPENDIX C

Table 5.1 Analysis Input Data for the NP-HWR Dynamic Cracked-Pipe Analysis Model

Coolant Piping

- 16-inch diameter, Sch 40 (0.500-inch)
- TP304 stainless steel

Boundary Conditions

- Fixed at reactor end
- Not specified at heat exchanger end

Loading

- Temperature, 230 F
- Pressure, 150 psig
- Dead weight loading
- Seismic load

  -horizontal excitation only

  -direction not specified
- Damping not specified

APPENDIX C

Table 5.2 The Effect of Various Boundary Condition Assumptions

Boundary Condition at Heat Exchanger	Natural Frequency (Hz)	Maximum Stress Node	Maximum Elastic Von Mises Stress (ksi)
fixed	21.8	18	78.4
moment free	11.0	13	23.8
free lateral translations	3.9	1	2.6

Table 5.3 Pipe System Displacements at SSE Loading from Linear Elastic Dynamic Analysis

Node	UY_{static} (inches)	UY_{min} (inches)	UY_{max} (inches)
3	-0.013	-0.062	0.029
7	-0.014	-0.586	0.475
10	-0.014	-0.977	0.834
13	-0.015	-1.341	1.153
18	-0.080	-1.487	1.159

Table 5.4 Von Mises Equivalent Stresses at SSE Loading from Linear Elastic Dynamic Analysis

Node	Static (ksi)	Minimum (ksi)	Maximum (ksi)
1	2.6	2.6	19.0
2	2.6	2.6	17.5
3	2.4	2.4	15.8
4	2.0	2.0	5.0
5	2.0	2.0	3.9
6	2.0	2.0	2.9
7	2.1	2.1	2.3
8	2.1	2.1	2.2
9	2.1	2.1	2.6
10	2.1	2.1	3.2
11	2.1	2.1	3.9
12	2.1	2.1	4.4
13	2.0	2.0	5.0
14	2.0	2.0	11.8
15	2.0	2.0	10.8
16	2.0	2.0	5.2
17	2.0	2.0	5.3
18	2.1	2.1	5.3

APPENDIX C

Table 5.5 Pipe System Displacements at 3 SSE Loading with a 10-Inch Long Through-Wall Crack

Node	UY_{min} (inches)	UY_{max} (inches)
3	-0.223	0.143
7	-1.971	1.777
10	-3.330	3.098
13	-4.524	4.273
18	-4.853	4.468

Table 5.6 Pipe System Von Mises Stresses at 3 SSE Loading with a 10-Inch Long Through-Wall Crack

Node	Minimum (ksi)	Maximum (ksi)
1	2.5	60.5
3	2.4	50.5
10	2.1	10.6
14	2.0	38.1

APPENDIX C

Table 5.7 Pipe System Displacements at 3 SSE Loading with a 40-Percent Deep 360-Degree Surface Crack and a 2-gpm Leaking (20.408-Inch Long) Through-Wall Crack

Node	UY_{min} (inches)	UY_{max} (inches)
3	-1.008	0.230
7	-5.945	2.745
10	-9.284	4.827
13	-12.060	6.701
18	-12.710	7.048

Table 5.8 Pipe System Von Mises Stresses at 3 SSE Loading with a 40-Percent Deep 360-Degree Surface Crack and a 2-gpm Leaking (20.408-Inch Long) Through-Wall Crack

Node	Minimum (ksi)	Maximum (ksi)
1	2.5	95.2
3	2.3	79.9
10	2.0	30.0
14	2.0	90.0

APPENDIX C

Table 5.9 Pipe System Displacements at 3 SSE Loading with a 75-Percent Deep 360-Degree Surface Crack and a 2-gpm Leaking (20.408-Inch Long) Through-Wall Crack

Node	UY_{min} (inches)	UY_{max} (inches)
3	-1.135	0.264
7	-6.520	3.158
10	-10.150	5.484
13	-13.210	7.587
18	-13.930	7.998

Table 5.10 Pipe System Von Mises Stresses at 3 SSE Loading with a 75-Percent Deep 360-Degree Surface Crack and a 2-gpm Leaking (20.408-Inch Long) Through-Wall Crack

Node	Minimum (ksi)	Maximum (ksi)
1	2.4	100.8
3	2.0	89.9
10	2.1	35.2
14	2.0	90.2

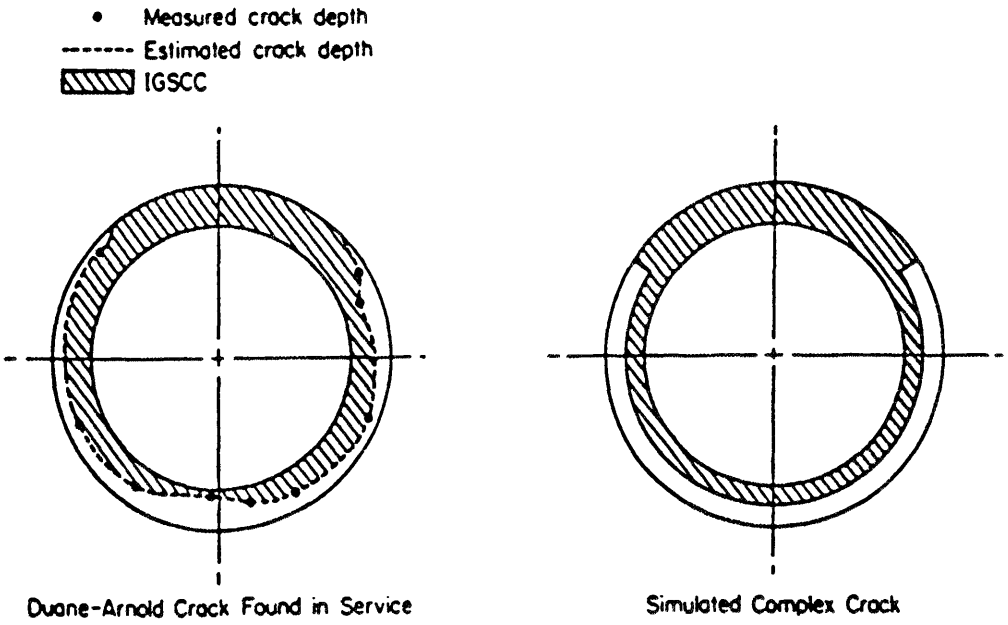

Figure 5.1 Complex-crack geometries from Duane Arnold safe ends found in service and simulated complex-cracks used in pipe experiments

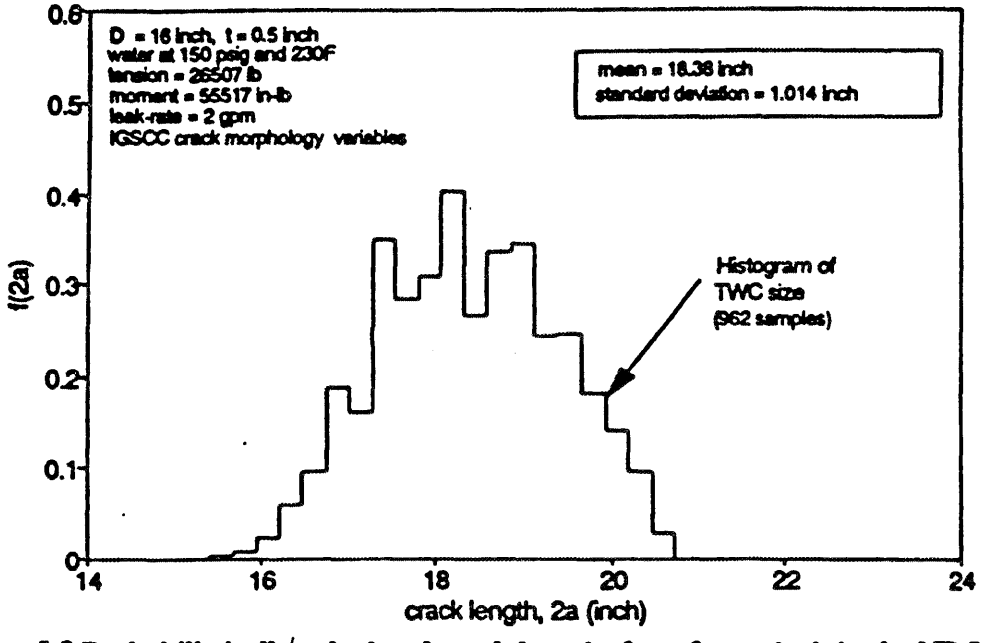

Figure 5.2 Probabilistically calculated crack lengths for a 2 gpm leak in the NP-HWR at the normal operating stresses from Battelle ANSYS calculations of a typical pipe loop

APPENDIX C

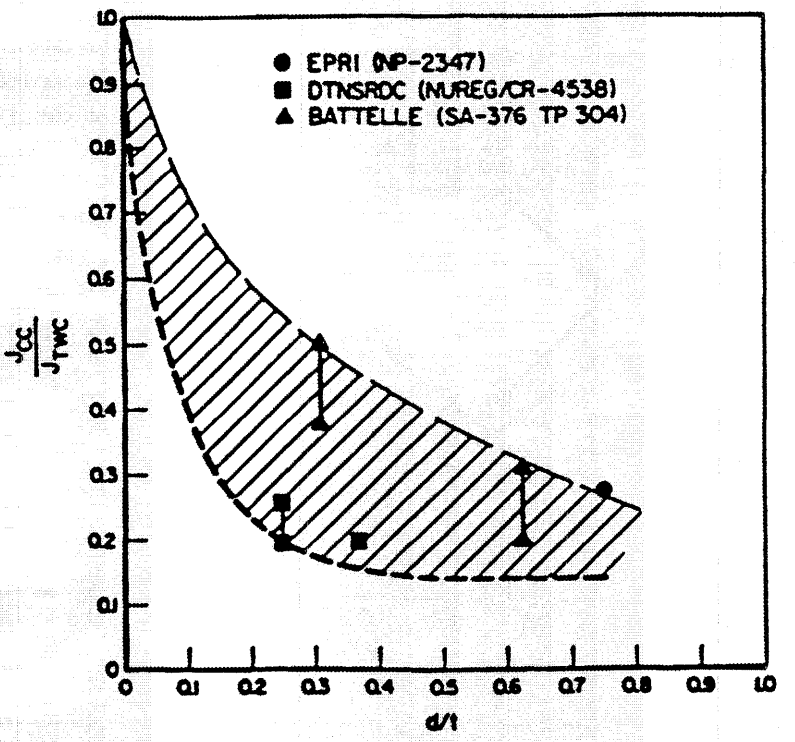

Figure 5.3 Constraint correction on J-R curve for complex-cracked pipe

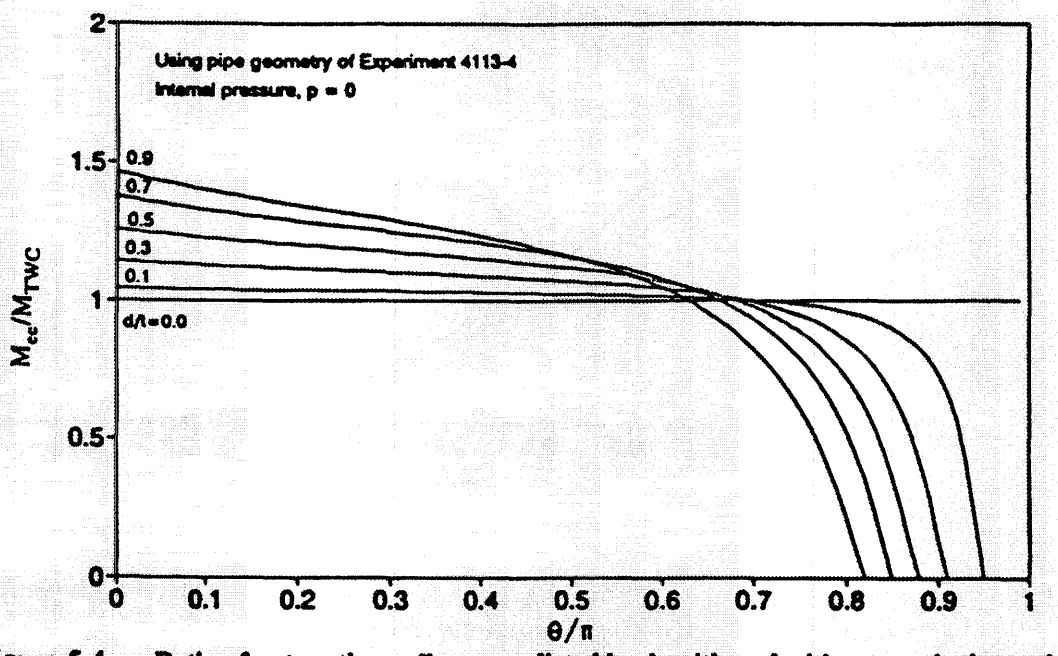

Figure 5.4 Ratio of net-section-collapse predicted loads with and without crack closure load correction

---

(a) TP304 complex-cracked pipe, Experiment 4112-2
(b) Inconel 600 complex-cracked pipe, Experiment 4112-4

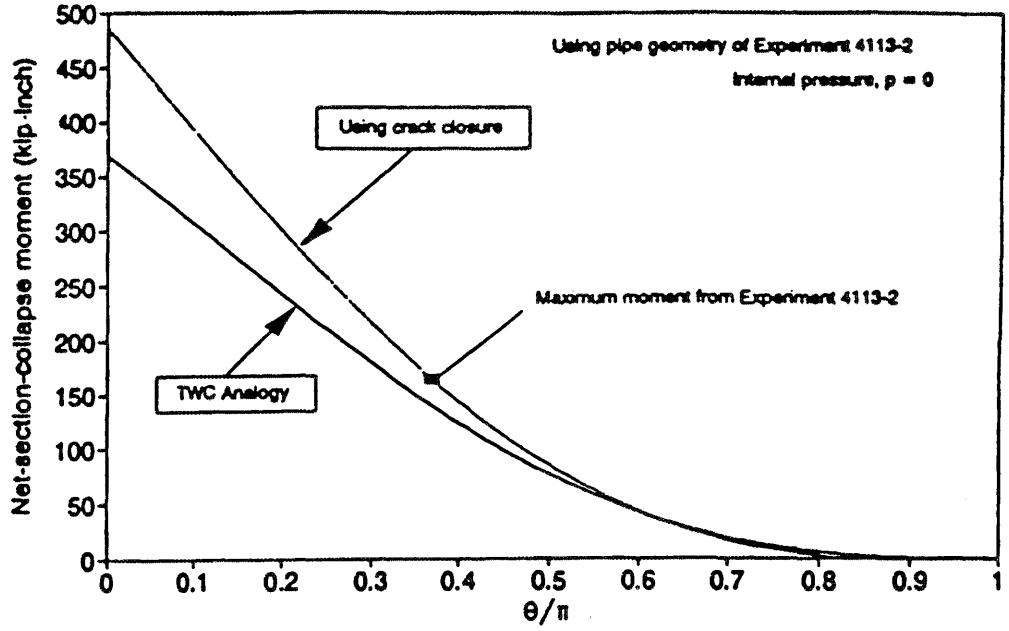

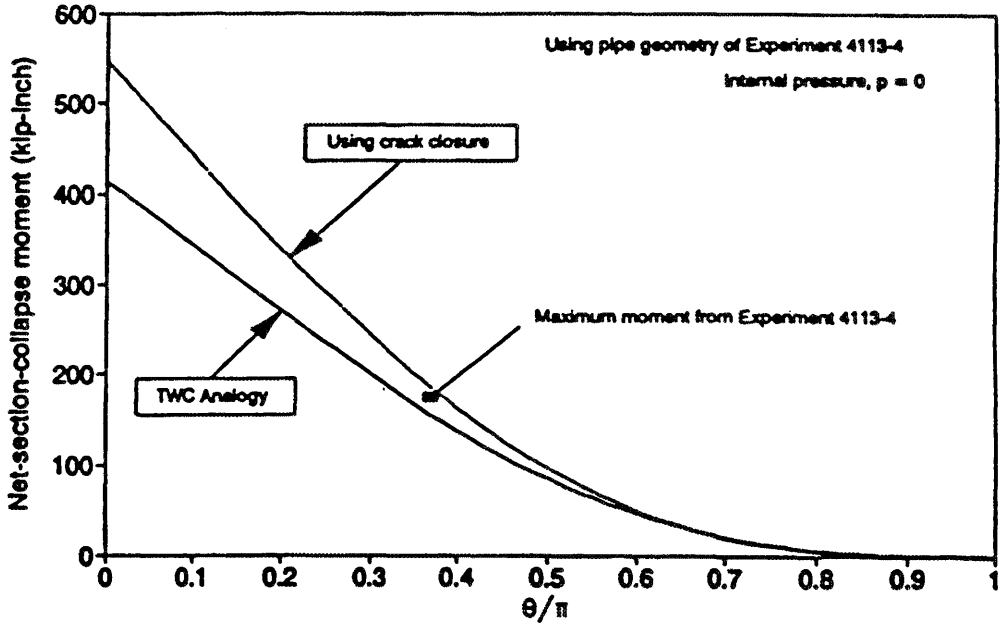

Figure 5.5 **Comparison of complex-cracked-pipe experiments to net-section-collapse analyses with and without crack-closure-load corrections**

(Crack lengths of both experiments nominally 37 percent of circumference for through-wall crack, and 60 percent of the thickness for the surface-crack depth.)

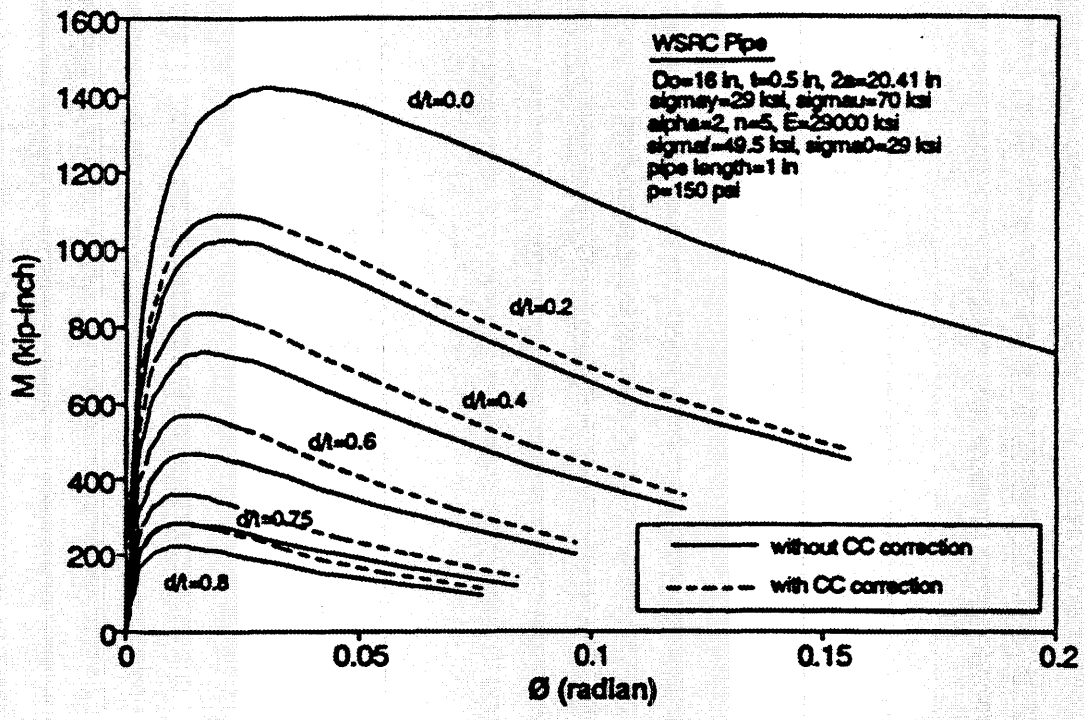

Figure 5.6 Calculated moment-rotation curves for various complex-cracked pipe with and without crack-closure load correction

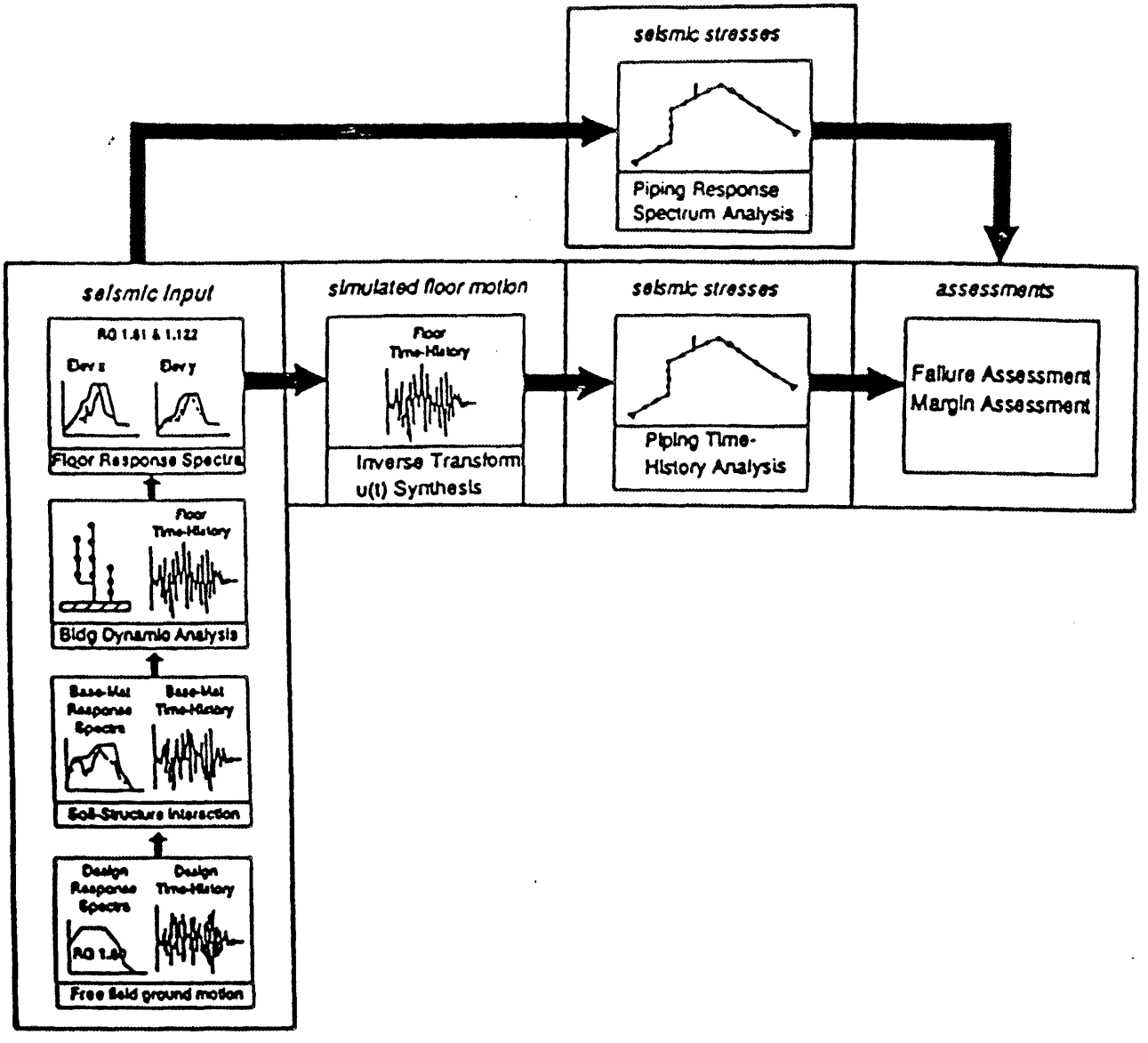

Figure 5.7 Seismic analysis flow chart

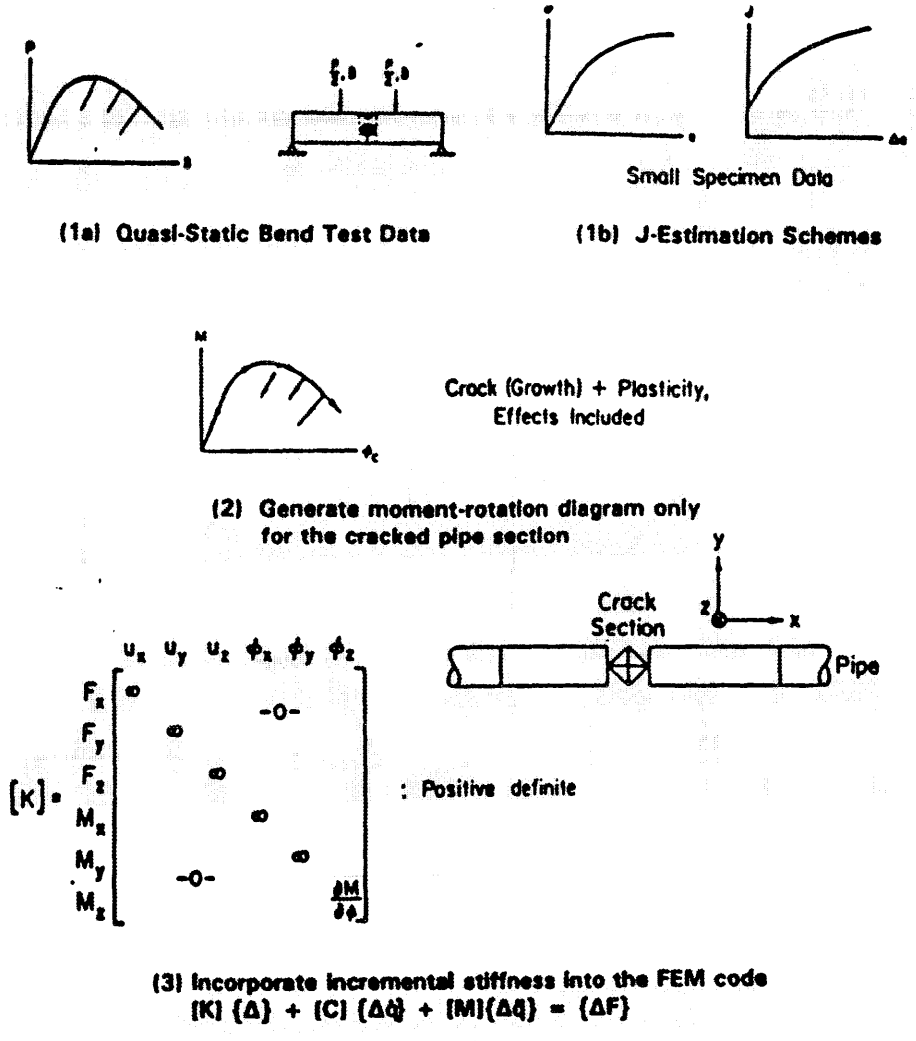

Figure 5.8 Nonlinear cracked-pipe modeling

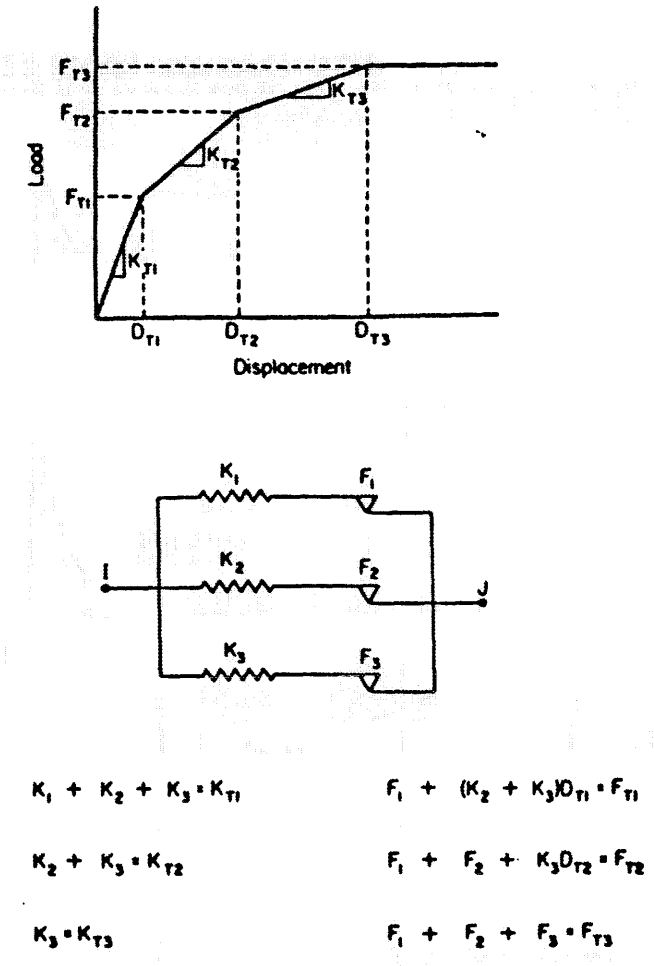

Figure 5.9 Multiple parallel spring-slider element behavior for modeling a surface crack in pipe

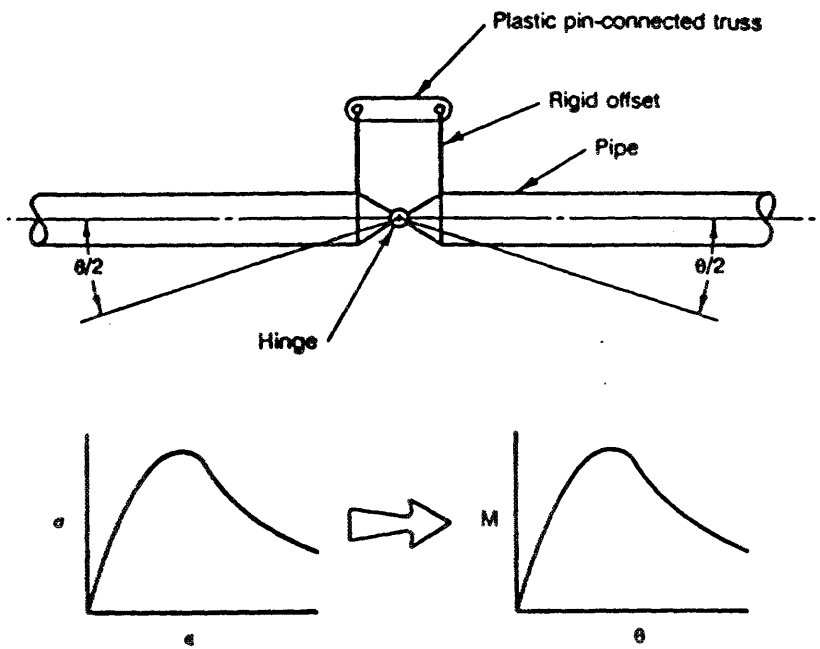

Figure 5.10 Through-wall crack model using a nonlinear truss

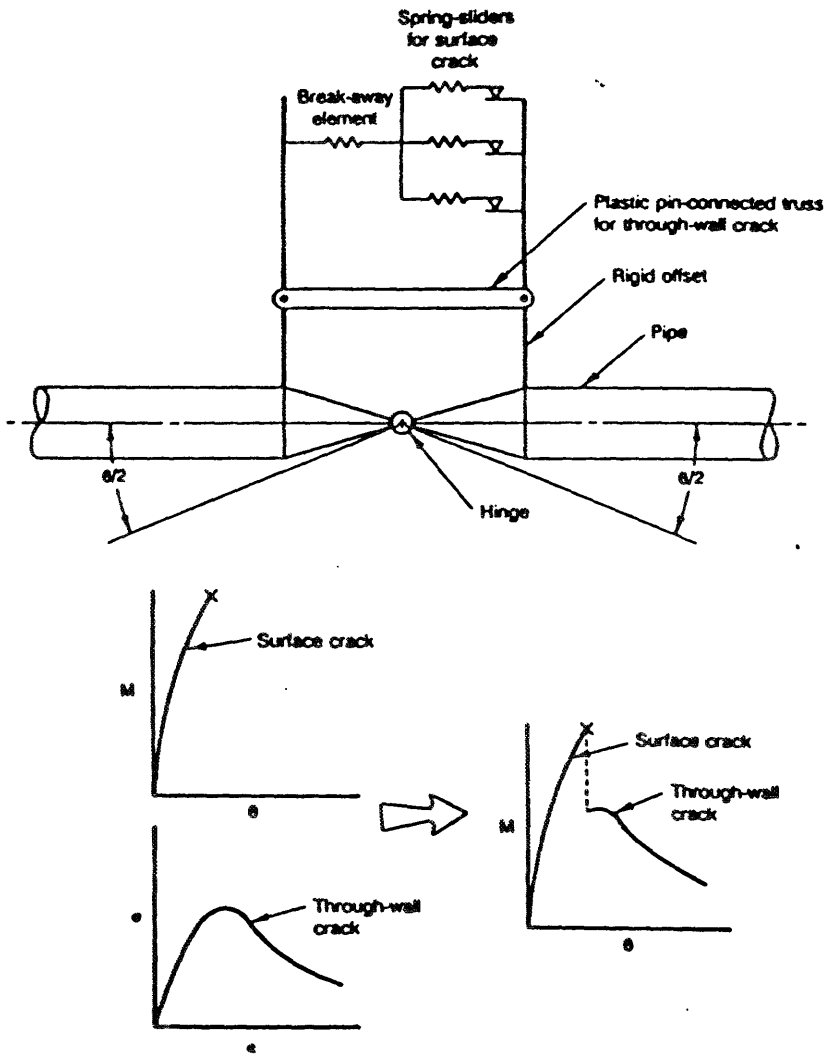

Figure 5.11 Combined surface-crack and through-wall crack model for analyzing dynamic surface to through-wall crack transitions

APPENDIX C

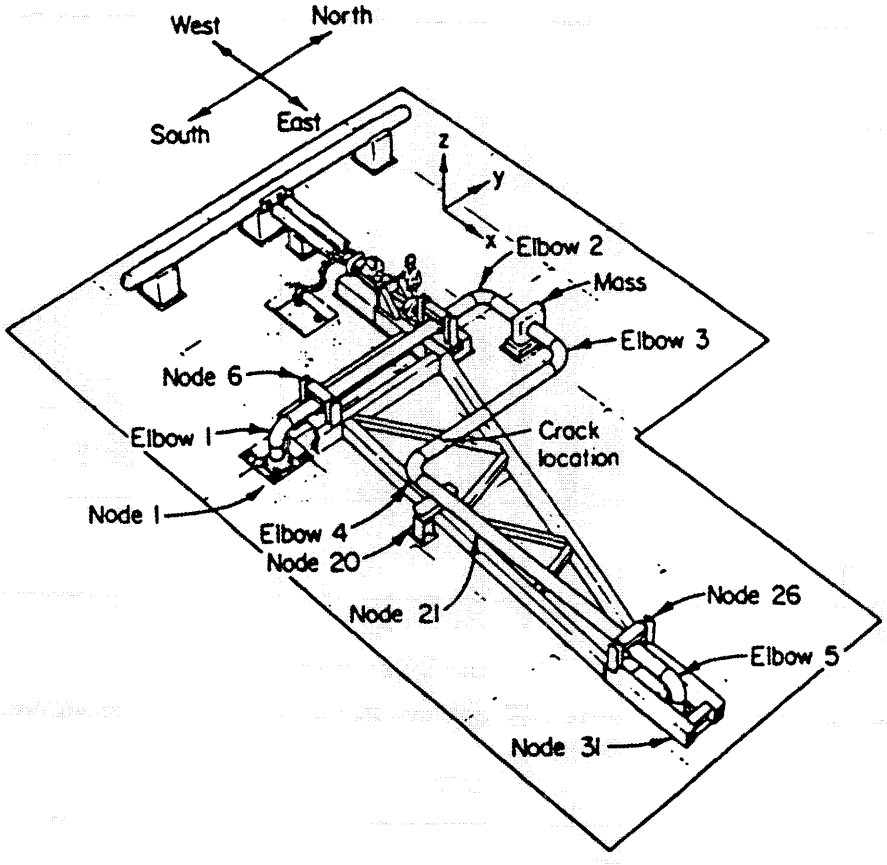

Figure 5.12 Artist's conception of the IPIRG simulated seismic cracked-pipe test facility

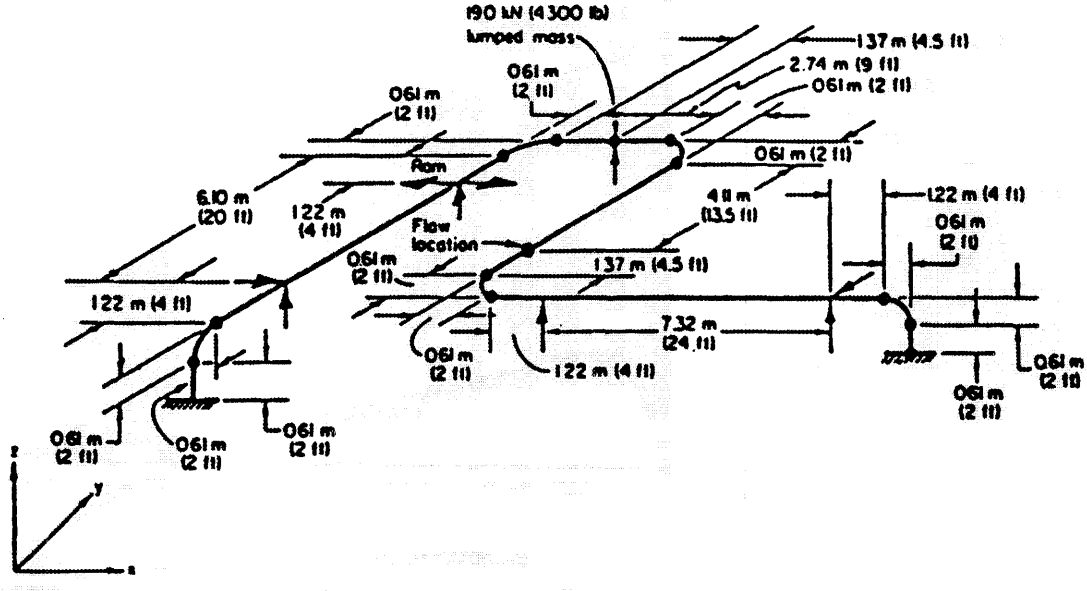

Figure 5.13 IPIRG pipe system geometry

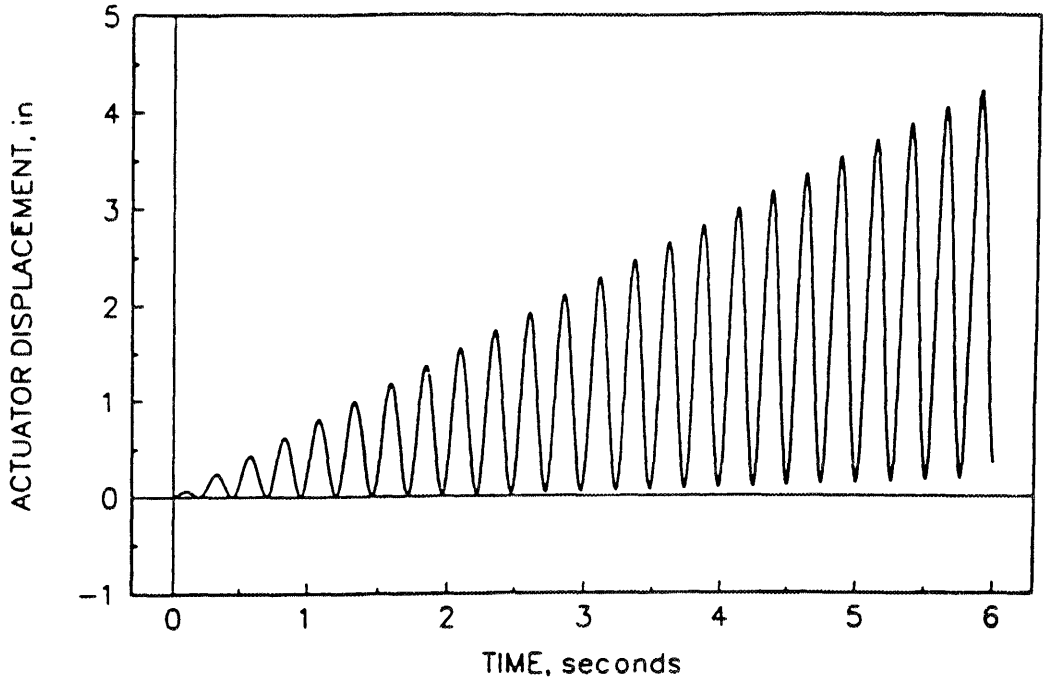

Figure 5.14 IPIRG-1 Experiment 1.3-7 (aged cast stainless steel) dynamic forcing function

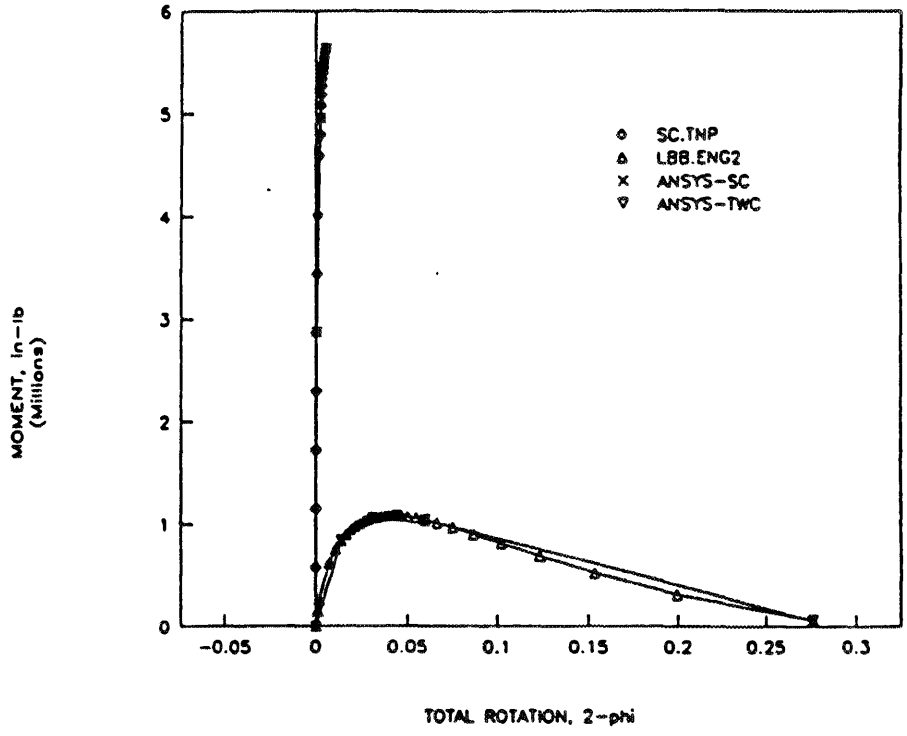

Figure 5.15 Surface and through-wall crack J-estimation scheme predictions of quasi-static moment-rotation behavior for IPIRG-1 Experiment 1.3-7

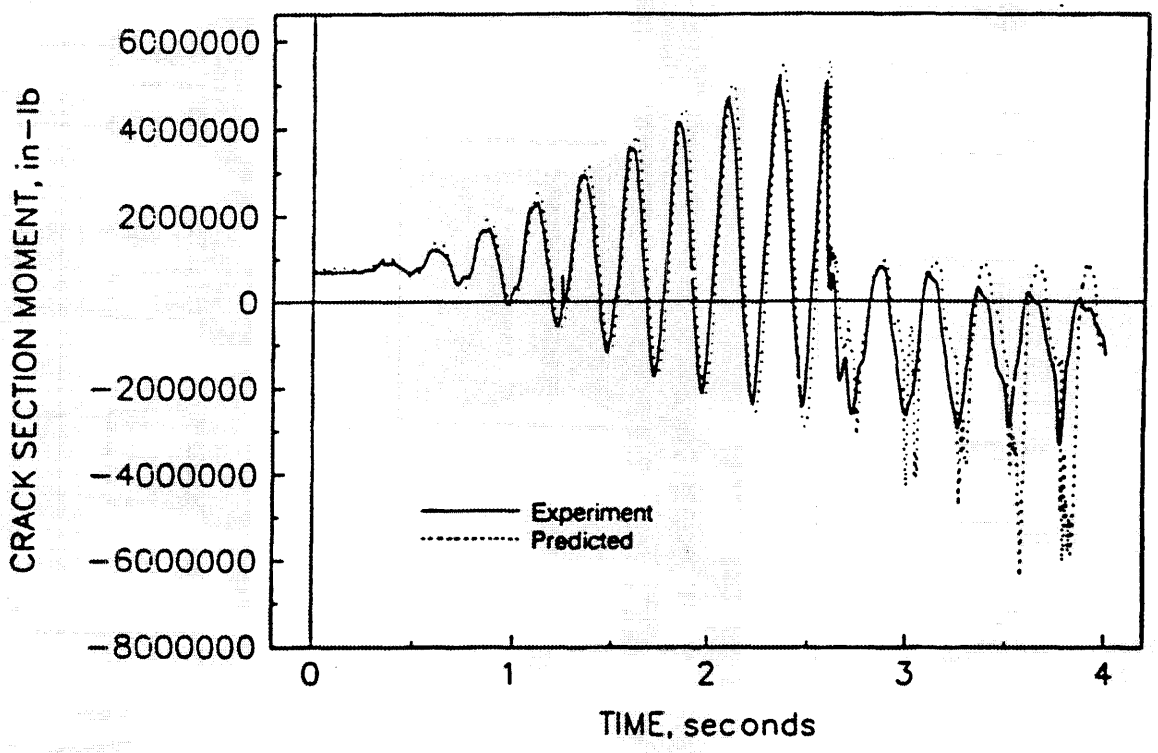

Figure 5.16 **Predicted moment-time dynamic response for IPIRG-1 Experiment 1.3-7 Showing a surface to through-wall crack transition**

APPENDIX C

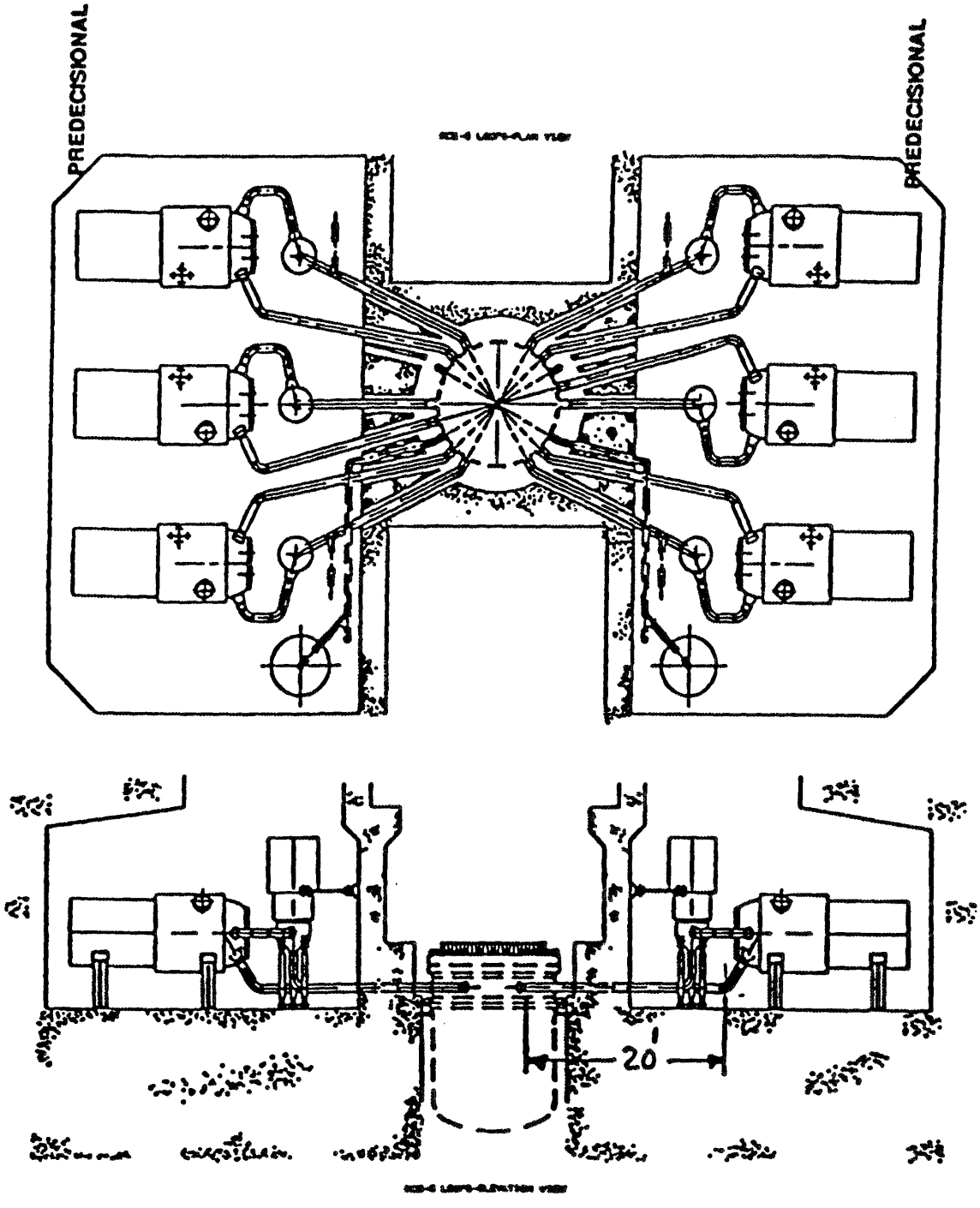

Figure 5.17 Preliminary NP-HWR coolant piping geometry

APPENDIX C

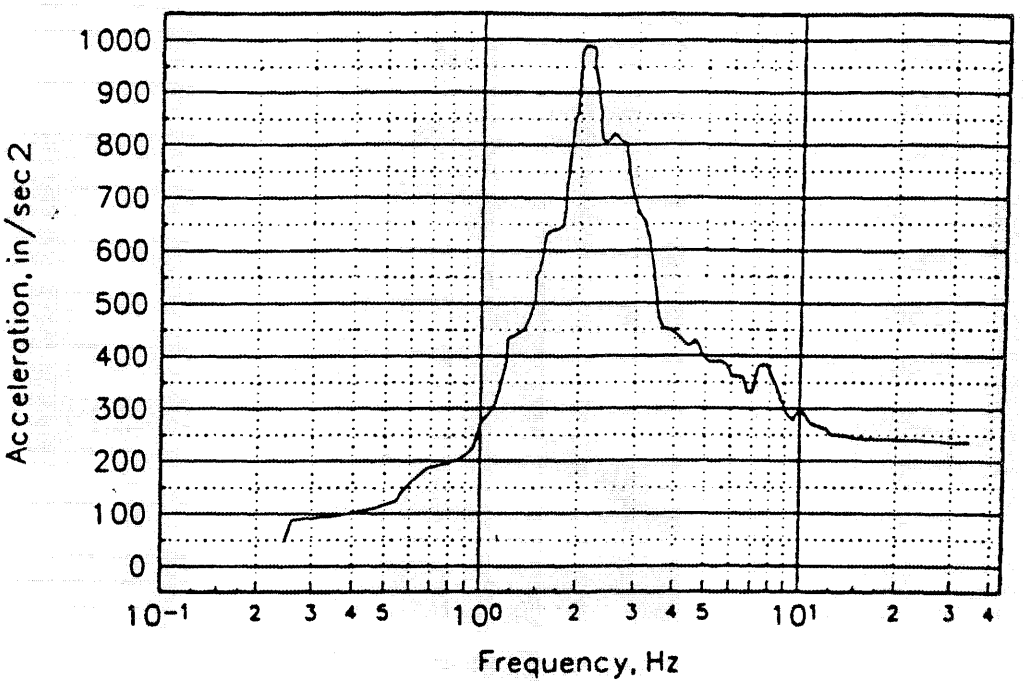

Figure 5.18 NP-HWR horizontal SSE seismic floor response spectrum

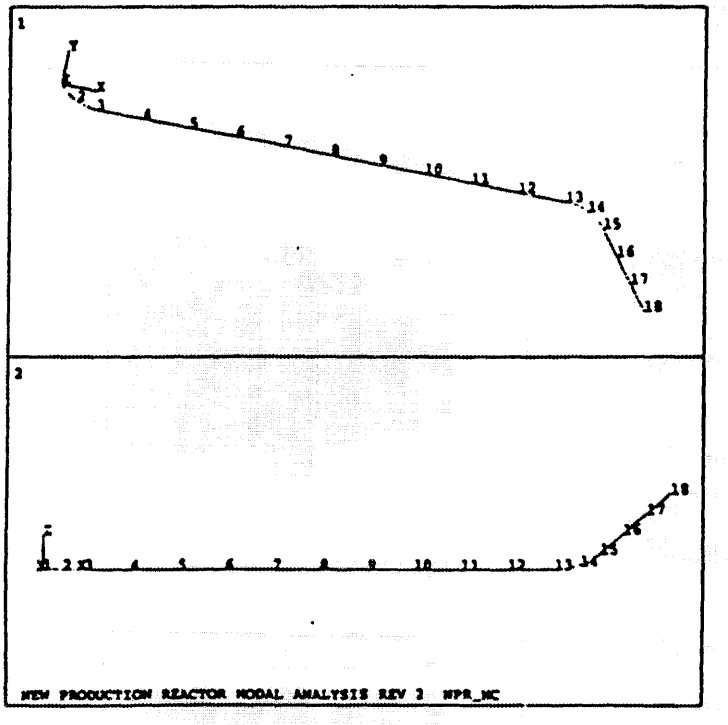

Figure 5.19 Plan and elevation views of the NP-HWR finite element model

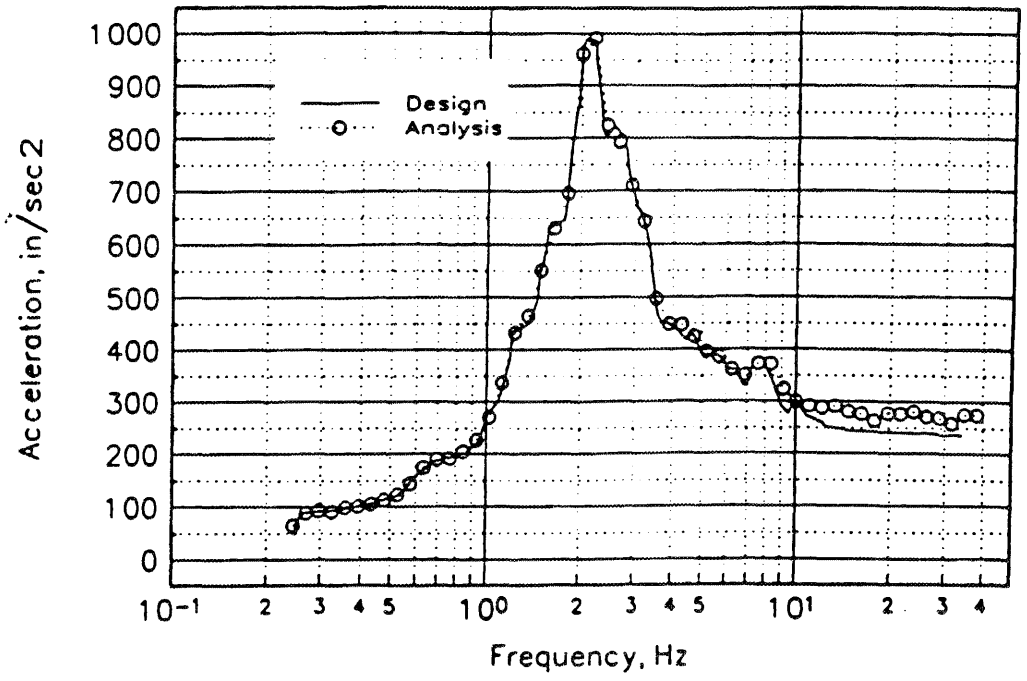

Figure 5.20 Comparison of NP-HWR design and analysis floor response spectra at one SSE level excitation

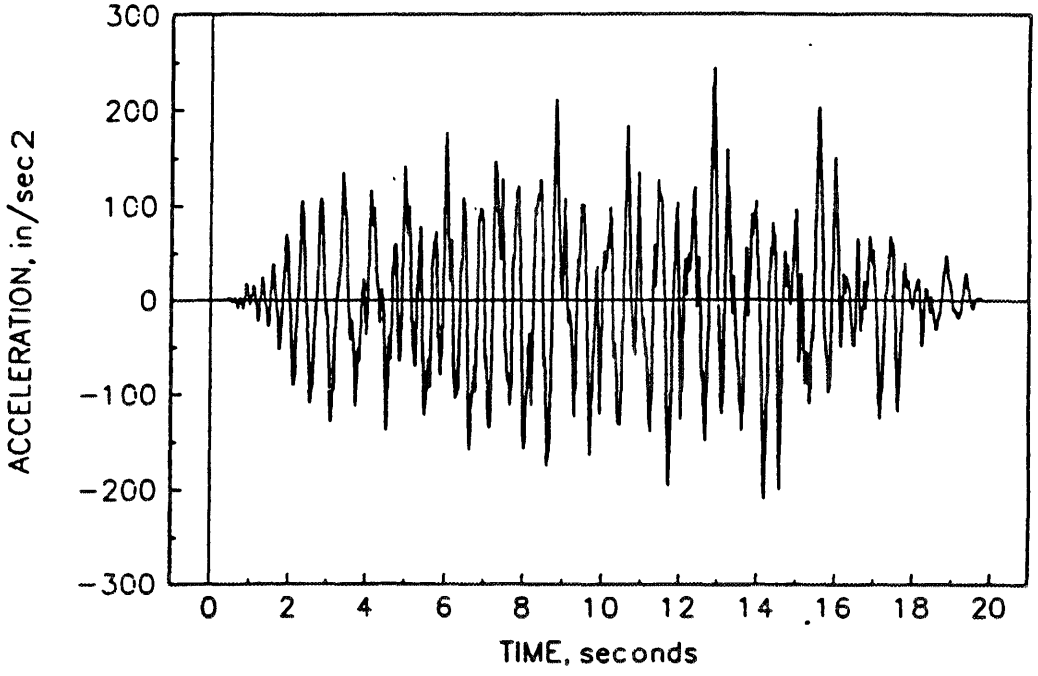

Figure 5.21 SSE spectrum-compatible time history

APPENDIX C

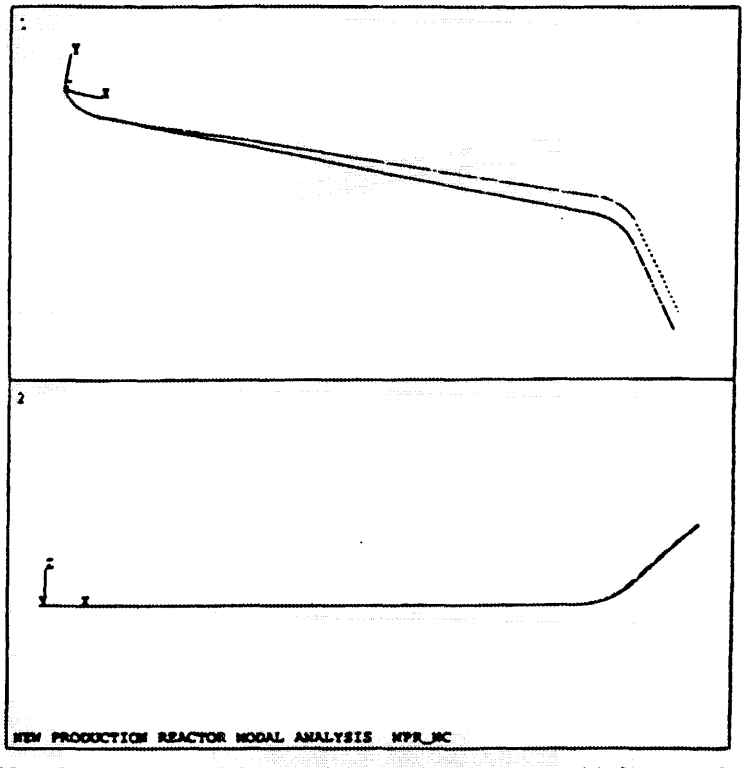

Figure 5.22 Mode Shape 1 (3.89 Hz) of the NP-HWR system with free translation boundary condition at the heat exchanger

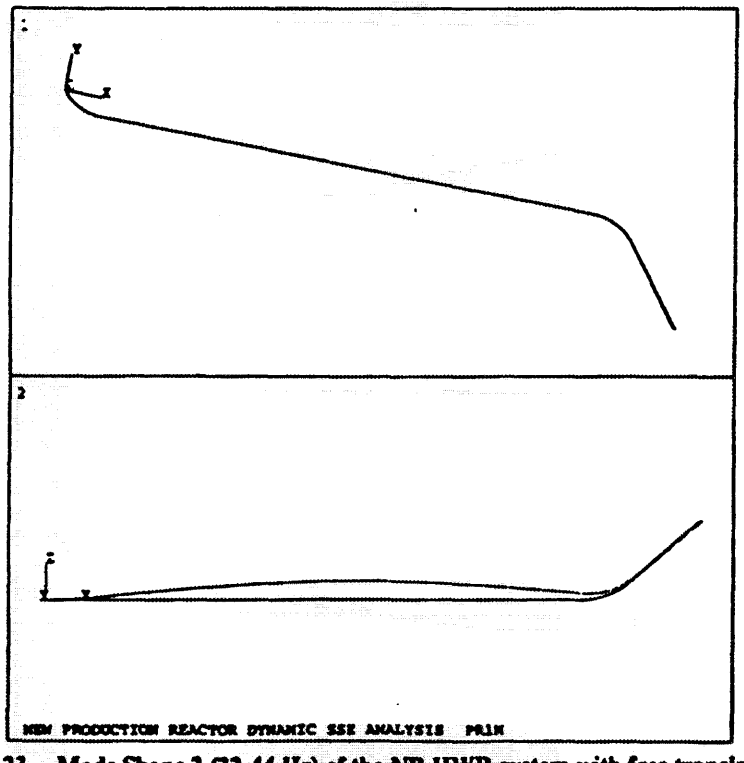

Figure 5.23 Mode Shape 2 (22.44 Hz) of the NP-HWR system with free translation boundary condition at the heat exchanger

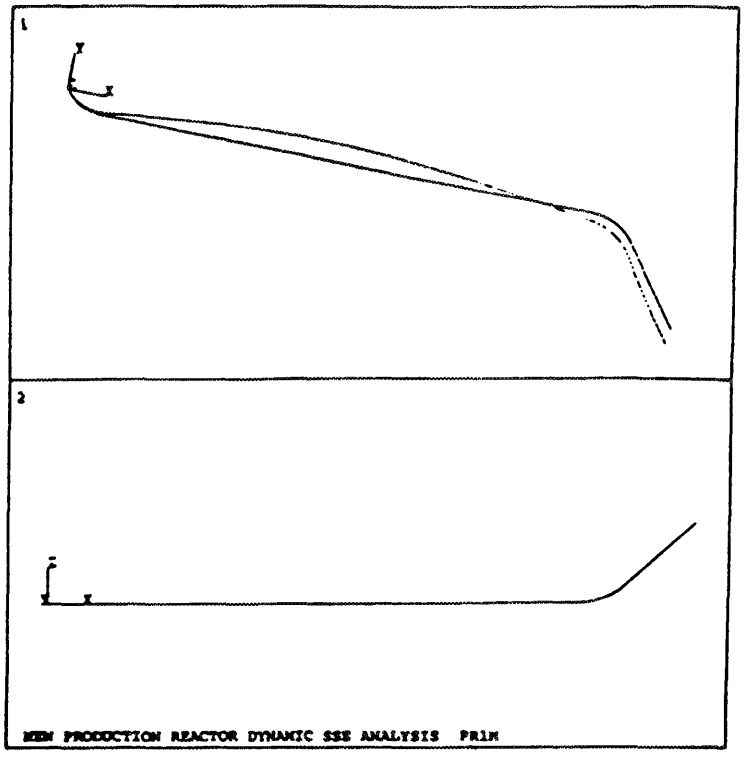

Figure 5.24 Mode Shape 3 (28.40 Hz) of the NP-HWR system with free translation boundary condition at the heat exchanger

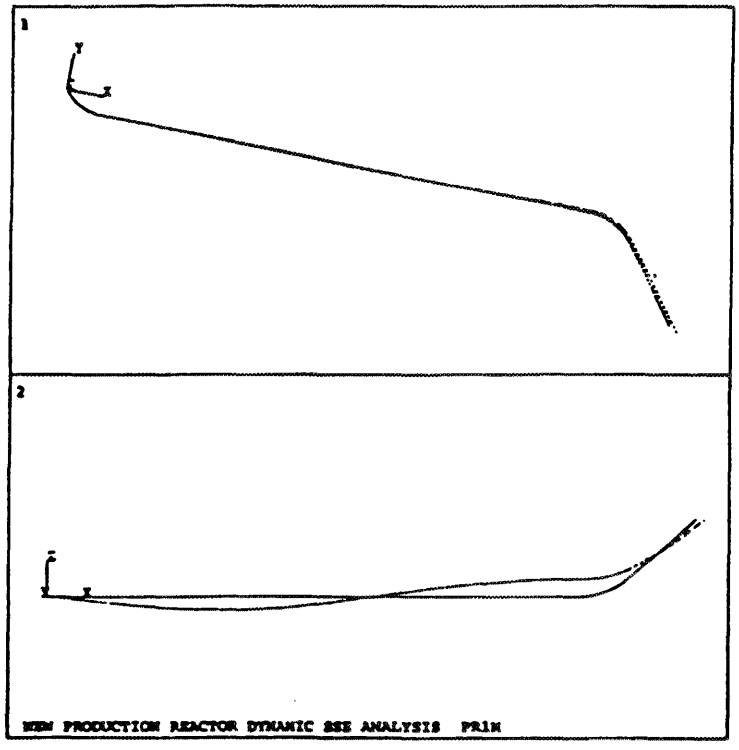

Figure 5.25 Mode Shape 4 (58.55 Hz) of the NP-HWR system with free translation boundary condition at the heat exchanger

APPENDIX C

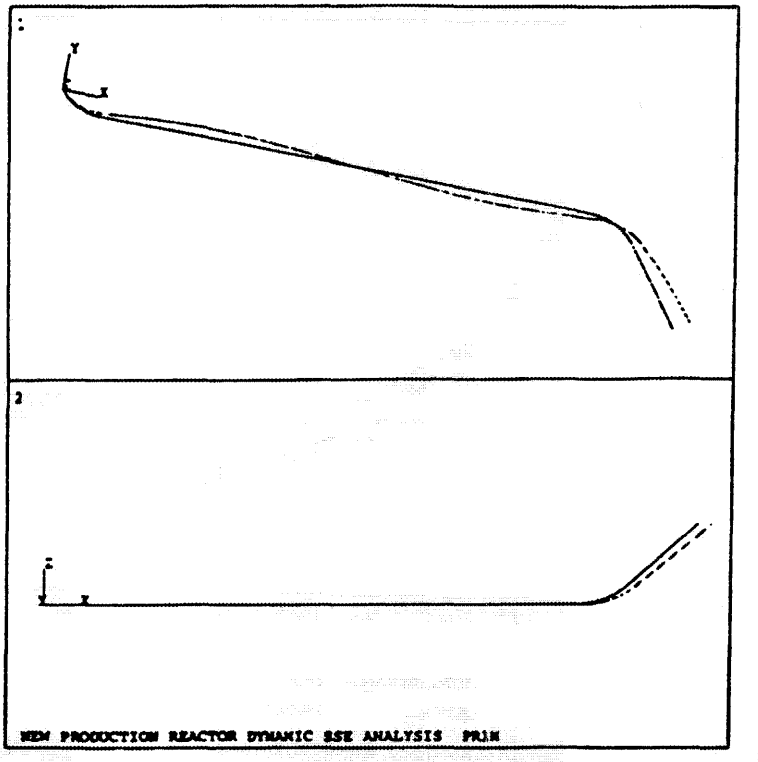

Figure 5.26 Mode Shape 5 (67.89 Hz) of the NP-HWR system with free translation boundary condition at the heat exchanger

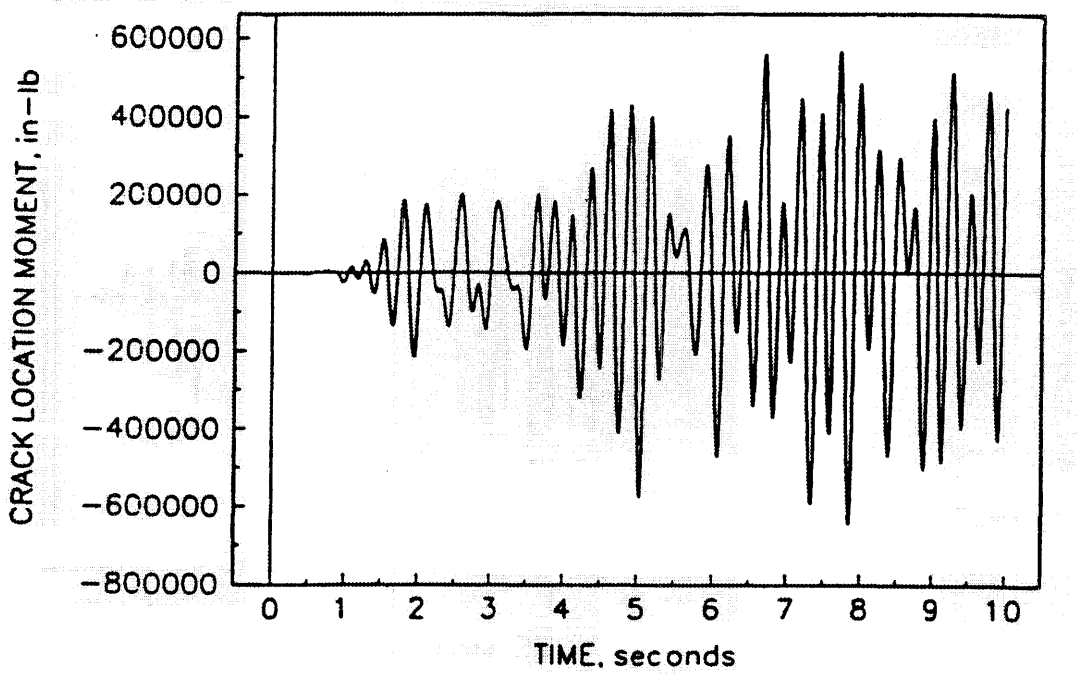

Figure 5.27 Linear elastically calculated N + 1SSE moment at the reactor pressure vessel nozzle (highest stressed location, assumed crack location)

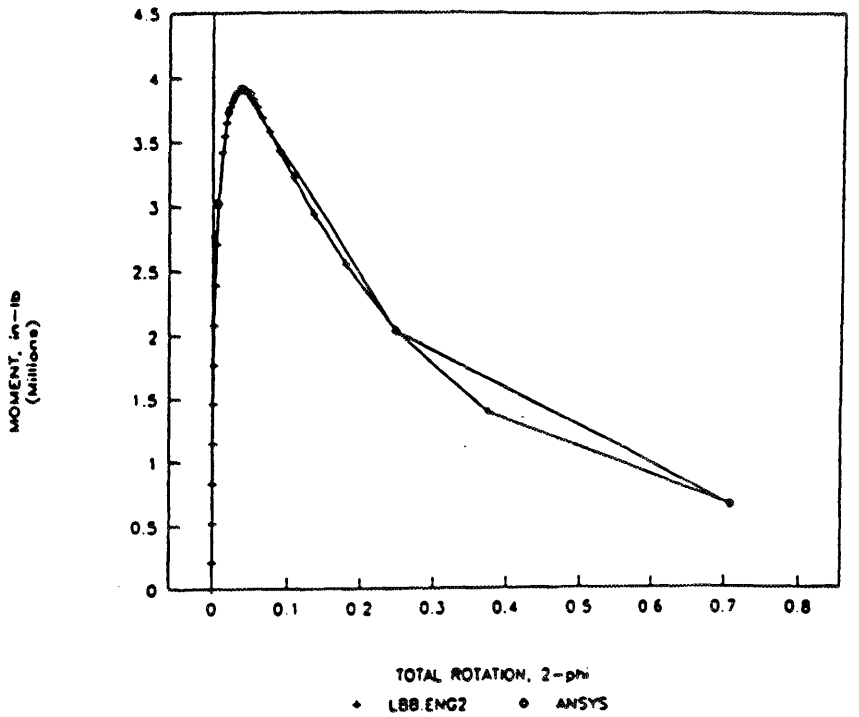

Figure 5.29 10-inch long through-wall crack moment-rotation response from a J-Estimation scheme

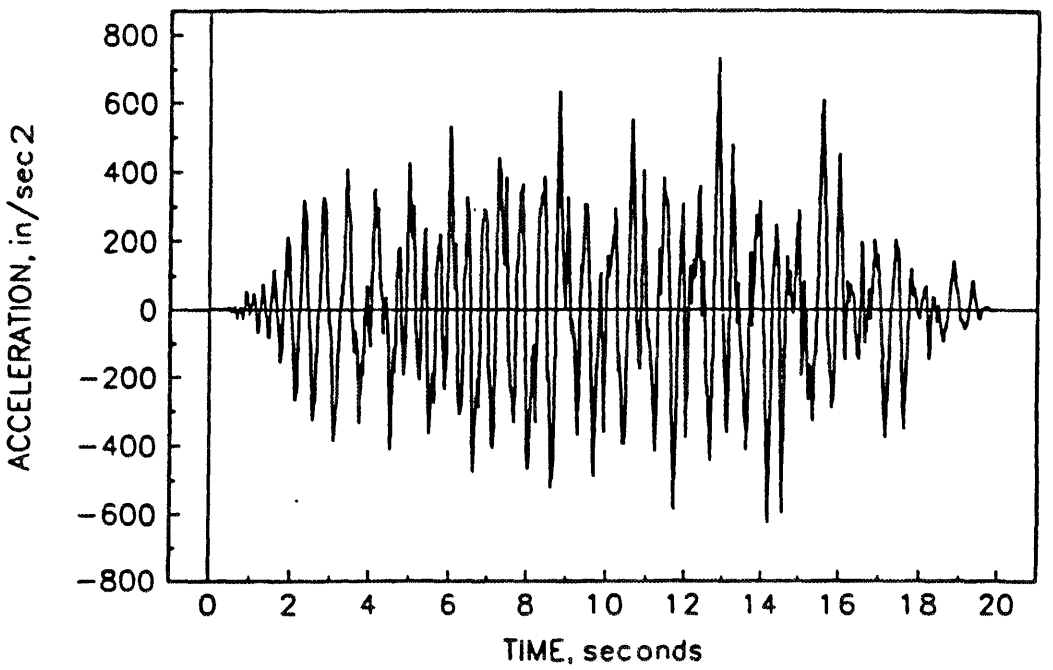

Figure 5.28 3 SSE floor motion acceleration

APPENDIX C

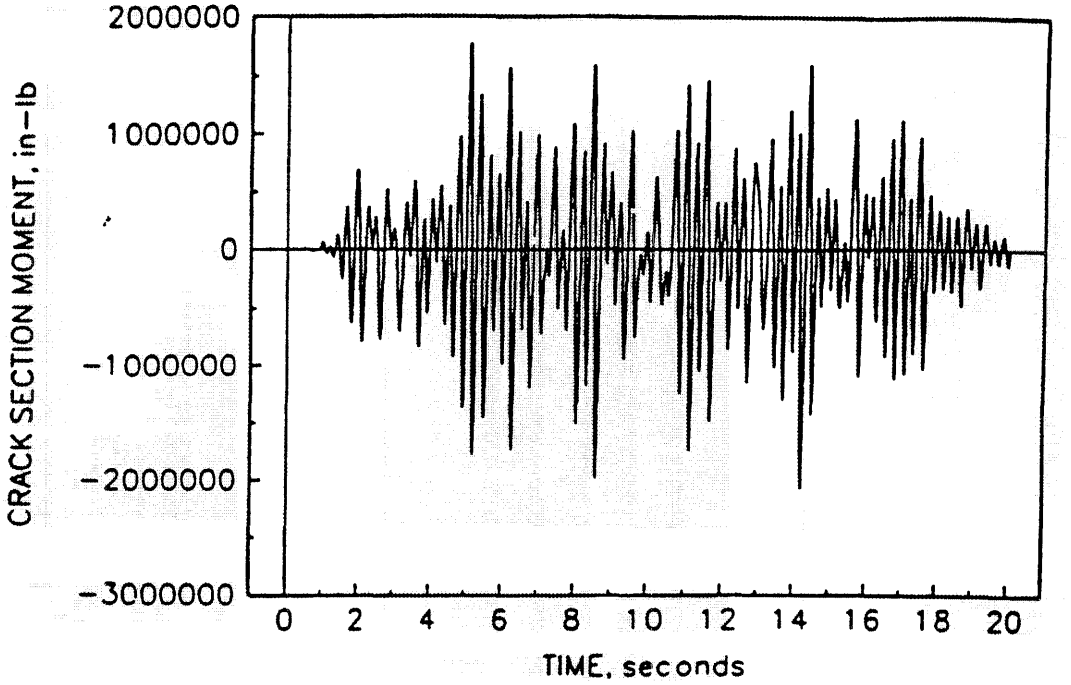

Figure 5.30 Crack-section moment for a 10-inch long through-wall crack at 3 SSE Loading

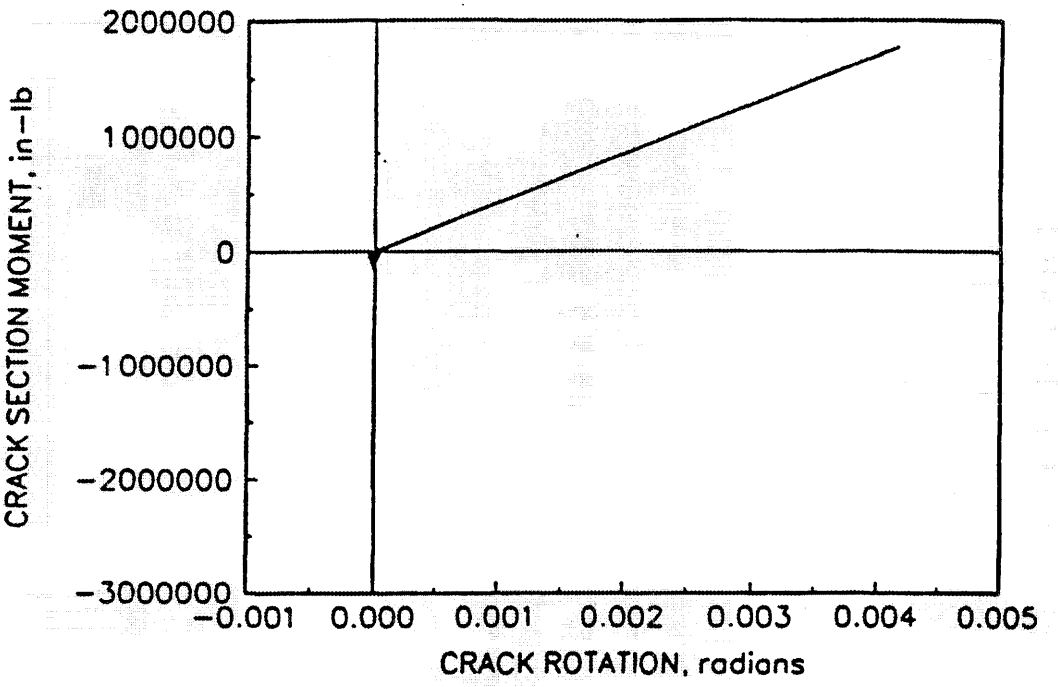

Figure 5.31 Crack-section response for a 10-inch long through-wall crack at 3 SSE Loading

APPENDIX C

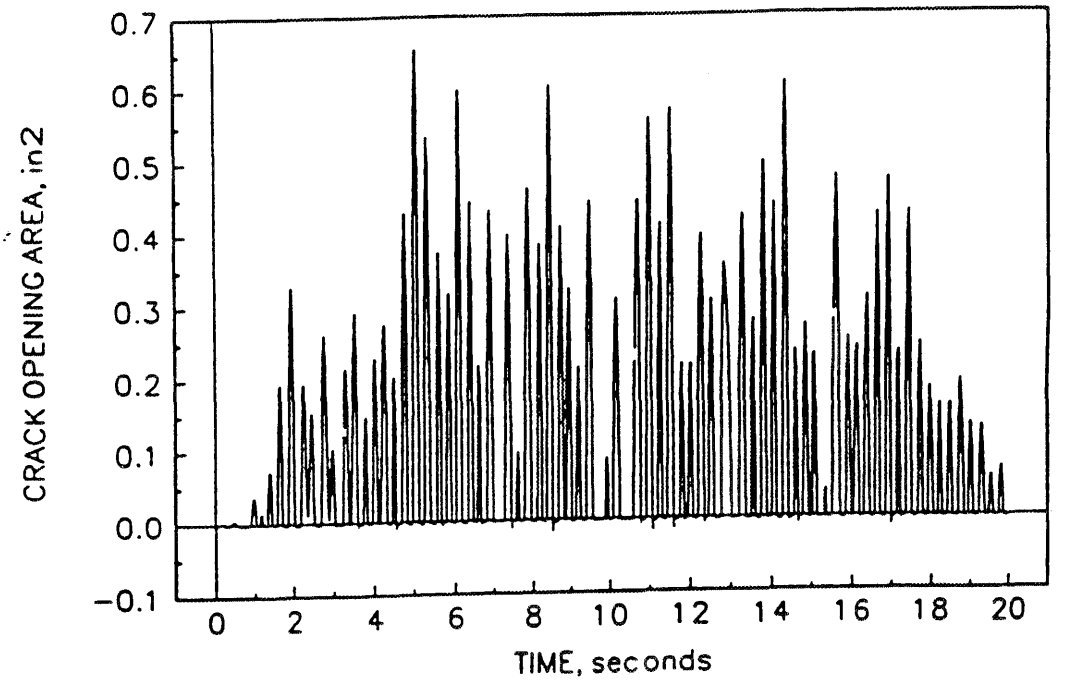

Figure 5.32 Crack-opening area for a 10-inch long through-wall crack at 3 SSE loading

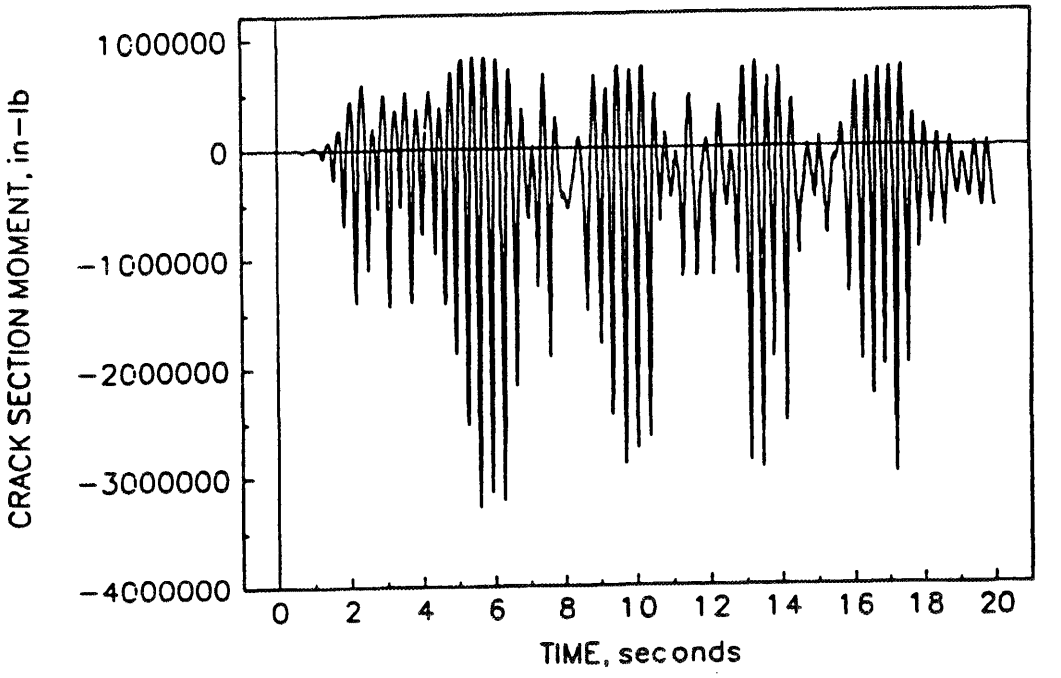

Figure 5.33 Crack-section moment for a 40-percent deep 360-degree surface crack with a 2-gpm leaking (20.408-inch long) through-wall crack at 3 SSE loading

APPENDIX C

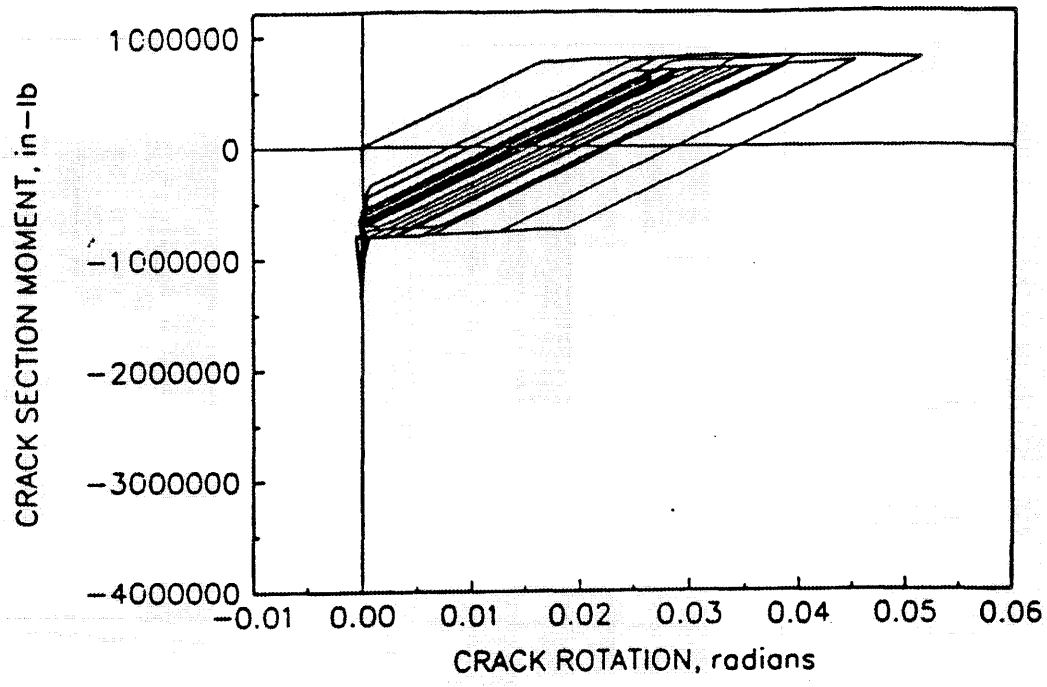

Figure 5.34 Crack-section response for a 40-percent deep 360-degree surface crack with a 2-gpm leaking (20.408-inch long) through-wall crack at 3 SSE loading

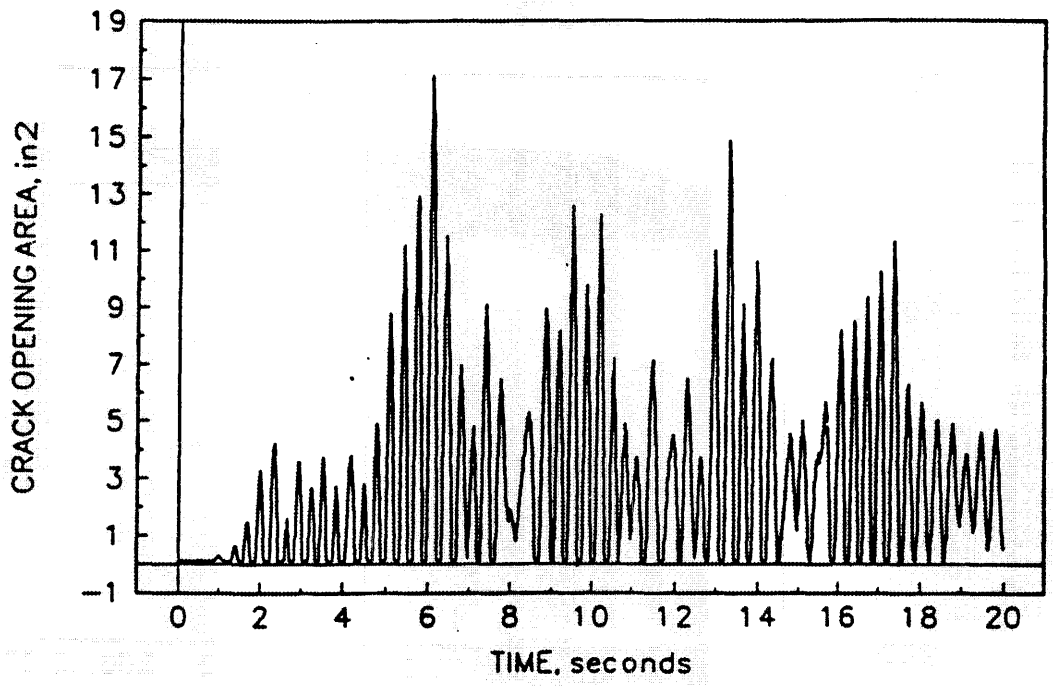

Figure 5.35 Crack-opening area for a 40-percent deep 360-degree surface crack with a 2-gpm leaking (20.408-inch long) through-wall crack at 3 SSE loading

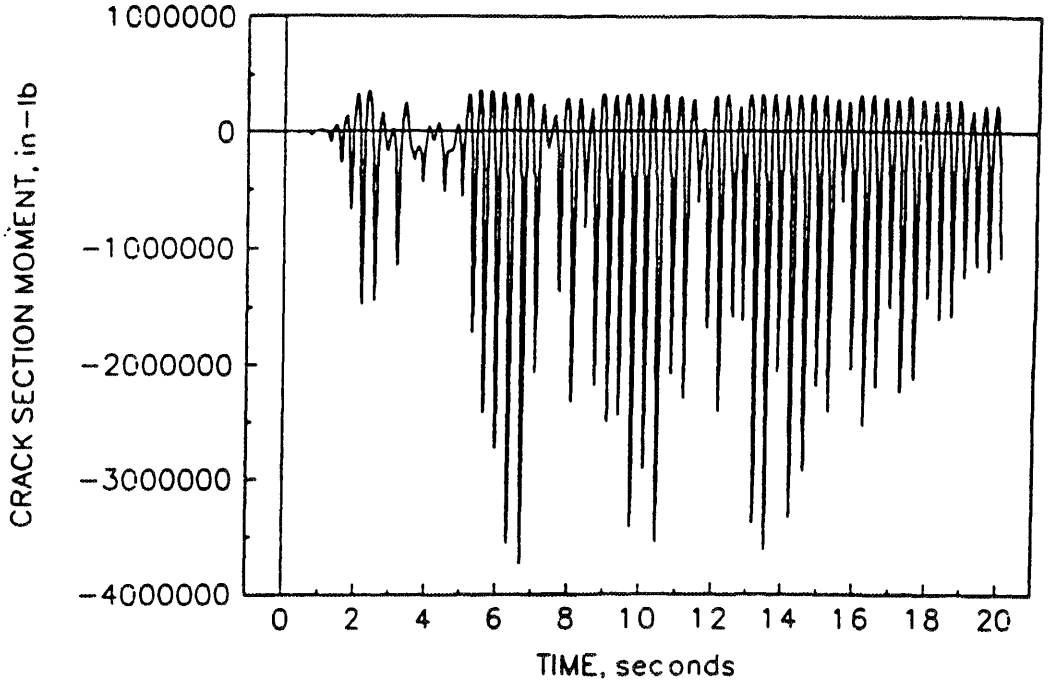

Figure 5.36 Crack-section moment for a 75-percent deep 360-degree surface crack with a 2-gpm leaking (20.408-inch long) through-wall crack at 3 SSE loading

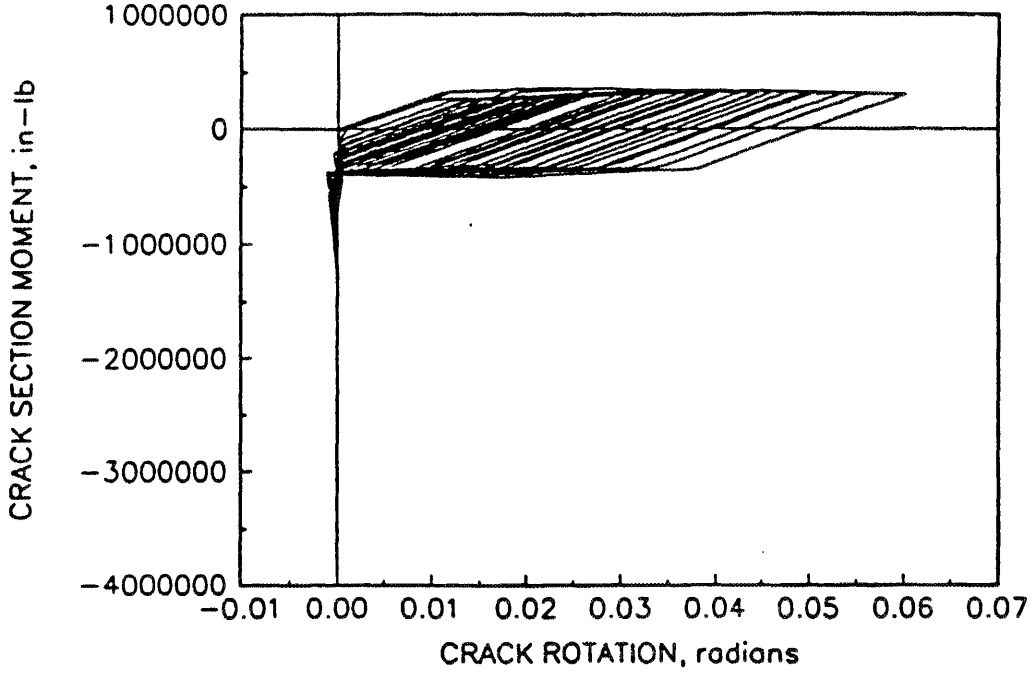

Figure 5.37 Crack-section response for a 75-percent deep 360-degree surface crack with a 2-gpm leaking (20.408-inch long) through-wall crack at 3 SSE loading

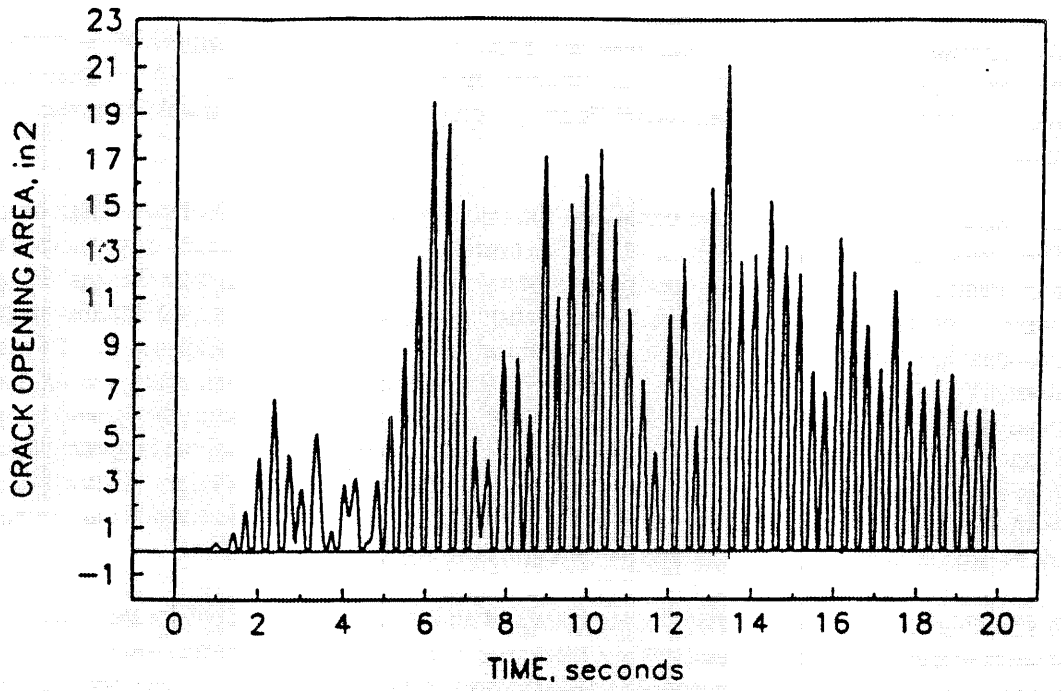

Figure 5.38 Crack-opening area for a 75-percent deep 360-degree surface crack with a 2-gpm leaking (20.408-inch long) through-wall crack at 3 SSE loading

6.0 CONCLUSIONS

From the four analytical efforts undertaken, the following conclusions can be drawn.

The first effort involved a sensitivity study to analytically find the family of surface cracks that could fail at various N+SSE stress levels. This can be considered a first step in an evaluation to assess what surface crack geometries could possibly lead to a pipe break. It is possible that a 360-degree surface crack is worse for stability considerations than a through-wall or complex crack. The results in Section 2 of this report would provide a basis for selecting surface-crack geometries for further dynamic evaluations as was done for the through-wall and complex-crack geometries in Section 5 of this report. Some international experts in the LBB arena consider the possibility of a DEGB from a surface crack more of a challenge to the integrity of the pipe system, since there is no possibility of detection of the crack by leak sensing equipment.

The second effort provided pretest predictions of the C-pipe experimental load, load-line displacement, crack growth, center-crack-opening displacement and the resulting crack-opening area. ORNL staff compared these predictions with their experimental data (not shown in this report) and found the agreement to be quite good. A judgement of how good the analyses actually are would require obtaining actual properties for the C-pipe tested at ORNL (typical values were used) and precise documentation of the pipe dimensions and average crack lengths through the thickness. This effort showed that reasonable predictions can be made by the J-integral estimation schemes, which are also a critical input to the nonlinear dynamic calculations conducted in the final effort in of this project.

The third effort in this project compared the cyclic crack growth in the ORNL low cycle fatigue test on the C-pipe with an extrapolation of high-cycle fatigue data for TP304 stainless steel from the

EDEAC data base. This agreement was extremely good, implying that in principle one could make slightly conservative, yet reasonably accurate, predictions of such crack growth. An evaluation of the predictive ability of an automated low-cycle fatigue crack-growth analysis should be assessed in the future.

The final effort in this project involved nonlinear time-history seismic analyses of one design of the NP-HWR pipe loop with a crack in it at 3 SSE loading. Although the exact dimensions and boundary conditions of the pipe loop modelled probably differ from what would be the final design conditions, this time-history nonlinear cracked-pipe analysis showed that there is considerable margin over conducting typical response-spectrum uncracked-pipe elastic stress analysis for fracture evaluations. The nonlinear time-history analysis of a 75-percent deep complex crack showed that there was margin of over a factor of 5 on the "failure" moment compared with predictions using elastic uncracked-pipe analyses. This margin comes from the short duration of the large amplitude cycles in the seismic event and the nonlinear behavior of the cracked-pipe section. Furthermore, even with the 75-percent deep complex crack the nonlinear time-history analysis showed only a small amount of ductile tearing occurred at the end of the 3 SSE loading.

The key findings of this work are that the occurrence of an instantaneous DEGB for the conditions examined is extremely unlikely, even with the most severe crack geometry that has been discovered in a commercial power plant. The analyses of the cracks evaluated suggest that they were a long way from a DEGB even occuring. Seismic aftershock loads may cause some additional cyclic crack growth, but probably much less than from the original event. There may be other conditions that will affect the dynamic results conducted to date. These are:

- The actual boundary conditions of the heat exchanger and the geometry of the pipe loop would probably differ from what was analyzed.

- Cyclic effects on the tearing resistance of the material were not included in this analysis. Since the load ratios are negative, and there are numerous cycles, experience to date suggests that the J-R curve will be lowered and more crack growth would occur than what is currently predicted. This is an evolving technology at this time, and incorporating these effects required more effort than allowed within the limitation of the project time and funds.

- Plasticity in the uncracked pipe remote from the crack will absorb energy and change the effective damping of the system. It is believed that this will reduce the dynamic loads, which would make the pipe less susceptible to a DEGB.

- Fatigue crack growth considerations were not incorporated into the dynamic calculations. Such a process is not automated to the point of including the growth in the dynamic analyses, but separate calculations with possible restarts of the dynamic calculations could be conducted. Not including this aspect will underestimate the crack growth in the dynamic calculations, but the magnitude of the error is probably small compared with the significance of the results obtained.

Should the NP-HWR program restart, the dynamic analyses should be repeated with the precise boundary conditions and geometry of the final design of the plant piping. The analyses should be extended to include the effects of low-cycle fatigue crack growth during the seismic event, as well as the ductile-tearing calculations that were done to date. Finally, analyses should be conducted to assess the propensity of fracture for a surface crack to propagate under dynamic loading, since all the work to date was on through-wall-cracked pipe. This dynamic surface-cracked pipe analysis would give some guidance for the maximum allowable surface-crack length for NDE inspection criteria.

APPENDIX D

ARGONNE NATIONAL LABORATORY
9700 South Cass Avenue, Argonne, Illinois 60439

Parametric Study of the Probability of Leaks in the NPR-HWR Pressurizer Surge Line

by

A. Stojimirovic and S. Majumdar

Materials and Components Technology Division

January 29, 1993

Work sponsored by

U.S. DEPARTMENT OF ENERGY
Office of New Production Reactors

Parametric Study of the Probability of Leaks in the NPR-HWR Pressurizer Surge Line

by

A. Stojimirovic and S. Majumdar

Abstract

The probability of leaks due to estimated steady-state and transient loadings in the pressurizer surge line of the New Production Reactor (NPR)-Heavy Water Reactor (HWR) was determined with the PRAISE code. The effects of earthquake loadings on the probability of leaks were found to be negligible. On the other hand, stress corrosion cracking in a welded joint can significantly increase the probability of leaks. Residual stress effects, which were not taken into account in this study, can further increase the probability of leaks.

1 Introduction

The U.S. Code of Federal Regulations requires that structures and components affecting the safe operation of nuclear power plants be designed to withstand the (random) combination of loads that results from normal operating conditions, postulated accidents, and natural phenomena that can occur at a plant site during its service life. Because reactor piping components form one of the most critical areas in terms of safe plant operation, a probabilistic fracture mechanics code known as the Piping Reliability Analysis Including Seismic Events (PRAISE)[1-10] was developed by the Nuclear Regulatory Commission (NRC). The PRAISE Code quantifies in probabilistic terms the safety or risk associated with the operation of a piping system. In addition to leaks, the code also computes the probability that a so-called double-ended guillotine break will not lead to a large loss-of-coolant accident (LOCA).

Piping deterioration, as incorporated in the current PRAISE code (a summary of the PRAISE code is given in the Appendix of Ref. 11), is caused by propagation of cracklike weld defects introduced during fabrication or created during plant service via stress corrosion. The mechanisms that govern defect evolution are (a) fatigue, reflecting the inherent cyclic mode of operation of the plant; and (b) stress corrosion cracking, which is triggered by the aggressive environment within the pipe.

This report describes the use of the PRAISE code to estimate the probability of leaks in the New Production Reactor - Heavy Water Reactor (NPR-HWR) pressurizer surge line. The basic assumptions, procedures, and application of the code are described in a series of earlier reports.[1-10] The code is available in versions for both mainframe and IBM-PC-compatible computers. The current studies were performed with the PRAISE PC version 2.1, modified to run on an Apple Macintosh Computer. Minimal changes, primarily in input and output routines, were needed for adaptation to the Macintosh. In addition, the capability for handling multiple-loading cases simultaneously (which is available in the mainframe version but was eliminated in the PC version because of the differences in how the mainframe and the PC manage arrays) was restored in the Macintosh version, because the Macintosh handles arrays in a manner similar to that required by the mainframe version. The source code for PRAISE was made available by John O'Brien of the NRC Office of Nuclear Regulatory Research through Sandia National Laboratories.

2 Input Parameters for Analysis of NPR-HWR Pressurizer Surge Line

2.1 Pipe Geometry and Material Properties

The pipe used in the pressurizer surge line is Type 316 stainless steel with an inner radius R = 7.5 in. and a thickness t = 0.5 in. Flow stress is taken as σ_{flo} = 48 ksi and is treated as a random variable with a standard deviation of 1.4 ksi. The fatigue crack growth law, $da/dN = C(\Delta K)^n$ is modeled with n = 4.16 and C as a log-normal-distributed random variable characterized by $\langle C \rangle = 1.12 \times 10^{-11}$ and $C_{90} = 2.50 \times 10^{-11}$, following the work of Poole.[12] This crack growth curve is conservative when compared with that given in

the 1990 edition of Section XI of the ASME Pressure Vessel Code and the experimental data of Ruther et al.[13]

Initial Crack-Size Distribution

In the absence of information on the statistical distribution of initial defects that are more applicable to the weld geometry of NPR-HWR piping systems, the distribution described in Ref. 9 was implemented. Crack depth was assumed to have a log-normal distribution, while the crack aspect ratio was taken to have an exponential distribution.

2.2 Service Inspections

Preservice and in-service inspections every 10 years are modeled. The effectiveness of all inspections is modeled probabilistically and is assumed to be equivalent to that for BWRs. Because of the thinner wall of the NPR-HWR surge line, which simplifies inspection in general, this should be a conservative assumption. Leaks are detected and the pipe repaired. A small leak is defined as any throughwall defect, the detectable leak rate (at and above which cracks are repaired) is 2 gal/min, and a big leak is considered to occur if the leak rate is ≥ 5 gal/min.

2.3 Operating Stresses and Transient Loading

The loads and transient histories of the surge line are the same as those used by Poole[12] in his deterministic studies (Table 1); they are estimated on the basis of experience with similar components in other reactor systems. The surge line is subjected to relatively low operating stresses: σ_{DW} = 0.64 ksi (due to dead weight), σ_{pr} = 0.18 ksi (due to coolant pressure), and σ_T = 4.10 ksi (due to constraints on thermal expansion). The transients considered here induce larger stresses (on the order of 10-15 ksi). Each transient represents an equivalent loading case for the subblock of transients that produce tension on the pipe inner wall. Transients are also characterized by their frequency, i.e., by the number of occurrences (cycles) per year (Table 1). The specific nature of the seismic transient warrants a somewhat different description and treatment in the PRAISE code, as described in Section 2.4.

APPENDIX D

Table 1. Summary of estimated NPR-HWR piping transient loading cases

Subblock No.	Stress Summary Loading Case	Total Cycles for 60 Yr	Equiv. Loading Case at Cycles/Yr
1	**CBT3** Unit Unloading	19,800	**CBT5** at
	CBT5 Off-Normal Step Temp. Decrease	3,000	36, 159 Cycles/Yr
	CBT6&7 SS Avg. Fluct.	2,144,100	
	CBT18 Normal React. Trip	540	
	CBT1 Full Gas Purge	2,100	
2	**CBT15** Normal Loop Start	300	**CBT10** at
	CBT8&9 SS & Random Fluct. (7%)	1,549,800	43,851 Cycles/Yr
	CBT10&11 SS & Random Fluct. (10%)	1,080,975	
3	**CBT16** Normal Loop Shutdown	300	**CBT14** at 55 Cycles/Yr
	CBT14 Coolant Recycling	3,000	
4	**CBT12&13** SS & Random Fluct. (15%)	476,400	**CBT12** at 7,946 Cycles/Yr
	CBT21 Inadvertent PWS Depressurization	180	
	CBT17 Loss of Power	180	
5	**CBT20** Reactor Trip with Accum. Inj. Cooldown	12	**CBT20E** at 1 Cycles/Yr
6	**CBT22** Fast Valve Closure Depressurization = 6.5P	600	**CBT22** at 10 Cycles/Yr
7	**CBT19** Reactor Trip with Cooldown	240	**CBT19** at 4 Cycles/Yr
8	**CBT26** Fast Valve Closure Depressurization = 4.75P	600	**CBT26** at 10 Cycles/Yr
9	**CBT27** Fast Valve Closure Depressurization = 2.90P	600	**CBT27** at 10 Cycles/Yr
10	**CBT32** Earthquake (Operating Base Earthquake)	120	**CBT32** at 30 Cycles/Occurr.

Source: Ref. 12.

Several transients arrive with relatively high frequency, i.e., cycling rates of dN/dt = 8,000–44,000 cycles/yr. They are:

- loading case CBT5** (σ = 10.26 ksi @ 36,159 cycles/yr).
- loading case CBT10** (σ = 11.47 ksi @ 43,851 cycles/yr).
- loading case CBT12** (σ = 13.29 ksi @ 7,946 cycles/yr).

Unit unloading, off-normal temperature decreases, steady-state (SS) average fluctuations, normal reactor trips, and full gas purges all combine to form the equivalent loading case CBT5. Likewise, normal loop startup, as well as SS and random fluctuations (7–10%), are represented by loading case CBT10, whereas loading case CBT12 covers SS and random fluctuations (15%), inadvertent depressurization of the primary water system, and loss of power.

The above high-frequency transients and the earthquake loading (equivalent loading case CBT32) are the only ones considered in the analysis.

The remainder of the transients occur only several times a year and induce stresses on the same order of magnitude as the three transients discussed above. Therefore, their influence on crack growth and subsequent failure probabilities is neglected.

2.4 Earthquake Loading

Over the course of a plant lifetime, the PRAISE code periodically evaluates the instantaneous effect of seismic events on failure probabilities. During an earthquake, a structure is subject to a number of cycles, whereas most other transients arrive with a single cycle. The PRAISE code handles earthquakes differently from the other transients, treating each earthquake as the first such occurrence. Thus, after an earthquake has been simulated and its influence on crack growth and associated failure probabilities has been evaluated, the crack dimensions are reset to their preevaluation values

** Poole's notation in Ref. 12.

and the simulation proceeds. Consequently, at the next evaluation time the earthquake occurrence is again the first occurrence.

In the simulation, an earthquake, during its duration, is characterized by a number of cycles and by a seismic stress amplitude. In the considered example, the number of cycles per arrival is 30, and the seismic stress amplitude is σ_{EQ} = 8.4 ksi (loading case CBT32).

2.5 Stress Corrosion Crack Initiation

The influence of stress corrosion cracking (SCC) was also examined. An average of one potential crack initiation site per 2 in. of a weld was assumed,[10] i.e., 19 potential initiation sites per weldment were modeled. The PRAISE code assigns to each of those sites an initiation time after which a crack will have formed. These initiation times are a monotonically increasing function of the variable tensile stress along the inside pipe surface and of the aggressiveness of the environment. Sites with initiation times within the plant lifetime enter the analysis. Once initiated, a crack grows for the remainder of the plant's lifetime.

The SCC models for initiation and growth in PRAISE are based primarily on data obtained under BWR conditions. For application to the NPR, the model was extrapolated to nominal NPR-HWR conditions, in which the dissolved oxygen concentration was taken to be 8 ppm at startup and 1 ppm during SS operation. The SS coolant temperature is 100°C (212°F). The presence of ionic impurities in the coolant is characterized by the relatively high coolant conductivity γ = 0.2 μS/cm, which is lower than that in the NPR-HWR but is a conservative estimate of the portion of the actual conductivity associated with aggressive species such as sulfates and chlorides. The PRAISE code conservatively assumes that all conductivity is associated with sulfates. This is not too conservative in the high-purity BWR environment, but is conservative in the case of the NPR-HWR because the relatively high coolant conductivity (≈2 μS/cm) is due primarily to the deliberate addition of nitric acid, which does not promote SCC.

The results of Ruther et al.[13] suggest that extrapolation of the crack growth model in PRAISE to NPR conditions gives very conservative results for SCC crack growth rates (approximately an order of magnitude too large). The initiation model in PRAISE was not systematically compared with the

experimental results of Ruther et al.[13] in simulated NPR environments because no significant SCC could be observed in these tests. The PRAISE model is undoubtedly conservative, but it is difficult to quantify the degree of conservatism.

The present calculations also ignore weld residual stresses. The current PRAISE residual stress models are based on results for the relatively heavy-walled piping used in BWRs and are probably not relevant to the much thinner walled piping used in the NPR.

3 Analytical Procedure

The PRAISE code can handle cracks of two different origins: a preexisting crack and an initiated crack (the latter created by stress corrosion). It is assumed that the design procedures for the PRAISE code prevent the initiation of cracks by fatigue.

When a preexisting crack is considered, one must account for the probability that it is present in the weld to begin with. In other words, the computed failure probabilities are conditional, relying on the initial presence of a crack in the weld. To obtain "absolute" (unconditional) probabilities, the obtained conditional probabilities should be multiplied by the probability of the occurrence of the initial crack.

The probability that one crack exists in the weld is (for a dilute crack concentration) proportional to the weld volume V,

$$P(1) \equiv Vp^* \tag{1}$$

where the coefficient of proportionality p^* represents the density of cracks per unit volume.[5] The weld volume also includes the heat-affected zone, which is taken to be two wall thicknesses wide. The weld volume is then

$$V = \pi D_i h(2h) = 2\pi D_i h^2, \tag{2}$$

where D_i is the pipe inner radius and h is the pipe wall thickness. A conservative estimate for the density of cracks per weld volume is $p^* = 10^{-4}/\text{in.}^3$. With this estimate, the probability of the existence of a crack in the weld of the considered pipe geometry is given by the equation

$$P(1) \cong 2\pi(15)(0.5)^2(10^{-4}) \cong 2.5 \times 10^{-3} \quad (3)$$

The value from Eq. 3 is used to obtain unconditional probabilities when only preexisting cracks are considered.

Where a crack initiated by SCC is considered, the computed failure probabilities are already absolute probabilities, because the PRAISE Code assumes that the crack will always form at the initiation site after the period of initiation time has passed.

4 Results

4.1 Fatigue Loading of a Preexisting Crack

The results of a simulation that includes all three sets of transients are presented in Figs. 1 and 2. The plant loading history causes no LOCA.

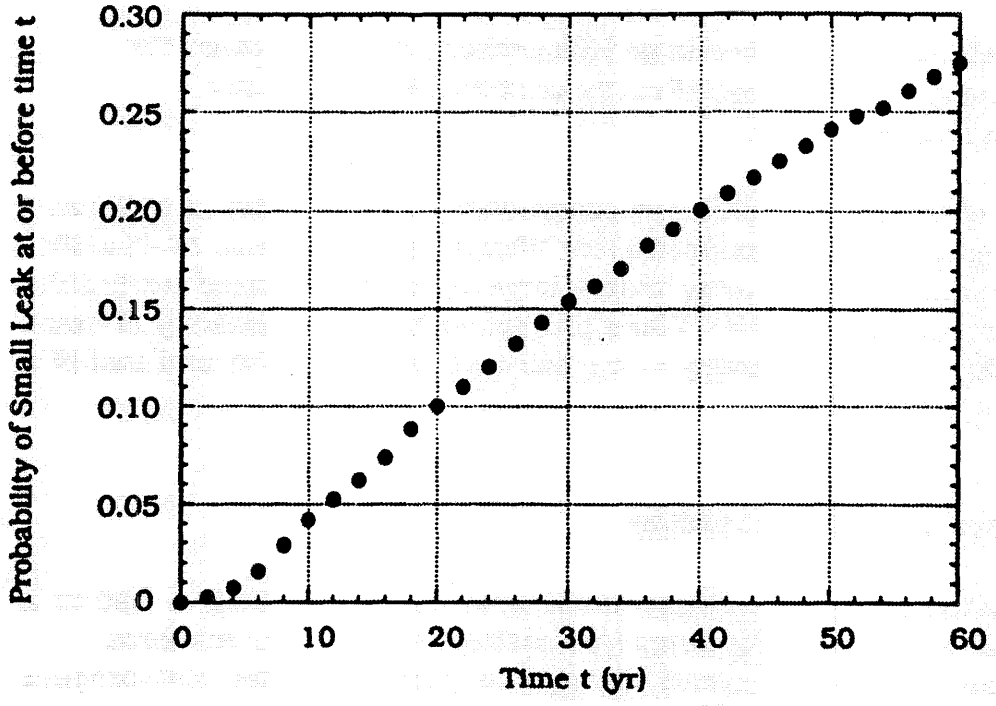

Fig. 1. Conditional cumulative small-leak probability for initial cracks growing under fatigue. Results are conditional on initial presence of a crack.

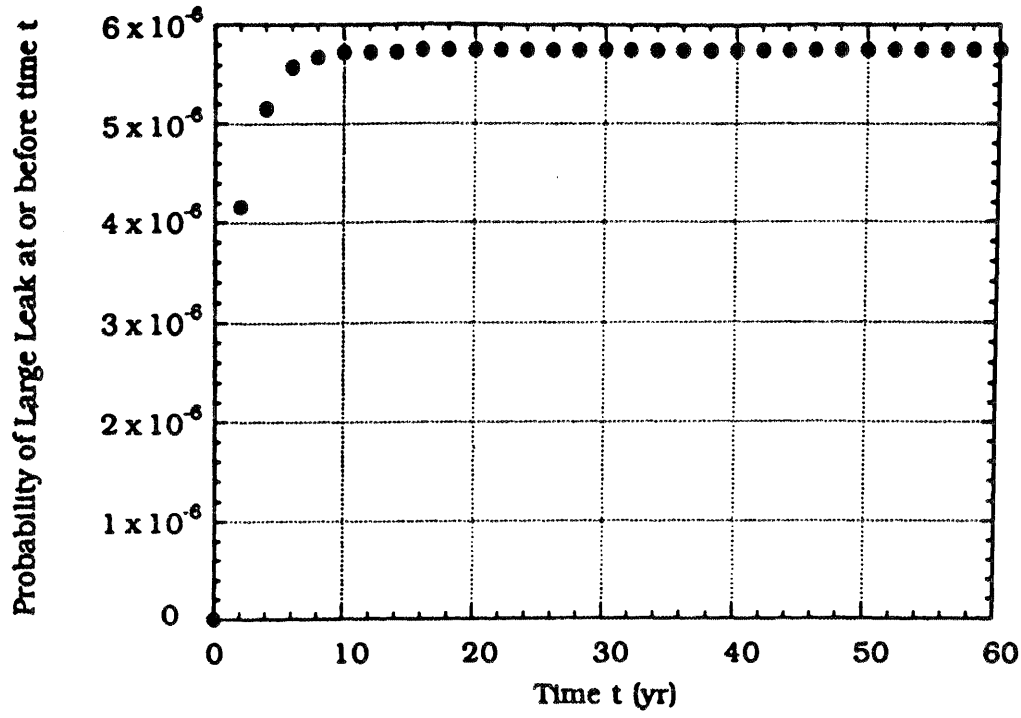

Fig. 2. Conditional cumulative large-leak probability for initial cracks growing under fatigue. Results are conditional on initial presence of a crack.

At the end of the plant lifetime, the *conditional* probability that a small leak has occurred during the assumed plant lifetime of 60 years is 27.45×10^{-2} and the *conditional* probability that a large leak has occurred during the plant lifetime is 5.74×10^{-6}. When multiplied by the probability of crack existence, Eq. 3, the probability of a small leak is 6.86×10^{-4} and that of a large leak is 1.43×10^{-8}.

Influence of Seismic Loading

The postulated additional seismic stresses were not sufficient to lead to a LOCA in a weld with a growing preexisting crack and, moreover, the relatively low number of cycles during the earthquake did not produce enough crack growth to cause a leak. To examine the influence of seismic loadings of possible larger magnitudes and to define the margin against failure under such loads, multiples (2, 2.5, 3, 3.5, 4) of the initially estimated seismic stress amplitude were considered. Even with

increasing levels of seismic stress, the probabilities of small and large leaks again did not change. LOCA probabilities were zero until stress levels reached 3 times the initial estimate (≈24 ksi, half the flow stress that governs net cross-section failure). The probabilities for a LOCA were largest at the beginning of the plant lifetime and then sharply attenuated after 2-4 years. This can be explained by the fact that only large initial cracks can lead to a LOCA, i.e., if the earthquake arrives later in the course of plant lifetime, large initial cracks will have already caused detectable leakage and will have been repaired.

Table 2 summarizes the results for the case of seismic loading. The last column accounts for the probability that a crack exists, which is ~ 2.5×10^{-3}. When compared with the computed small- and large-leak probabilities, the influence of earthquakes is negligible.

Table 2. Influence of seismic stress level on probabilities of a LOCA at plant startup (t = 0).

seismic stress magnitude (ksi)	conditional LOCA	LOCA
1 x 8 ksi = 8	0	0
2 x 8 ksi = 16	0	0
2.5 x 8 ksi = 20	0	0
3 x 8 ksi = 24	7.48×10^{-16}	1.87×10^{-18}
3.5 x 8 ksi = 28	2.16×10^{-14}	5.40×10^{-17}
4 x 8 ksi = 32	4.23×10^{-12}	1.05×10^{-14}

4.2 Simultaneous action of Fatigue and Stress Corrosion on Preexisting and Stress Corrosion Induced cracks

The influence of SCC is twofold: it can initiate additional cracks, and provide mode of crack growth, besides fatigue, for cracks that have been initiated previously or were present during fabrication. Where the probability of more than one preexisting crack is low, the cumulative probability of failure of a weld within time t, event F_t, due to the presence of cracks, can be written as

APPENDIX D

$$P(F_t) = P[F_t|\text{no initial crack}] * [1 - P(1)] + P[F_t|1 \text{ initial crack}] * P(1) \quad (4)$$

where P(1) is the probability of having one initial crack.[3] Thus, failure probability is computed from Eq. 4 in two separate program runs, one with only SCC-initiated cracks growing under both fatigue and SCC, and another allowing only for initial defects, growing under both fatigue and SCC. The results for no initial defects are presented in Fig. 3. The cumulative probability of a small leak at the end of the plant lifetime (60 yr) is 1.55×10^{-3}. No large leak is generated by this case.

The result for one preexisting crack is presented in Fig. 4. The only difference between Fig. 4 and Fig. 1 is that besides fatigue, stress corrosion is an additional driving force for a preexisting crack. For the case of a preexisting crack, stress corrosion appeared to contribute relatively little to the probability of a small leak compared with the contribution of a fatigue crack growth mechanism, i.e., the *conditional* probability of a small leak at the end of plant lifetime is 27.57×10^{-2} (compared with 27.45×10^{-2} in the case of fatigue only). Fatigue also dominates the conditional probability for

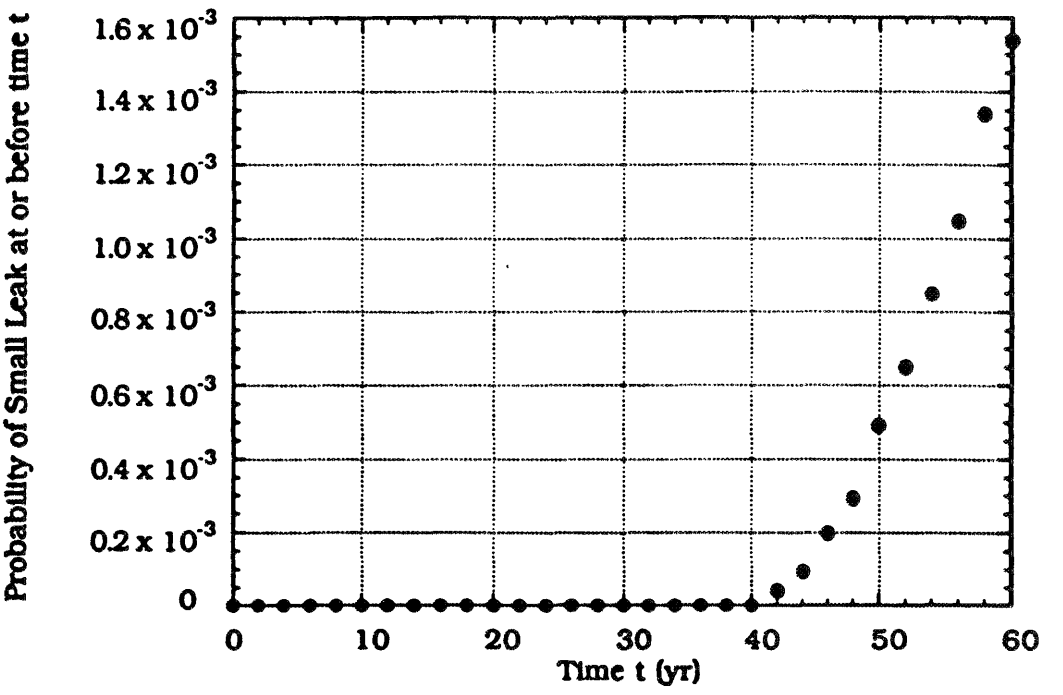

Fig. 3. Cumulative small-leak probability for the case of initiated cracks growing under both fatigue and SCC (no initial cracks present).

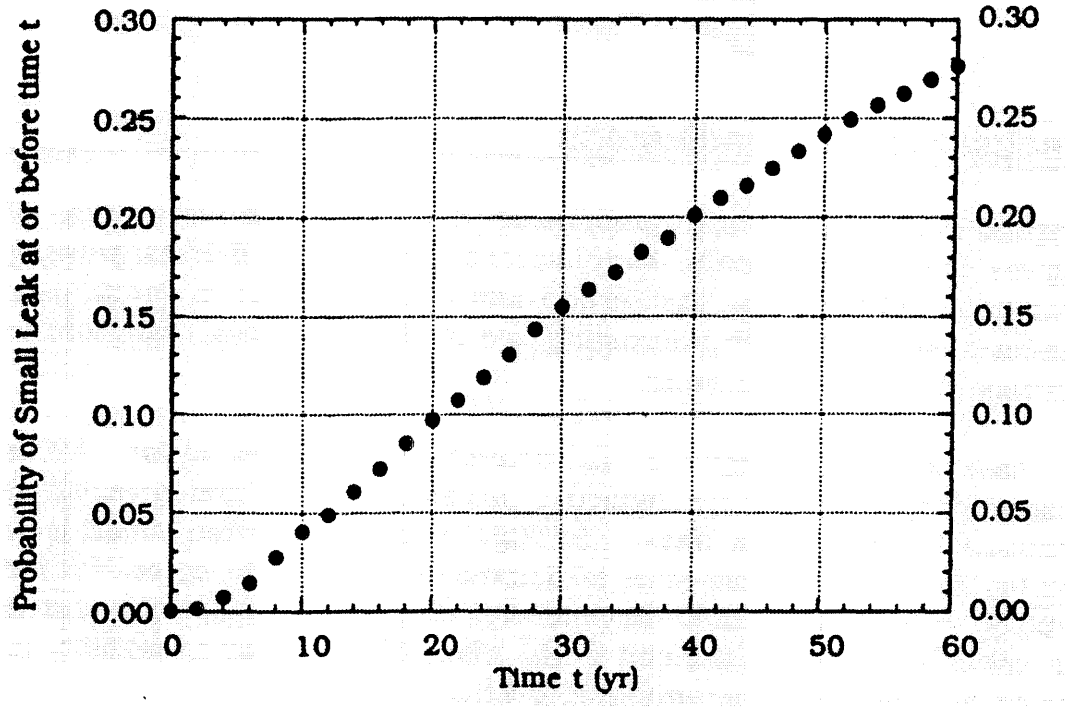

Fig. 4. Conditional cumulative leak probability for initial cracks growing under both fatigue and SCC. Results are conditional on initial presence of a crack.

large leaks where the results that include stress corrosion produce only indistinguishable changes in Fig. 2.

According to Eq. 4, the probabilities of leaks in the case of SCC-initiated and preexisting cracks, driven by both fatigue and SCC, are

$$\begin{aligned} P[\text{Small Leak}] &= 1.55 \times 10^{-3} \cdot (1 - 2.5 \times 10^{-3}) + 0.2757 \cdot 2.5 \times 10^{-3} \\ &= 1.54 \times 10^{-3} + 6.89 \times 10^{-4} \\ &\approx 2.2 \times 10^{-3}, \end{aligned} \tag{5}$$

and

$$
\begin{aligned}
P[\text{Large Leak}] &= 0 \cdot (1 - 2.5 \times 10^{-3}) + 5.74 \times 10^{-6} \cdot 2.5 \times 10^{-3} \\
&= 0 + 1.43 \times 10^{-8} \\
&= 1.43 \times 10^{-8}.
\end{aligned}
\tag{6}
$$

5 Discussion and Conclusions

The results of the analysis are summarized in Table 3. The first column of data gives the results for the simulation of preexisting defects growing under fatigue only, whereas the second and third are used to obtain leak probabilities caused by both preexisting and initiated cracks growing under both fatigue and SCC (last column).

In the case represented by the last column, the time evolution of the small-leak probability can be divided into contributions from preexisting and initiated cracks. As shown in Fig. 5, the calculated small-leak probability for 316 stainless steel is dominated by preexisting cracks for the first 50 yr of plant lifetime. Beyond that time, the influence of initiated cracks prevails, so that at the end of the plant lifetime, leak probability is controlled by stress-corrosion-initiated cracks.

When the first and last columns of data are compared, it is evident that the probability of a small leak at the end of the plant lifetime increases from 6.86×10^{-4} in the case of fatigue of initial defects to 2.2×10^{-3} when aggressive environmental action is considered. The corresponding probability of a large leak, for practical purposes, does not increase because small leaks are continually repaired. However, even with the conservative assumptions for crack growth rates used in the study, the actual probabilities of a large leak are still quite low.

The values in the first and last columns of data give zero computational LOCA probability over the sample of selected cracks. The variance induced in this result by sampling errors can be estimated.[14]

Table 3. Probability of occurrence of three events, given various defect origins and crack growth modes

Event	Defect Origin			
	Preexisting Crack [a]	Preexisting Crack [b]	SCC-initiated Crack [b]	Preexisting & SCC-initiated Cracks -Eq. 4[b]
Small leak	6.86×10^{-4}	6.89×10^{-4}	1.54×10^{-3}	2.20×10^{-3}
Large Leak	1.43×10^{-8}	1.43×10^{-8}	0	1.43×10^{-8}
LOCA	0	0	0	0

[a] Growth mode = fatigue
[b] Growth mode = fatigue and SCC

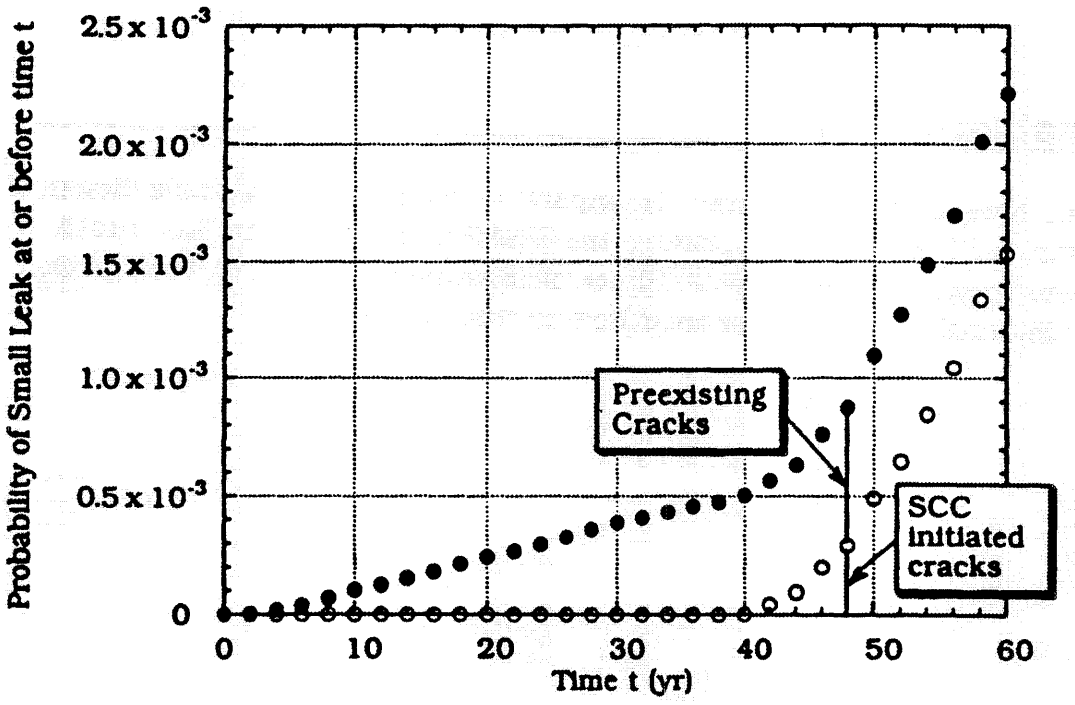

Fig. 5. Contributions of preexisting and initial cracks to the probabilities of a small leak in the case of cracks growing under both fatigue and SCC.

Because it is assumed that the design rules prevent the initiation of fatigue cracks, the number of fatigue failures is strongly limited by the relatively low probability of existence of initial cracks (on the order of 10^{-3}) due to small weldment volume. When SCC is considered, however, many more crack initiation sites are potentially available, some of which become true crack initiation sites during the plant lifetime and subsequently lead to faster pipe deterioration, as demonstrated in Fig. 5. Even with the large conservatisms introduced by extrapolating the current SCC models in PRAISE to NPR conditions, the overall probabilities are still quite small. However, the present analysis does not take into account residual stress effects. These would tend to increase the failure probabilities somewhat, although the degree on nonconservatism due to the neglect of residual stresses is almost certainly smaller than that introduced by the use of the current PRAISE correlations for SCC under NPR water chemistry conditions.

Acknowledgments

The authors thank Mr. Loren Thompson of Argonne's Materials Science Division for his help in installing the PRAISE code on the Macintosh II personal computer and Dr. W. J. Shack of Argonne and Mr. A. B. Poole of Oak Ridge National Laboratory for their helpful discussions.

References

1. S. Lu, R. D. Streit, and C. K. Chou, *Probability of Pipe Fracture in the Primary Coolant Loop of a PWR Plant, Volume 1: Summary, Load Combination Program, Project I Final Report*, NUREG/CR-2189, Vol. 1, UCID-18967, Vol. 1, Prepared for U.S. Nuclear Regulatory Commission by Science Applications, Inc., and Lawrence Livermore Laboratory (1981).

2. A. C. Eberhardt, *Probability of Pipe Fracture in the Primary Coolant Loop of a PWR Plan, Volume 2: Primary Coolant Loop Model, Load Combination Program, Project I Final Report*, NUREG/CR-2189, Vol. 2, UCID-18967, Vol. 2, Prepared for U.S. Nuclear Regulatory Commission by Science Applications, Inc., and Lawrence Livermore Laboratory (1981).

3. A. L. Chan, S. C. Lu, E. F. Rybicki, and D. J. Curtis, *Probability of Pipe Fracture in the Primary Coolant Loop of a PWR Plan, Volume 3: Nonseismic Stress Analysis, Load Combination Program, Project I Final Report*, NUREG/CR-2189, Vol. 3, UCID-18967, Vol. 3, Prepared for U.S. Nuclear Regulatory Commission by Science Applications, Inc., and Lawrence Livermore Laboratory (1981).

4. S. C. Lu, S. M. Ma, and R. A. Larder, *Probability of Pipe Fracture in the Primary Coolant Loop of a PWR Plant, Volume 4: Seismic Response Analysis, Load Combination Program, Project I Final Report*, NUREG/CR-2189, Vol 4, UCID-18967, Vol. 4, Prepared for U.S. Nuclear Regulatory Commission by Science Applications, Inc., and Lawrence Livermore Laboratory (1981).

5. D. O. Harris, E. Y. Lim, and D. D. Dedhia, *Probability of Pipe Fracture in the Primary Coolant Loop of a PWR Plant, Volume 5: Probabilistic Fracture Mechanics Analysis, Load Combination Program, Project I Final Report*, NUREG/CR-2189, Vol. 5, UCID-18967, Vol. 5, Prepared for U.S. Nuclear Regulatory Commission by Science Applications, Inc., and Lawrence Livermore Laboratory (1981).

6. R. D. Streit, *Probability of Pipe Fracture in the Primary Coolant Loop of a PWR Plant, Volume 6: Failure Mode Analysis, Load Combination Program, Project I Final Report*, NUREG/CR-2189, Vol. 6, UCID-18967, Vol. 6, Prepared for U.S. Nuclear Regulatory Commission by Science Applications, Inc., and Lawrence Livermore Laboratory (1981).

7. R. Mensing and L. George, *Probability of Pipe Fracture in the Primary Coolant Loop of a PWR Plant, Volume 7: System Failure Probability Analysis, Load Combination Program, Project I Final Report*, NUREG/CR-2189, Vol. 7, UCID-18967, Vol. 7, Prepared for U.S. Nuclear Regulatory Commission by Science Applications, Inc., and Lawrence Livermore Laboratory (1981).

8. R. D. Streit, *Probability of Pipe Fracture in the Primary Coolant Loop of a PWR Plant, Volume 8: Pipe Fracture Indirectly Induced by an Earthquake, Load Combination Program, Project I Final Report*, NUREG/CR-2189, Vol. 8, UCID-18967, Vol. 8, Prepared for U.S. Nuclear Regulatory Commission by Science Applications, Inc., and Lawrence Livermore Laboratory (1981).

9. E. Y. Lim, *Probability of Pipe Fracture in the Primary Coolant Loop of a PWR Plant, Volume 9: PRAISE Computer Code User's Manual, Load Combination Program, Project I Final report*, NUREG/CR-2189, Vol. 9, UCID-18967, Vol. 9, Prepared for U.S. Nuclear Regulatory Commission by Lawrence Livermore Laboratory (1981).

10. D. O. Harris, D. D. Dedhia, E. D. Eason, and S. D. Patterson, *Probability of Failure in BWR Reactor Coolant Piping, Volume 3: Probabilistic Treatment of Stress Corrosion Cracking in 304 and 316NG BWR Piping Weldments*, NUREG/CR-4792, Vol. 3, UCID-20914, Vol. 3, Prepared for U.S. Nuclear Regulatory Commission by Failure Analysis Associates and Lawrence Livermore Laboratory (1986).

11. A. Stojimirovic, and S. Majumdar, *Use of the PRAISE Code to Estimate Probability of Leaks in the NPR-HWR Pressurizer Surge Line*, ANL/NPR-92/4, Argonne National Laboratory, (1992).

12. A. B. Poole, Oak Ridge National Laboratory, personal communication (1991).

13. W. E. Ruther, T. F. Kassner, W. J. Shack, and W. K. Soppet, *Environmentally Assisted Cracking of Austenitic Stainless Steels in Simulated NPR Water*, ANL/NPR-91/7, Argonne National Laboratory, (1991).

14. T. Yamane, *Elementary Sampling Theory*, Prentice-Hall, Inc., Englewood Cliffs, NJ (1967).

Internal Distribution

Central Research Library
Document Reference Section
Laboratory Records Department (2)
Laboratory Records, ORNL RC
NPR-RMS-DCC-RC
ORNL Patent Section
R. L. Battiste
R. D. Cheverton
J. A. Clinard (5)
J. M. Corum
G. F. Flanigan
R. C. Gwaltney
H. A. Glovier
R. M. Harrington
D. O. Hobson
F. J. Homan
J. E. Jones Jr.
J. G. Merkle
S. E. Moore
D. L. Moses
R. K. Nanstad
A. B. Poole (5)
T. B. Powell
C. E. Pugh
J. B. Richard
P. L. Rittenhouse
D. L. Selby
J. O. Stiegler
C. D. West
D. L. Williams, Jr.
G. T. Yahr

External Distribution

Argonne National Laboratory, 9700 South Cass Avenue, Building 208, Argonne, IL 60439
L. W. Deitrich
A. E. Klickman

Argonne National Laboratory, Materials Science and Technology Division, Building 212, 9700 South Cass Avenue, Argonne, IL 60439
S. Majumdar
W. J. Shack
A. Stojimirovic

Babcock & Wilcox Company, 3315 Old Forest Road, Lynchburg, VA 24506-0935
J. D. Aadland
R. J. Beauregard
T. A. Thornton
W. T. Withers

Brookhaven National Laboratory, Building 130, Upton, Long Island, NY 11973
J. R. Weeks

Department of Energy, Office of New Production Reactors, 1000 Independence Avenue, SW, Washington, DC 20585
R. J. August, NP-41 (2)
K. A. Klein, NP-30 (5)
W. A. Stringfield, NP-43

Department of Energy, DOE Headquarters, Washington, DC 20585
K. Jamali, DP-62
J. P. Mulkey, NE-47

Department of Energy, Barnwell County Project Management Office, Hitchcock Office Park, 35 Varden Drive (NP-70), Aiken, SC 29803
M. C. Kirkland, NP-70

Ebasco Services Incorporated, Two World Trade Center, New York, NY 10048
R. C. Iotti

Lawrence Livermore National Laboratory, P.O. Box 808, Livermore, CA 94551
G. S. Holman

Los Alamos National Laboratory, P.O. Box 1663, Mailstop K-575, Los Alamos, NM 87545
C. R. Bell
W. L. Kirchner
E. Rodriguez

Sandia National Laboratories, P.O. Box 5800, Division 6402, Albuquerque, NM 87185-5800
K. D. Bergeron

Westinghouse - Savannah River Company
N. G. Awadalla, Savannah River Laboratory, P.O.Box 616, Aiken, SC 29801
K. F. Cooper, 37 Varden Drive, Aiken, SC 29801
M. R. Louthan, Savannah River Laboratory, P.O. Box 616, Aiken, SC 29801
F. J. McCrosson, Savannah River Site, Building 773-41A, Aiken, SC 29802
C. Thiessen, 37 Varden Drive, Aiken, SC 29801

Review & Synthesis Associates, 630 Cedar, Richland, WA 99352
Spencer H. Bush

U.S. Nuclear Regulatory Commission, NLS-007, Washington, DC 20555
Lawrence C. Shao
Robert J. Bosnak

RPK Structural Mechanics Consulting, Inc., 18971 Villa Terrace, Yorba Linda, CA 92686
Robert P. Kennedy

Teledyne Engineering Services, 10 Forbes Road, Woburn, MA 01801
Donald F. Landers

Everett C. Rodabaugh, Consultant, 7025 Scribner Way, Dublin, OH 43017

G. C. Slagis Associates, 3520 Eris Court, Walnut Creek, CA 94598-4669
G. C. Slagis

Battelle Columbus Laboratories, 505 King Avenue, Columbus, OH 43201
Gery M. Wilkowski
R. J. Olson

Electric Power Research Institute, 3412 Hillview Avenue, Palo Alto, CA 94304
S. W. Tagart
B. Chexal
J. D. Gilman

Office of Assistant Manager, Energy Research and Development, DOE-ORO, Oak Ridge, TN 37831

Office of Scientific and Technical Information (2), P.O. Box 62, Oak Ridge, TN 37831